Table of contents

Zusammenfassung

Die Calsyntenine wurden im Labor von Prof. Peter Sonderegger im Rahmen einer Suche nach axonal sezernierten Proteinen mittels eines kompartimentierten Zellkultursystems und zwei-dimensionaler Gelelectrophorese entdeckt. Die drei Mitglieder der Calsyntenin-Genfamilie, Calsyntenin-1, -2, und -3, haben eine Aminosäuren-Identität von ungefähr 70%. Die biologische Funktion der Calsyntenine ist noch weitgehend unerforscht. Eines der bisher festgestellten Charakteristika der Calsyntenine weist darauf hin, dass eine Region mit bevorzugt sauren Aminosäuren im zytoplasmatischen Segment von Calsyntenin-1 bei der Verarbeitung von neuronalen Calcium-Signalen eine Rolle spielen könnte. Auf Grund der Calcium-bindenden Funktion des ersten Vertreters wurden die Mitglieder dieser Genfamilie als Calsyntenine benannt. Die Calcium-bindende Funktion des zytoplasmatischen Segments von Calsyntenin-1 motivierte uns zu den vorliegenden Studien, welche zum Ziel hatten, eine mögliche Rolle der Calsyntenine im Excitotoxizitäts-induzierten neuronalen Zelltod zu studieren und charakterisieren.

Anstelle der zeitaufwändigen Erzeugung des Gen-Knock-Outs bei Mäusen verwendeten wir Vektor-basierte siRNA (small interfering RNA) um die Expression und Funktion der Calsyntenine zu unterdrücken. Die siRNA-Sequenz, welche einer Sequenz des angezielten Gens entspricht, wurde hinter dem Promotor der RNA-Polymerase III eingefügt. Die resultierenden siRNA-Transkripte imitieren Zwischenstufen des RNA-Interferenz-Weges, welche schlussendlich den Sequenz-spezifischen mRNA-Abbau zur Folge haben. Mittels EGFP (enhanced Green Fluorescent Protein) als Ziel-Gen konnten wir mit unserem Vektor-basierten siRNA-System in den Säugetier-Zelllinien HEK293T und NG108-15 effiziente und spezifische Gen-Suppression erzielen. Ebenso wurde die Expression von transfiziertem Calsyntenin-1 durch die Co-Transfektion eines Calsyntenin-1-spezifischen siRNA-Konstrukts, pBlueU6-siCst1.1, in der Neuroblastoma-Glioma-Zelllinie NG-108-15 stark unterdrückt.

Die effiziente Einführung eines fremden Gens in eine Nervenzelle ist mit den heute gängigen Transfektionsmethoden in der Regel schwierig. Deshalb haben wir einen Vektor zu Hilfe genommen, der aus dem Adeno-assoziierten Virus (AAV) entwickelt wurde. Unser rekombinanter AAV (rAAV) mit der siRNA-Kassette gegen Calsyntenin-1 wurde in 90% der Neurone aufgenommen. Die Analyse der Zellen mittels Immunoblot und Immunozytochemie zeigte eine Suppression von Calsyntenin-1 von bis zu 60%. Auf die gleiche Art konnten wir auch die Ueberexpression von Calsyntenin-1 herbeiführen. Wir zählten die primären und sekundären Dendriten der Neurone mit Knock-down und Ueberexpression von Calsyntenin-1 und inspizierten sie bezüglich morphologischer Auffälligkeiten. Zum

Schluss untersuchten wir die Reaktion von Neuronen, die mit rAAV infiziert wurden, nach Exposition von 100 µM NMDA, um einen möglichen Einfluss von Ueberexpression oder Mangel an Calsyntenin-1 auf den Excitotoxizitäts-induzierten neuronalen Zelltod zu ermitteln.

Die bisher vorliegenden Resultate nach rAAV-induziertem Knock-down und Ueberexpression von Calsyntenin-1 lassen noch kein abschliessendes Urteil darüber zu, ob Calsyntenin-1 eine Rolle beim Excitotoxizitäts-induzierten Nervenzelltod innehat. Insbesondere werden auch weitere Experimente notwendig sein, um die Rolle der anderen Familienmitglieder, Calsyntenin-2 und -3 zu studieren und deren mögliche kompensatorische Rolle nach der Ausschaltung von Calsyntenin-1 zu ermitteln. Zur gezielten Ausschaltung aller drei Calsyntenine wurde bereits eine siRNA-Kassette konstruiert, welche eine Sequenz enthält, die eine den drei Calsynteninen gemeinsame Sequenz anzielt. Damit sind die Voraussetzungen für einen Triple-Knockdown der Calsyntenine gegeben.

I. Abstract

Using a compartmentalized culturing system and two-dimensional gel analysis, a novel protein family was discovered in embryonic chicken neuron cultures in the laboratory of Dr. Peter Sonderegger in 2001. The three members, calsyntenin-1, 2, and 3 share 70% amino acid identity. The protein family was named calsyntenin because of the acidic stretches in the cytoplamsic domain, consistent with a calcium binding function. Later, highly conserved homologues in human and mouse were also identified. The biological function of calsyntenin remains unknown but many of the properties that have been characterized provide clues for further investigation. The restricted localization in the CNS and the calcium binding motif in the cytoplasmic part of calsyntenin suggest its potential function in calcium buffering and signaling in neurons, which motivated our efforts to explore the roles of calsyntenin in calcium regulation in neurons and in excitotoxic neuronal cell death.

Instead of the time-consuming generation of knockout animals, DNA vector-based siRNA was used in this project to achieve loss-of-function. RNA polymerase III promoters, which can produce small transcripts extending from a well-defined starting point to a 5T–in-row terminal, were isolated and cloned into vectors to conduct siRNA transcription. The siRNA template derived from a target gene sequence was cloned downstream to the promoter to produce siRNA transcripts that mimic intermediates in the RNA interference pathway and eventually induce sequence-dependent mRNA degradation. Using EGFP as a target gene, we demonstrated efficient and highly specific gene suppression by our vector-based siRNA system in the mammalian cell lines HEK293T and NG108-15. The co-transfected calsyntenin-1 expression was also strongly inhibited by introducing the corresponding siRNA construct pBlueU6-siCst1.1 in the NG-108 cell line.

Efficient gene delivery has proven difficult in neurons with electroporation and lipofectamine transfection. We have developed a solution involving the recombinant adeno-associate virus (rAAV) vector, which offers a promising tool to introduce foreign DNA into neurons *in vitro* and *in vivo*. Our rAAV carrying siRNA cassette against calsyntenin-1 transduced 90% of neurons in primary hippocampal neuronal culture under optimized conditions. Calsyntenin-1 suppression was evaluated with immunoblotting and immunocytochemistry, revealing a drastic calsyntenin-1 down-regulation by up to 60%. Gain-of-function was achieved by introducing calsyntenin-1 over-expressing rAAV into neurons.

The numbers of primary dendrites originating from neuronal soma and the secondary dendritic branches were counted in the calsyntenin-1 knockdown and

over-expressing neurons to screen for morphological changes in dendritic development. So far, no obvious changes were observed. To explore the potential involvement of calsyntenin in excitotoxicity, rAAV transduced neurons were exposed for 30 minutes to 100 µM NMDA to induce excitotoxic neuronal cell death. Nuclear condensation in apoptotic cells and apoptotic-like cells indicated by DAPI and Hoechst staining assays did not show significant differences in either calsyntenin-1 down-regulated or over-expressing cells.

The preliminary data obtained from the calsyntenin-1 knockdown experiment is not sufficient to draw a conclusion whether calsyntenin plays a role in neuronal excitotoxicity. To exclude a compensatory effect by calsyntenin-2 and 3, a siRNA cassette targeting the common sequence shared between these two proteins was incorporated into the calsyntenin-1 knockdown vector. This approach makes the triple knockdown of all three calsyntenins possible.

Further morphological investigations such as the analysis of total dendritic length and synaptic density will be conducted to give a more comprehensive understanding of the role of calsyntenins in neuronal development. Facilitated by the rAAV vehicle, calsyntenin suppression and over-expression *in vivo* can now be easily realized. Reversible focal cerebral ischemia induced by temporary middle cerebral artery occlusion may serve as a good model to answer the question whether the calsyntenins play a role in excitotoxic neuronal cell death.

Abbreviations

Abbreviations

AA	Amino acid
AAV	Adeno-associated virus
Aβ	β-amyloid
Ab	Antibody
AD	Alzheimer's Disease
acetyl-CoA	Acetyl-coenzyme A
AIF	Apoptosis inducing factor
AMPA	A-amino-3hydroxy-5methyl-4-isoxazole-propionic acid
AP	Akaline phosphatase
APP	Amyloid precursor protein
ATP	Adenosine triphosphate
bp	Base pair
BLAST	Basic Local Alignment Search Tool
BSA	Bovine serum albumine
CA	Cornu ammonis
CaM	Calmodulin
CaMK	Calmodulin-dependent protein kinase
cAMP	Cyclic adenosine monophosphate
caspase	Cysteinyl-aspartate-cleaving protease
CCE	Capacitive Ca^{2+} entry
CHS	Chalcone synthase
cDNA	Complementary deoxyribonucleic acid
CNS	Central nervous system
cADPR	Cyclic ADP ribose
Cst	Calsyntenin
Cy3	Cytochrome-3
Cy5	Cytochrome-5
DAG	Diacylglycerol
DG	Dentate gyrus;
dsRNA	Double-stranded RNA
DMEM	Dulbecco/Vogt Modified Eagle's Minimal Essential Medium
ECL	Enhanced electrochemiluminescence
EDTA	Ethylenediamine
ER	Endoplasmatic reticulum
FCS	Fetal calf serum
FGFR-1	Fibroblast growth factor receptor 1
GFP	Green fluorescent protein
Glu	Glutamate
GluR	Glutamate-specific receptor

HAT	Hypoxantine, Aminopterin,Thymidine)
HBSS	Hank's balanced saline solution
HEPES	4-(2-hydroxyethyl)-1-piperazineethanesulfonic acid
HEK293T	Human embryonic kidney 293 cell line
HGFR	Hepatocyte growth factor receptor
HRP	Horse radish peroxidase
HSPG	Heparin sulfate proteoglican
Ig	Immunoglobulin
Ins-1,4,5,-P3	Inositol-1,4,5-trisphosphate
iGluRs	Ionic glutamate-gated channels
ITRs	Inverted terminal repeats
KA	Kainic acid
kDa	Kilodalton
KLC	Kinesin light chain
MAPK	Mitogen-activated protein kinase
mGluR	Metabotropic glutamate receptor
miRNA	micro RNA
mPTP	Mitochondrial permeability transient pore
mRNA	Messenger ribonucleic acid
NAADP	Nicotinic acid dinucleotide phosphate
NAD	Nicotinamid-adenine dinucleotide
NADH	Nicotinamide adenine dinucleotide
NCBI	National Center for Biotechnology Information
NCS	Newborn calf serum
NMDA	N-methyl-D-asparate
nt	Nucleotide(s)
ORFs	Open reading frames
PART-1	polyADP-ribose polymerase-1
PAZ	Piwi Argonaute Zwille
PBS	Phosphate-buffered saline
PFA	Paraformaldehyde
pH	*pondus hydrogenii*
PLC	phospholipase C
PIWI	P-element induced wimpy testis
PIP2	Phospotidylinositol 4,5-bisphosphate
PKC	Protein kinase C
PMCA	Plasma-membrane calcium-ATPase
PNK	polynucleotide kinase
PSD	Post-synaptic density
PVDF	Polyvinylidene Difluoride
RBE	Rep-binding element
RdRP/RDEs	RNA-dependent RNA polymerase
RE	Restriction endonuclease
RISC	RNA-induced silencing complex

RLC	RISC loading complex
RNase	Ribonuclease
RNAi	RNA interference
ROC	Receptor operated channel
ROS	Reactive oxygen species
RyR	Ryanodine
RT	Room temperature
SDS-PAGE	Sodium dodecyl polyacrylamide gel electrophoresis
SERCA	Sarcoendoplasmic reticular calcium ATPases
SOCs	Store-operated channels
siRNA	Small interfering RNA
shRNA	Short hairpin RNA
TBS	Tris-buffered saline
TBST	Tris-buffered saline Tween-20/Triton-X-100
TGS	Transcriptional gene silencing
TKs	tyrosine kinases
Tris	Trishydroxymethylaminomethane-2-amino-2-hydroxymethyl-1,3-propanediol
TRP	Transient receptor protein
Vg	Vector genome
viRNA	Virus-derived siRNA
VOCs	Voltage-operated channels
UTR	Untranslated region

II. Introduction

2.1 Calsyntenin protein family

In 2001, calsyntenin-1 was first discovered as a novel secreted protein by 2-dimentional gel electrophoresis in the laboratory of Professor P. Sonderegger when the researchers screened for extracellularly cleaved proteins from supernatant of chicken spinal cord neurons growing in compartmentalized culturing system. The new protein shows apparent molecular mass of 115kD and p*I* value of approximate 6.0 in the 2-dimentional gel analysis (Figure 2.1). Full cDNA sequence of the protein was subsequently revealed when searching available genomic database with cDNA fragment deduced from the 13 amino acids in the N-terminus by reverse genetics. Using the chicken calsyntenin-1 sequence, the homologues of this gene in mouse and human were identified by blast in corresponding genomes. Later, other two highly conserved members of calsyntenin family lately named calsyntenin-2 and calsyntenin-3 were discovered with the same approach from human and mouse genome databases. So far, three different genes encoding three calsyntenin members were found in mammals and avians but only one gene was revealed in *C.elegans*, *D. melanogaster* and *D. rerio* (Vogt et al., 2001).

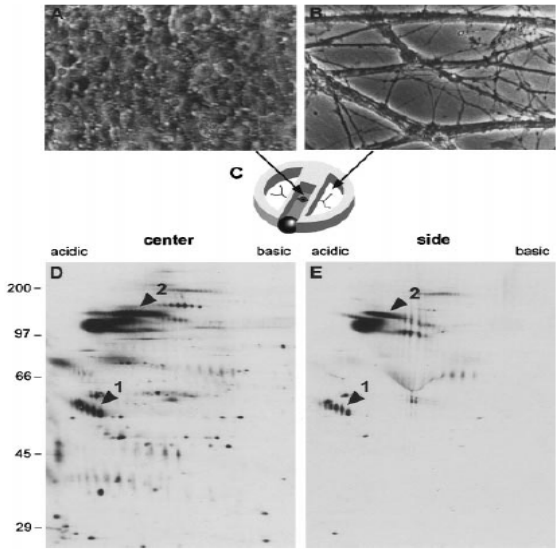

Figure 2.1: Calsyntenin-1 was identified from supernatant of compartmented cell culture by 2-dimentional gel electrophoresis (Vogt et al., 2001)

A: Dissociated neurons from the ventral halves of E6 chicken spinal cords were seeded into the center compartment of compartmental culturing device. **B**: The neuritis extended to the side compartment after 6 days in culture. **C**: The compartmental cell culture system, in which the culture surface is subdivided into three compartments by a Teflon divider. **D** and **E**: Proteins released into the conditioned media of both the central and the side compartments were analyzed by two-dimensional SDS-PAGE and fluorography.

The open reading frame (ORF) of calsyntenin cDNAs flanked over approximate 2900bp, encoding full length protein of roughly 140KD in molecular mass. The deduced protein sequences indicated that they are type I transmembrane proteins. According to two cadherin-like domains found in extracellular N-terminus, the proteins were considered belong to cadherin superfamily. The three members of calsyntenin family share high-degree homology on amino acid sequence of extracellular parts but distinct in their sequences of cytoplasmic domains.

The cytoplasmic sequences of calsyntenin-1 and -2 are characterized with striking acidic amino acids clusters usually found in calcium-binding proteins, suggesting their potential calcium binding property. Later, in vitro calcium-overlay assay truly demonstrated the ability of calsyntenin-1 to bind calcium ions in a manner of low affinity but high capacity. Uniquely, calsyntenin-3 does not contain the acidic stretch in its relatively short C-terminus.

In situ hybridization revealed that the calsyntenins are overwhelmingly expressed in CNS with distinct dominance in different subpopulation of neurons and in different brain regions. Calsyntenin-1 shows the strong expression in cortical neurons, pyramidal neurons and granule neurons in hippocampus, whereas the distribution of calsyntenin-2 and -3 is confined to layer V and VI in cortex, CA2 and CA3 regions in hippocampus. In cerebellum, calsyntenin-1 was only found in granule cells while calsynenin-1 and -3 exclusively present in Purkinjie cell layer (Hintsch et al., 2002) (Figure 2.2).

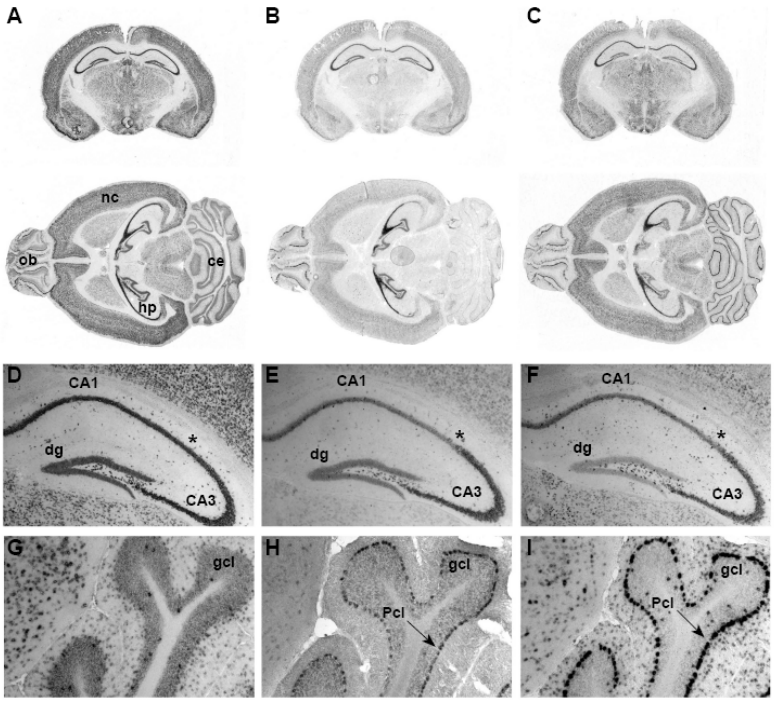

Figure 2.2: Expression pattern of Calsyntenins in the adult mouse brain (Hintsch et al., 2002)

A-C: In situ hybridization of coronal and horizontal whole-brain sections with DIG-labeled antisense riboprobe against calsyntenins show different expression pattern of the three calsyntenins in the neocortex (nc), the hippocampus formation (hc), the thalamus and the hypothalamus (ht). **D-F**: Localization of calsyntenin mRNAs in the hippocampus. Calsyntenin-1 is strongly expressed in all pyramidal cells of the CA1-CA3 regions, in the granule cells of the dentate gyrus and in some interneurons of all dendritic layers and hilus. Calsynetnin-2 and calsyntenin-3 expression is the strongest in CA2-CA3 pyramidal cells and subpopulations of interneurons in all compartments. Considerably lower levels of calsyntenin-2 and-3 mRNA are found in the CA1 region. **G-I**: Celluar localization of calsyntenin mRNAs in horizontal sections of the cerebellar cortex. Calsynternin-1 expression is strong in granule cell layer; no expression was detected in Purkinje cell layer. Low levels of calsyntenin-2 mRNA are restricted mainly to Purkinje cells. Calsyntenin-3 expression is very strong in Purkinje cells.

The full-length calsyntenins are located in postsynaptic densities by immunoelectromicroscopy using polyclonal antibodies generated by immunizing Rabbit with peptides derived from calsyntenins. When cleaved by unknown protease, calsyntenin-1 ectodomain is released into extracellular fluids and the calcium-binding transmembrane stump is internalized to the membrane of the spine apparatus, give rising to a speculation that the proteins may play roles in postsynaptic calcium buffering or signaling (Figure 2.3).

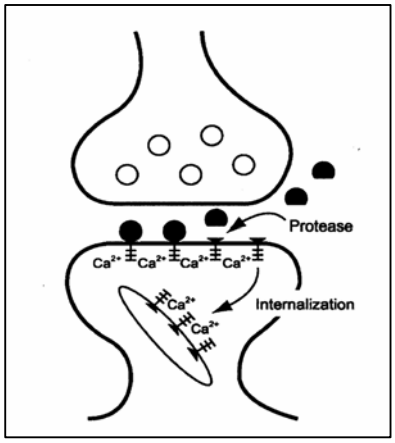

Figure 2.3: Proposed mechanism of protease-dependent translocation of the postsynaptic Calsyntenin-1 (Vogt et al., 2001)

Full-length calsyntenin-1 mainly located on postsynaptic membrane. After proteolytic cleavage by an extracellular protease in the synaptic cleft, the transmembrane stump is internalized into the membrane of the spine apparatus

More hypothesis concerning functions of calsyntenins were raised according to recent observations in immunoprecipitation and yeast two-hybrid for screening their potential partners. When the yeast two-hybrid assay was performed with the bait derived from cytoplasmic domain of calsyntenin-1, a kinesin light chain (KLC) clone was isolated. Further pull down analysis confirmed that calsyntenin is highly associated with kinesin light chain which mediates microtubule-dependent transportation, suggesting the calsyntenins may be involved in the cargo vesicle delivery in neuron. The KLC-binding sites were clearly revealed by mapping with a serial of deletion mutants (Konecna et al., 2006).

Additionally, calsyntenin-1 was identified as a binding partner to X11L/Mint2 and amyloid-beta precursor protein (APP) in the yeast two-hybrid screen by a group of Japanese scientists. The immunopercipitation assay resulted in stable tripartite complex consisting of APP, X11L/Mint2 and calsyntenin-1, which is coincident to previous founding. X11L/Mint2 is known as an adaptor protein to APP which stabilizes the full-length APP on the cell membrane by suppressing APP metabolism to a reduced amyloid-beta generation. Calsyntenin-1, sharing the similar binding motif of APP to X11L/Mint2, demonstrated an enhanced stabilization of APP in the in vitro co-expression assays (Araki et al., 2003).

Since the extracellular senile plaques comprised mainly by amyloid-beta represent a critical pathologic feature of neurodegenerative Alzheimer's Disease (AD), APP/ amyloid-beta processing and molecular mechanisms underlying intracellular trafficking of APP become very important to understand AD pathogenesis. The APP/ amyloid-beta metabolism is a strictly regulated process and the disturbance has vital impacts on the amyloid-beta accumulation leading to AD. Based on this knowledge and the possible involvement of calsynenin-1 in APP metabolism, the protein was named differently as Alcadein (Alzheimer-related cadherin-like protein) by the Japanese scientists.

Among all the properties of calsyntenins which have been revealed, the translocation and internalization of putative calcium-binding stump after extracellular cleavage draw our attention to explore their potential roles in calcium buffering or signaling which may be further linked to neuronal excitotoxicity.

2.2 Calcium signaling and Excitotoxicity

2.2.1 Calcium and calcium signaling

As the most ubiquitous and versatile intracellular modulator, free cytosolic calcium ion (Ca^{2+}) impacts nearly entire aspect of cellular physiology by playing vital roles in cell signaling pathways. The common mechanism behind calcium signaling is to convert a variety of external signals that do not cross the plasma membrane into numerous intracellular calcium-sensitive processes by generating temporally and spatially controlled pulses of free cytosolic calcium. For this purpose, cells exploit broad group of pumps, channels, transporters and Ca^{2+} binding proteins to achieve the fine tune of Ca^{2+} signals (Clapham, 2007).

Most of the cellular Ca^{2+} ions are isolated from cytoplasm by intracellular compartments. Endoplasmic reticulum (ER) is generally the predominant intracellular Ca^{2+} store where Ca^{2+} are bound to high capacity-low affinity Ca^{2+} buffering proteins such as calsequestrin and calreticulin. There are many other proteins in the cytoplasm and other organelles such as mitochondria act as Ca^{2+} buffers by transiently binding to Ca^{2+}. The level of free cytosolic Ca^{2+} is normally maintained to resting concentration at a low range of 10-100nM through the combined actions of a number of buffering proteins and Ca^{2+} compartmentalization mechanisms. Cytosolic Ca^{2+} increases to active level of roughly 1000nM as a result of either Ca^{2+} uptake from extracellular environment or the release from intracellular stores through certain calcium channels. The stimuli binding on the receptors turn on the ON mechanism to activate those channels and finally trigger the Ca^{2+} signaling by generating various Ca^{2+} mobilizing signals to feed Ca^{2+} into cytoplasm.

There are many proteins identified as Ca^{2+} entry channels on the plasma membrane for delivering Ca^{2+} from external medium in response to stimuli including membrane depolarization, extracellular agonists or intracellular messengers. Those channels were traditionally classified into three groups according to the ways how they are activated:

voltage-operated channels opening in response of voltage change, receptor-operated channels opening upon binding with external stimuli, and store-operated channels opening in response to depletion of internal Ca^{2+} stores (Berridge et al., 2003).

The release of Ca^{2+} from the intracellular stores is controlled by Ca^{2+} itself or by a group of Ca^{2+} mobilizing messengers, such as inositol-1,4,5-trisphosphate (Ins-1,4,5,-P3), ryanodine (RyR), cyclic ADP ribose (cADPR) and nicotinic acid dinucleotide phosphate (NAADP). The formation of Ins-1,4,5,-P3 is a focal point of major signaling pathways, one is initiated by a family of cell surface receptors, G protein-coupled receptors and the other is triggered by receptors linked with tyrosine kinases (TKs) either directly or indirectly. When activated by stimulus, those receptors are coupled to energy-dependent transducing mechanisms which activate phospholipase C (PLC) enzymes to generate inositol-1,4,5-trisphosphate (Ins-1,4,5,-P3) and diacylglycerol (DAG) by hydrolyzing phosphotidylinositol 4,5-bisphosphate (PIP_2). Ins-1,4,5,-P3 then bind to ER channel inositol-1,4,5-trisphosphate receptor ($InsP_3R$) to enable the releases of stored Ca^{2+} from ER, thus to promote a increase in free cytoplasmic Ca^{2+}concentration. Other Ca^{2+} mobilizing messengers like cyclic ADP ribose (cADPR) and nicotinic acid dinucleotide phosphate (NAADP) generated from nicotinamid-adenine dinucleotide (NAD) modulate Ca^{2+} release from ER through different mechanisms. The Ca^{2+} released to cytoplasm activates a wide range of Ca^{2+} sensors and Ca^{2+}-sensitive processes, thus initiate different cytoplasmic and nuclear actions which finally lead to divergent cellular processes such as membrane excitability, metabolism, vesicle trafficking, gene transcription or cell proliferation and fertilization (Clapham, 1995, , 2007) (Figure 2.4).

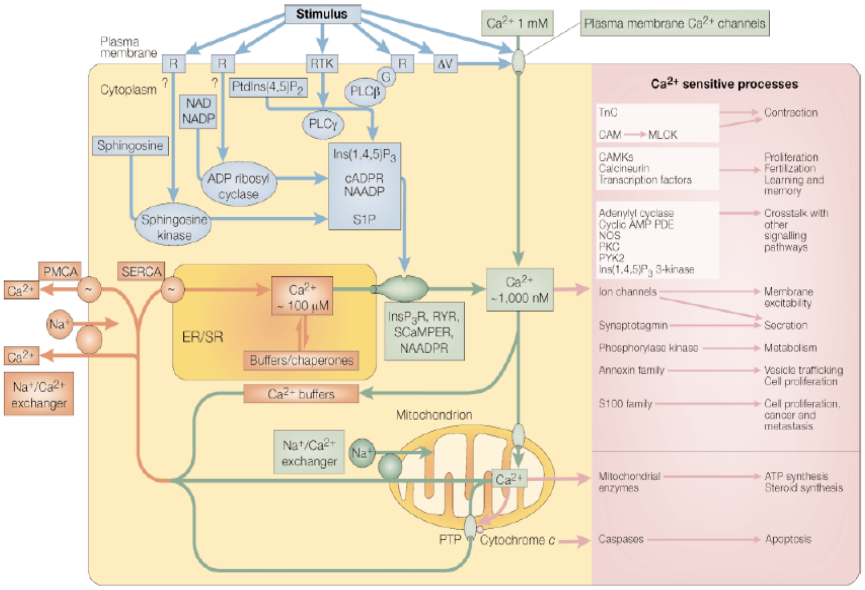

Figure 2.4: Ca^{2+} signaling network (Berridge et al., 2000)

Cells have an extensive signaling toolkit that can be mixed and matched to create Ca2+ signals of widely different properties. **BLUE**: Ca2+-mobilizing signals generated by stimuli acting through a variety of cell-surface receptors(R). **GREEN**: ON mechanisms that respond to transmitters or the Ca2+-mobilizing signals, leading to the Ca2+ influx into cytoplasm. **PURPLE**: Ca2+ sensors activated by ON mechanisms, allowing the activation of a wide range of Ca2+ sensitive processes. **RED**: OFF mechanisms that pump Ca2+ out of cytoplasm.

Upon entering into cytosol, only very small portion of Ca^{2+} end up being free since most of them rapidly bind either to Ca^{2+} buffering proteins such as calretinin, calbindin and parvalbumin, or to Ca^{2+} sensors and effectors such as calmodulin and Ca^{2+}-sensitive enzymes. So far over 200 Ca^{2+}-binding proteins have been identified as Ca^{2+}-buffering proteins or effectors in human genome. The buffering proteins function as the spatial and temporal fine-tunes to Ca^{2+} signaling by chelating and releasing Ca^{2+} in different Ca^{2+} levels to alter the amplitude or duration of individual Ca^{2+} signals. Ca^{2+} buffering proteins such as parvalbuin and calbindin exist in high concentration in neurons that enable the confined and localized Ca^{2+} signaling in synapses. The most common motif shared within the Ca^{2+} binding proteins is the EF hand helix-turn-helix in which seven negatively charged oxygen atoms cage Ca^{2+} tightly. The EF-hand Ca^{2+} binding proteins can be divided into two classes: signaling proteins and buffering proteins. The former one typically undergoes a conformational change upon the Ca^{2+} binding to open a binding site for target proteins, while the latter one is represented by calbindin D9k which does not undergo calcium dependent conformational changes (Burgoyne and Weiss, 2001).

Some of the Ca^{2+} binding proteins such as troponin C and calmodulin (CaM) play vital roles as sensor or adaptor that converts Ca^{2+} signals to protein interaction. The small acidic protein Calmodulin (CaM) ubiquitously expressed in all eukaryotic cells is the most extensively studied Ca^{2+} signaling protein. Since it contains four EF-hand motifs, each calmodulin molecule could bind up to four Ca^{2+}, offering a diversified capacity to Ca^{2+}. Additionally, the post-translational modifications such as phosphorylation, acetylation, methylation and proteolytic cleavage could modulate the calcium binding properties of calmodulin and subsequently further diversify its actions. By undergoing pronounced conformational change upon Ca^{2+} binding, the hydrophobic groups from inner residues are exposed to the surface of calmodulin protein which consequently allows the interaction with the complementary hydrophobic region on different protein targets. Through activating a wide range of targets, Calmodulin (CaM) orchestrates comprehensive cellular responses to cell excitation resulting from the simple elevation of intercellular Ca^{2+} concentration. The calmodulin (CaM) is used as a Ca^{2+} signal transducer in those processes since most of the protein targets that the calmodulin binds to are not able to interact with Ca^{2+} directly. The calmodulin also extends the reach of Ca^{2+} by activating a number of different Ca^{2+}-regulated enzymes and pathways, such as phosphorylation pathways, protein kinase C (PKC), cyclic AMP phospodiesterase, Ca^{2+}-activated proteases (calpains) and Ca^{2+}/calmodulin-dependent protein kinases (CaMK). Those calcium-sensitive effectors finally allow different cellular actions including gene transcription, channel activity, metabolism, proliferation and differentiation (Ivings et al., 2002). In addition to the general modulator like calmodulin, there are many other Ca^{2+} binding proteins engaged in specific functions, such as Ca^{2+} sensor synaptotagmin which is fully specified for exocytosis of membrane vesicles in synapses.

2.2.2 Calcium Homeostasis

Calcium homeostasis refers to the regulation of the concentration of calcium ions in

cytoplasm. The disturbed intracellular calcium homeostasis causes general metabolic dysfunction eventually leading to cell death. Through combined action of pumps and exchangers, Ca^{2+} level is controlled by the “on” reaction that introduce Ca^{2+} into cytoplasm between the “off” reactions that remove the Ca^{2+} signal from cytoplasm. Influx and efflux of cytosolic Ca^{2+} during the ON and OFF reactions should be balanced to avoid the net loss or gain of cytosolic Ca^{2+}. Ca^{2+} could be turned to toxic signals when delivered in wrong level, wrong time and wrong place.

Entry of extracelluar Ca^{2+} is driven by various channels that open either in response to different external signals or in the presence of a large electrochemical gradient across the plasma membrane as described before. NMDA (N-methyl-D-aspartete) receptor which belongs to receptor-operated channel (ROC) induces Ca^{2+} entry in response to glutamate binding. The voltage-operated channels (VOCs) in excitable cells generate the rapid Ca^{2+} influxes inducing fast cellular process such as muscle contraction or exocytosis at synaptic cleft. There also are many other channel types that are sensitive to a diverse array of stimuli, such as cyclic-nucleotide-gated channel and arachidonic-acid-sensitive channel which represent second-messenger-operated channels controlled by internal messengers, and the store-operated channels, thermosensor or stretch-activated channels that belong to the board transient receptor protein (TRP) ion-channel family. Members of TRP channels are particularly important in controlling slow cellular processes such as cell proliferation since they share the common property of slow conductance and therefore operated over longer time scales to drain Ca^{2+} into the cells.

Once Ca^{2+} has carried out its signaling function, it should be rapidly removed from the cytoplasm. Although the plasma-membrane Ca^{2+}-ATPase (PMCA) pump and Na^{+}/ Ca^{2+} exchanger (NCX) are responsible for driving the extrusion of Ca^{2+} from the cells, the maintenance of the cytoplasmic Ca^{2+} homeostasis mainly relies on sequestering Ca^{2+} with intracellular compartments and buffering with specific calcium binding proteins. To maintain Ca^{2+} in the low resting concentration in cytoplasm, Ca^{2+} is actively and constantly translocated into ER and sometimes into mitochondria through the action of sarcoendoplasmic reticular calcium ATPases (SERCA) and mitochondrial uniporter respectively (Berridge et al., 2000).

Ca^{2+} sometimes acts to control Ca^{2+} management within cell as a feedback mechanism such as capacitive Ca^{2+} entry (CCE) which modulates Ca^{2+} influx through store-operated channels (SOCs) activated by depletion of intracellular Ca^{2+} stores. Additionally, passive Ca^{2+} release from ER is dependent on ER lumenal Ca^{2+} level with the evidence that low ER Ca^{2+} concentration greatly reduces the leakage. Ca^{2+} level in ER lumen can even affect the IP3R and SERCA activities during Ca^{2+} translocation (Bano and Nicotera, 2007).

2.2.3 Calcium signaling in Neuron

Basically, neuron shares the same Ca^{2+} signaling mechanism with other different cell types. Through numerous calcium-regulated pathways, Ca^{2+} signals govern most, if not all

of cellular activities in neuron such as neurotransmission, synaptic activity, plasticity, potentiation, growth and gene expression. Since that, neurons must maintain the Ca^{2+} homeostasis in a tightly controlled manner to ensure the efficient signaling. The resting Ca^{2+} concentration is balanced at a low level of approximately 100nM to enable the high signal-to-noise ratio so that small increase in Ca^{2+} concentration is sufficient to trigger physiological actions. Therefore, delicate and complex mechanisms have been evolved in neurons to orchestrate Ca^{2+} influx, Ca^{2+} buffering, Ca^{2+} storage and Ca^{2+} efflux for maintaining cytosolic free Ca^{2+} homeostasis (Arundine and Tymianski, 2003).

The diversity of neuronal cell functions controlled by Ca^{2+} results from distinct types of Ca^{2+} signaling that differ in spatial and temporal aspects. Except for general Ca^{2+} sensor proteins such as calmodulin, a number of other Ca^{2+} binding proteins such as neuronal calcium sensor protein (NCS) family are either exclusively expressed or enriched in the nervous system, where they have distinct roles in regulating neuronal functions. Members of NCS protein family share similar compact globular structure in which four EF-hand motifs are present for Ca^{2+} binding while they show big differences in Ca^{2+} affinity, Ca^{2+} binding dynamics, subcellular localization, targets and expression patterns which contribute vast diversity of the functions of this protein family. These NCS proteins have been implicated in a group of Ca^{2+} signaling related events such as neurotransmitter release, channel and receptor regulation, neuronal growth, survival and gene transcription (Haeseleer et al., 2002; Burgoyne, 2007). Neurons have several Ca^{2+} sensitive pathways located in different regions. In the synaptic ending, membrane depolarization produces a localized pulse of Ca^{2+} that triggers exocytosis, whereas in the cell body and dendrites, the same depolarization can induce Ca^{2+} entry to activate a number of targets such as adenylyl cyclase, mitogen-activated protein kinase (MAPK) and Ca^{2+}/calmodulin-dependent protein kinase (CaMK).

2.2.4 Calcium-dependent excitotoxicity

Nerve cell damage induced by excessive glutamate load was initially described as excitotoxicity by Olney in 1969. Over the years, the mechanism of excitotoxicity is formulated stepwise by intensive and extensive studies. Briefly, excitotoxicity refers the over-activation of postsynaptic excitatory neurotransmitter receptors induced by excessive synaptic release of glutamate or other excitotoxins, which allows the massive influx of calcium ions into the neuron and consequently leads to the disturbed regulation of calcium-dependent enzymes and signaling cascades which eventually cause neuronal cell death (Sattler and Tymianski, 2000).

Excitotoxicity is believed to be major mechanism contributing to neurodegeneration in many central nervous system diseases such as ischemia, stroke, Multiple sclerosis, Alzheimer's disease, Pakinson's disease and Huntington's disease. The failure in the clearance of excessive excitatory transmitter causes sustained gating of receptor-operated channels, leading to prolonged neuronal depolarization and excessive Ca^{2+} load. As the major excitatory neurotransmitter in mammalian, glutamate mediates most of the excitatory neurotransmissions and also plays a vital role as prime excitotoxin

in the excitotoxic neuronal cell death (Bano and Nicotera, 2007).

Glutamate receptors are categorized into two distinct classes of ligand gated ion channels (ionotropic glutamate recepters) and G-protein coupled receptors (metabotropic receptors) based on their prototypic pharmacological agonists. The former could be further subdivided into three groups: AMPA, NMDA and kainite receptors, according to their pharmacology structural similarities; whereas the latter are subdivided into three groups: Group I, Group II and Group III, according to their sequence similarities, pharmacology and intracellular signaling mechanisms. The neurotransmitter glutamate generates Ca^{2+} signals either by activating receptor-operated channels such as NMDA receptor, or by stimulating the metabotropic glutamate receptor mGluR to produce Ins(1,4,5)P3 to mobilize internal Ca^{2+} from the endoplasmic reticulum (ER). Although most of glutamate receptor subtypes involve in mediating excitotoxic neuronal cell death, NMDA receptors play the most critical role because of their high permeability to Ca^{2+}. Due to a voltage-dependent block of the channel pore by magnesium ions, NMDA receptors are inactive at resting membrane potentials. The impulses generated by sustained activation of other receptors such as AMPA receptor could depolarize the postsynaptic membrane to release the channel block of NMDA receptors and thus allowing Ca^{2+} influx into the postsynaptic cells. Under certain conditions like prolonged depolarization, the magnesium block may be completely removed, leading to massive influx of Ca^{2+}. Group I mGluR coupled to PLC through G-protein is also involved in Ca^{2+} signaling since its activation leads to an increase in IP3 production which mediate intracellular Ca^{2+} signaling by inducing Ca^{2+} release from ER to cytoplasm. Group II and group III receptors are negatively coupled to adenylyl cyclase through G protein. When those receptors are over-stimulated, the production of an important Ca^{2+} regulator cAMP will be inhibited, leading to a interrupted Ca^{2+} signaling (Berliocchi et al., 2005).

In pathological condition, excessive Ca^{2+} entry through NMDA receptor and other channels causes the excitotoxic Ca^{2+} overload exceeding the capacity of regulatory mechanism, triggering abnormal activation of Ca^{2+}–sensitive processes. For instance, excessive Ca^{2+} in cytosol could result in protease calpain activation, which leads to general proteolysis of proteins in the cytoskeleton, ion channels, enzymes, cell surface receptors and consequent irreversible cell damage. Other calcium-dependent enzymes such as endonucleases, ATPase and phospholipases are also involved in the process of excitotoxicity when they are over-activated. The transcription factors such as c-Fos, c-Jun and c-Myc are induced, leading to transcriptional activation of certain genes involved in cell death. Additionally, cells overexcited by excess Ca^{2+} accumulate toxic free radicals such as superoxide and nitric oxide participated in unwanted side reactions, resulting in cell damage. For example, the activation of neuronal nitric oxide synthase leads to DNA damage by over-production of nitric oxide and peroxynitrite (Dawson and Dawson, 1998). PARP-1 activation triggers the release of the apoptosis inducing factor (AIF) from mitochondrial membranes, which participates in large-scale DNA fragmentation. (Susin et al., 1999) In turn, the disrupted plasma membrane and ion channels allow the uncontrolled influx of Ca^{2+} into the cell, which ultimately leads to an irreversible buildup of

the intracellular Ca^{2+} concentration. All these mechanisms lead to cell death through necrosis or apoptosis (Arundine and Tymianski, 2003)(Figure 2.5).

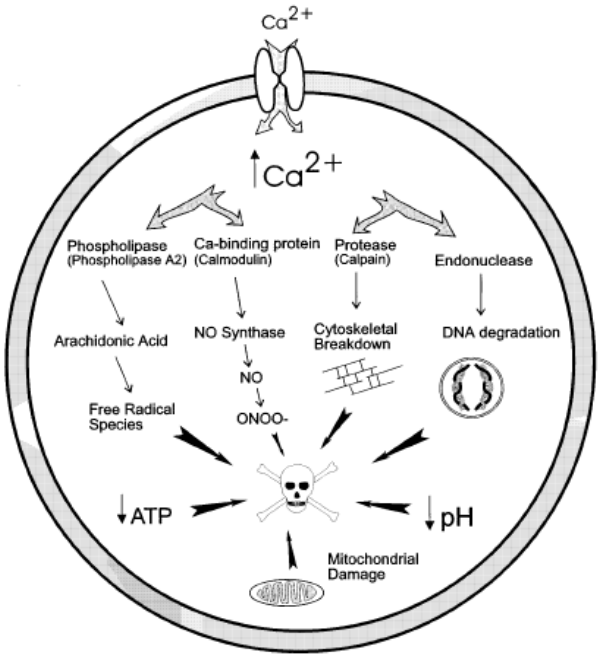

Figure 2.5: proposed mechanisms of Ca^{2+}-dependent excitotoxicity (Sattler and Tymianski, 2000)

This is a schematic and descriptive presentation of proposed mechanisms by which intracellular Ca2+ elevation may trigger secondary Ca2+ dependent phenomena, which result in neurotoxicity. NO: Nitric oxide; ONOO: peroxynitrite; ATP: adenosine triphosphate; ADP: adenosine diphosphate; DNA: desoxyribonucleic acid.

Mitochondria are usually described as "power plants" because they generate most of the cell's supply of adenosine triphosphate (ATP) as a source of chemical energy. But in pathological condition, mitochondria are thought to be the target organelles of Ca^{2+} dependent excitotoxic processes. It has been known for long time that the mitochondria are capable of accumulating Ca^{2+} but its importance as intracellular Ca^{2+} store was considered as minimal since mitochondrial Ca^{2+} uptake mechanism is not related to physiological increases in cytosolic Ca^{2+}. Mitochondria Ca^{2+} is regulated by fundamentally distinct mechanisms that differ from those used in ER. Primarily, mitochondria take up Ca^{2+} rapidly through the mitochondrial uniporter driven by membrane potential. Mitochondrial Ca^{2+} is balanced by Ca^{2+} extrusion through mitochondrial Na^{+}/ Ca^{2+} exchanger in cardiomyocytes and neurons, and through H^{+}/Ca^{2+} exchanger in hepatocytes (Montero et al., 2001). Another mechanism involved in Ca^{2+} efflux is the formation and opening of mitochondrial permeability transient pore (mPTP) when factors such as mitochondrial membrane depolarization or oxidized NAD/NADP and superoxide anions were accumulated. The prolonged opening of mPTP triggers a rapid excessive release of Ca^{2+} and mitochondrial metabolites including apoptotic factors such as cytochrome C. The excessive cytosolic Ca^{2+} accumulation results in subsequent abnormal increase of Ca^{2+} in mitochondria lumen, demonstrating a synchrony between

$[Ca^{2+}]i$ and $[Ca^{2+}]mt$ oscillations (Hajnoczky et al., 1995) (Won et al., 2002).

The mitochondria become the focal point of Ca^{2+} dependent excitotoxic processes since the dysfunction of mitochondrial Ca^{2+} regulation causes Ca^{2+} accumulation in mitochondria and subsequently disturb ATP synthesis due to the collapse of mitochondrial electron transportation and oxidative phosphorylation. The activation of many key mitochondrial enzymes involved in ATP production, such as puruvate dehydrogenase and NAD-isocitrate dehydrogenase, are related to Ca^{2+} concentration. The ATP production could be stopped unexpectedly when the Ca^{2+} regulation goes wrong in mitochondria. (McCormack et al., 1990) ATP is the main energy source for the majority of cellular functions. In glutamate excitotoxicity, the inadequate ATP first eliminates electrochemical gradients of certain ions required for removing glutamate from the extracellular space. Additionally, ATP-dependent ion transporters fail, leading to cell depolarization and allowing Ca^{2+} to flow into the cell. Cell membranes are disrupted by activated phospolipases, allowing more ions and toxic chemicals flow into the cell. Ion pumps fail to transport Ca^{2+} out of the cell, amplifying the accumulation of Ca^{2+} which triggers the release of excitatory amino acid neurotransmitter glutamate. This results in a buildup of glutamate and further damaging activation of glutamate receptors on the postsynaptic membrane. The glutamate stimulates both Ca^{2+}-permeable AMPA receptors and NMDA receptors to allow more Ca^{2+} influx into cytoplasm. During the excessive Ca^{2+} entry, mitochondria metabolism has been damaged, causing increased reactive oxygen species (ROS) production and the initiation of caspase-dependent apoptosis cascade. Finally, mitochondria are swelling and even broken down to release proteins that can lead to cell death into cytoplasm (Arundine and Tymianski, 2003).

2.3 RNA interference (RNAi)

RNA interference (RNAi) is evolutionarily mechanism that hinders specific gene expression by causing homology-dependent RNA degradation, which represents a protective mechanism to combat the invasion from virus and genetic parasites.

The phenomenon was first observed in plant petunias in 1990 by Rich Jorgensen and his colleagues when they attempted to overexpress pigment-producing chalcone synthase (CHS) in petunia petals by introducing chimeric petunia CHS gene into the plant. Surprisingly, instead of expected dark violet color, most of the flowers appeared unpigmented white or variegated. RNase protection analysis showed that the mRNA level of both introduced and endogenouse CHS genes were reduced drastically. They termed this bizarre phenomenon as “co-suppression” of homologous genes, but the mechanism behind remained unclear (Napoli et al., 1990).

Soon after, similar observation was noted in a wide range of organisms. In filamentous fungi Neurospora crassa, introduction of exogenous sequences derived from

carotenogenic albino-3 (al-3) and albino-1 (al-1) genes provoked a severe impairment in the expression of the endogenous al-1 or al-3 genes, leading to an wild-type or intermediate phenotype, which is termed as “quelling” (Romano and Macino, 1992). In Drosophila, rather than the expected gene dosage effect, the expression of Alcohol dehydrogenase (Adh) gene is progressively reduced both in larvae and adults by the introduction of promoter-Adh fusion gene, which is strongly analogous to "co-suppression" phenomena described in plant species (Pal-Bhadra et al., 1997).

For a long time, the “co-suppression” and the “quelling” were considered as a simple antisense-mediated silencing mechanism depending on hybridization between homologous RNA transcripts since many evidences indicated that the suppression occurred post-transcriptionally (J.M. Kooter et al. 1994). Based on this hypothesis, in 1995, Guo and Kamphues first make attempt to use the artificial RNA fragment to shutdown gene expression in nematode worm Caenorhabditis elegans. They demonstrated a successful blocking of par-1 gene expression with the RNA fragments complementary to par-1 mRNA. But, surprisingly, they found that the sense RNA fragment could also provoke target gene silencing, challenging the proposed antisense-mediated silencing mechanism since the sense RNA can not pair with the mRNA to block the translation (Guo and Kemphues, 1995).

The phenomenon remains mysterious until the study of the similarity between natural viral-induced and transgene-induced gene silencing in plants reveals that viral defense and RNA-induced posttranscriptional gene silencing (PTGS) may share a common innate biological mechanism, suggesting the homology-dependent gene silencing may represent an evolved RNA-mediated antiviral response mechanism in the organisms (Frank Ratcliff, et al. 1997). In 1998, Andrew Fire reported that double-stranded RNA (dsRNA) was substantially more effective at triggering potent and specific gene silencing than either strand does individually in Caenorhabditis elegans. A few molecules of the dsRNA could achieve pronounced decrease or elimination of endogenous gene expression in affected cell, while extensively purified antisense and sense RNAs had only marginal interference activity even injected in high dose. Additionally, they found that the silencing effect of dsRNA could be passed through germ line cells to progeny for several generations (Fire et al., 1998). Those features further argue against the previous hypothesis that the interference relies on stochiometric binding between introduced RNA and endogenous mRNA.

Fire and his colleagues termed the phenomenon as RNA interference (RNAi) to differ it from the passive antisense RNA silencing. They proposed that exogenous dsRNAs act as initiators in RNAi process, activating unknown cellular mechanisms of signal amplification and sequence-specific RNA degradation when they were introduced into cell. This explanation adds on an entirely new understanding of gene regulation and offers possibility to develop a potent approach for achieving loss-of-function to determine the role of gene by depleting specific mRNA with synthetic dsRNAs. Since that, RNAi became one of the most exciting biological discoveries, calling on extensively studies for

mechanistic base behind it.

RNAi has since been discovered in most eukaryotic organisms. In addition to its biological roles in protecting the genome against RNA invasion and instability caused by transposons (Ketting et al., 1999), RNAi was proved involved in developmental gene regulation and genome maintenance since the disruption of genes required for RNAi causes several developmental defects (Bernstein et al., 2001a). A group of 21-23 nucleotide RNA molecules encoded in genomes were identified as microRNAs (miRNAs) from eukaryotic cells emerging as important endogenous RNAi modulators in cellular pathways such as growth and proliferation, apoptosis, and developmental timing (Ruvkun, G. 2001).

Artificial dsRNA has long been used for eliminate specific gene expression in many organisms. Following the observation of synthetic short RNA mediated the sequence-specific mRNA degradation in mammalian cells in 2001, small interfering RNA(siRNA) was immediately developed as a potential therapeutic strategy for silencing disease-related genes (Elbashir et al., 2001). Since Fire and Mello first clearly elucidated the silencing trigger and established the fundamental understanding to RNAi mechanism, they were eventually awarded Nobel Prize in Physiololgy or Medicine in 2006 for the great discovery of RNAi.

2.3.1 Mechanism of RNAi in post-transcriptional gene silencing

Some components required in the RNAi network were first identified by genetic screening in some C. elegans mutants which resistant to dsRNA-mediated RNA interference (Tabara et al., 1999). The protein encoded by one of RNAi-resistant genes shares homology to RNase D, supporting the idea that RNAi is dsRNA-directed enzymatic RNA degradation (Ketting et al., 1999). Soon after, when the RNAi was examined in the in vitro system derived from Drosophila S2 cells, it was discovered that the introduced dsRNAs were processed to segments in 21-23 nucleotides in length during the RNAi reaction. Cleavage of target mRNA occurs at homologous sites sharing same 21-23 nucleotides cleavage interval observed for the dsRNA trigger itself, suggesting that the 21-23 nucleotide fragments cleaved from the dsRNA are guiding mRNA cleavage (Zamore et al., 2000). Chemically synthesized 21nt RNA fragments targeting firefly luciferase gene show efficient target mRNA cleavage in the Drosophila in vitro system, leading to the conclusion that 21-23 nucleotides small interfering RNA (siRNA) is indeed the mediator of sequence-specific mRNA degradation (Elbashir et al., 2001).

In 2001, the enzyme responsible for producing siRNA was identified as Dicer, an evolutionary conserved member of RNase III family of nucleases that specifically cleave dsRNA. It also revealed that the cleavage of target mRNA was conducted independently by RNA-induced silencing complex (RISC) in which the Argonaute proteins may play the role in mRNA slicing. Thus, the RNAi pathway was divided conceptually into initiation

phase in which the dsRNA trigger was converted into siRNA, and effectors phase in which mature RISC mediated cleavage of target mRNA (Bernstein et al., 2001b).

Piece by piece, the puzzle of RNAi mechanism was assembled rapidly. The current model of RNAi implies that the RNAi pathways are initiated by the enzyme Dicer, which processes exogenous dsRNA or endogenous pre-miRNA into 21-23 nucleotides siRNA and miRNA respectively. One of strands from siRNA or the unwinding miRNA paired with complementary sequences of target mRNA and incorporated into RISC. The catalytic components of RISC complex finally conducted the mRNA degradation, leading to the post-transcriptional gene silencing (Figure 2.6).

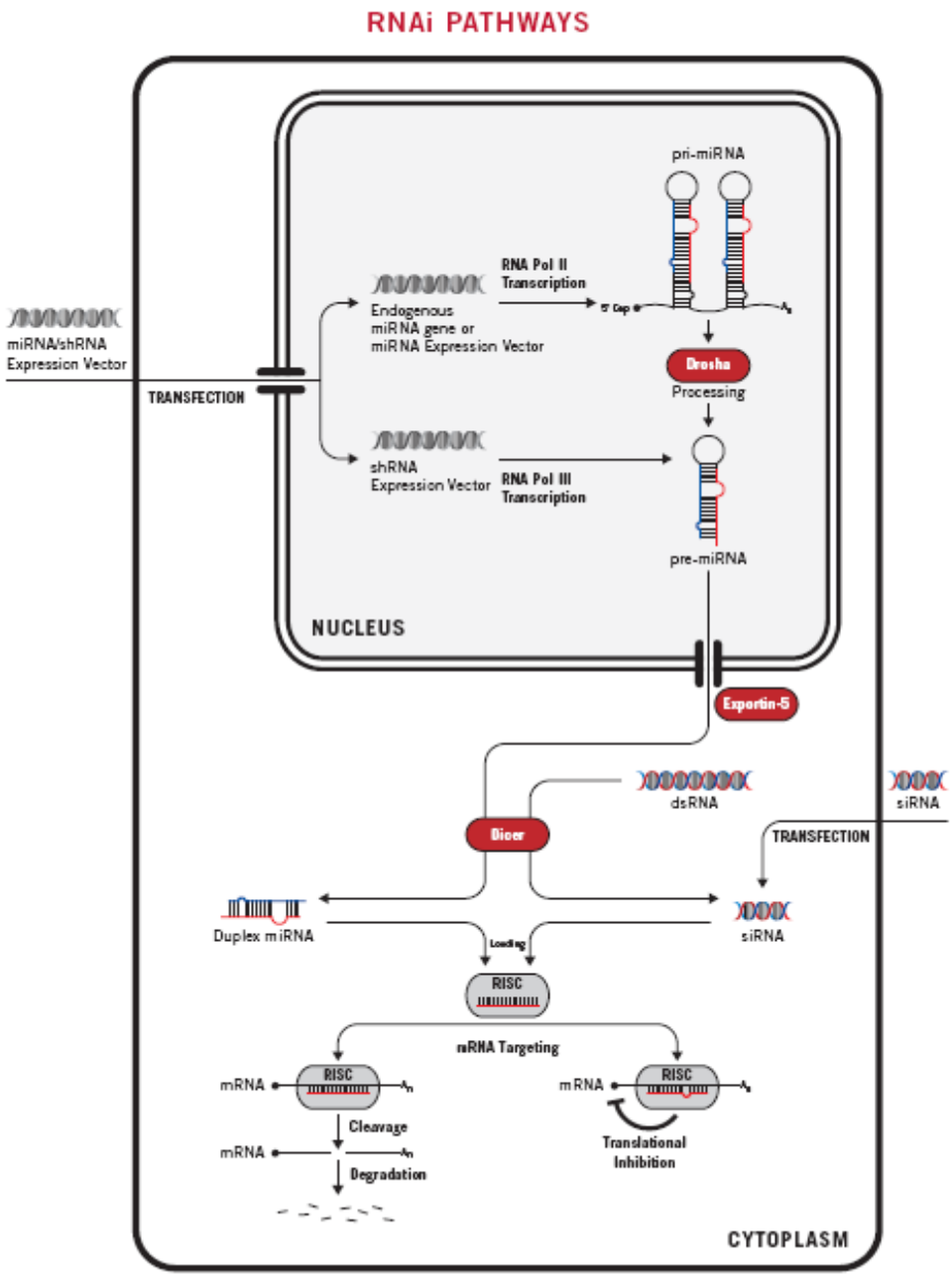

Figure 2.6: Outline of RNAi Mechanism in mammalian cell (From www.mirusbio.com)

The RNAi pathways are initiated by the enzyme Dicer, which processes exogenous dsRNA or endogenous pre-miRNA into 21-23 nucleotides siRNA and miRNA respectively. One of strands from siRNA or the unwinding miRNA paired with complementary sequences of target mRNA and incorporated into RISC. The catalytic components of RISC complex conducted the mRNA degradation, leading to the post-transcriptional gene silencing.

2.3.1.1 Initiation phase: processing of RNA triggers

It is clearly known that dsRNA plays a very important role in RNAi pathway not only as silencing trigger but also as an intermediate. Silencing triggers in the form of dsRNA may be presented in the cells as synthetic RNA, RNA viruses or transcripts copied from aberrant mRNA from nuclear genes by RNA-dependent RNA polymerase (RdRP or RDEs). Upon entering into cytoplasm, those dsRNA triggers were recognized and processed to discrete sizes of ~25 nucleotides by Dicer, a ~200 kDa highly conserved RNase III family containing two catalytic RNase III domains, Piwi Argonaute Zwille (PAZ) motifs and RNA helicase. Biochemical analysis revealed that the Dicer functions as dimeric complex in which two enzymes aligned in antiparallel manner, giving rise to unique structure with two active compound catalytic centers consisting of RNase III domains from both monomers. When recognized and captured by PAZ motifs of the Dicer, dsRNA substances were then successively cleaved in certain interval by the dual catalytic domains, producing precisely sized siRNA fragments. (Hannon, 2002) The cutting interval is determined by the spacing of the two catalytic centres within the Dicer. That characteristic feature of Dicer offers a good explanation to the species-specific variation in siRNA length (Figure 2.7).

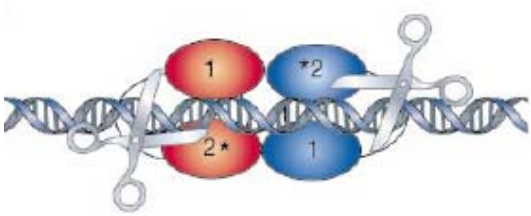

Figure 2.7: Diagrammatic representation of Dicer binding and cleaving dsRNA (Hannon, 2002)

Two separate Dicer molecules are colored differently. Deviations from the consensus RNase III active sites in the second RNase III domain inactivate the central catalytic sites, resulting in target mRNA cleavage at 22-nucleotide intervals.

Primary miRNA (pri-miRNA) transcripts containing imperfect stem-loop pairing structure are first processed by Drosha within nucleus. The resulting precursor miRNA (pre-miRNA) are then exported into cytoplasm to enter RNAi pathway. In Drosophila, miRNA and siRNA are produced by distinct Dicers, whereas in vertebrates both miRNA and siRNA are produced by the only one Dicer.

2.3.1.2 Effector phase: RISC assembly and mRNA degradation

The resulting siRNA duplexes from the Dicer cleavage shared a common configuration of phosphorylated 5' termini and 3' overhang with two nucleotides, which

have been proven functionally important for incorporation to nuclease to form RNA-induced silencing complex (RISC).

Although the mechanism of mRNA cleavage is not fully revealed, the responsible RNase has been identified to be distinct from Dicer. To find out the “slicer”, RISC was isolated through co-immunopercipation with biotin-conjugated siRNA for further evaluation .The biochemical studies elucidate that the RISC is a multiprotein complex of 500kDa, mainly containing siRNA and Argonaute family proteins which have been implicated in RNAi pathways in screens of RNAi-deficient mutants. Family members of Argonaute share two characteristic domains: PAZ which was also found in Dicer, and PIWI (P-element induced wimpy testis) which is unique to this protein family. The Argonaute family can be divided into Ago subclass and Piwi subclass according to their functions and distributions. Ago proteins are ubiquitously expressed whereas Piwi proteins are restricted to germ line cells. X-ray crystallography reveals that the PIWI domain within Ago protein isolated from archaeal shares remarkable similarity to the RNase H enzymes on the secondary structure, indicating its potential role as mRNA slicer in RISC (Song et al., 2004). Further biochemical conducted with the immunopercipitated Ago complexes from human 293T cells show that one of Ago (Ago2) indeed performs endonucleolytic cleavage on mRNA in RNAi pathway (Liu et al., 2004).

In mammalian cells, the core component of RISC loading complex (RLC) consisting of Dicer (Dcr-2) and R2D2 heterodimer binds to the 2-nucleotide overhangs of siRNA 3’ end. Then the key RISC component Ago2 displaces Dcr-2/R2D2 heterodimer in ATP-dependent manner to form mature RISC. Ago2 is also responsible for unwinding of the siRNA duplex, which removes the passenger strand and incorporates the remained guide strands into RISC. Active RISC containing only guide strand performs mRNA cleavage by the endonuleolytic PIWI domain of Ago protein. It is believed that the PIWI motif of Ago recognizes and anchors the 5’ phosphorylated end of siRNA guide strand, while the PAZ domain offers a binding pocket to characteristic 3’ end of siRNA, allowing the rest of guide siRNA to pair to complementary site of target mRNA which were also incorporated by PIWI domain (Matranga et al., 2005; Rand et al., 2005) (Figure 2.8).

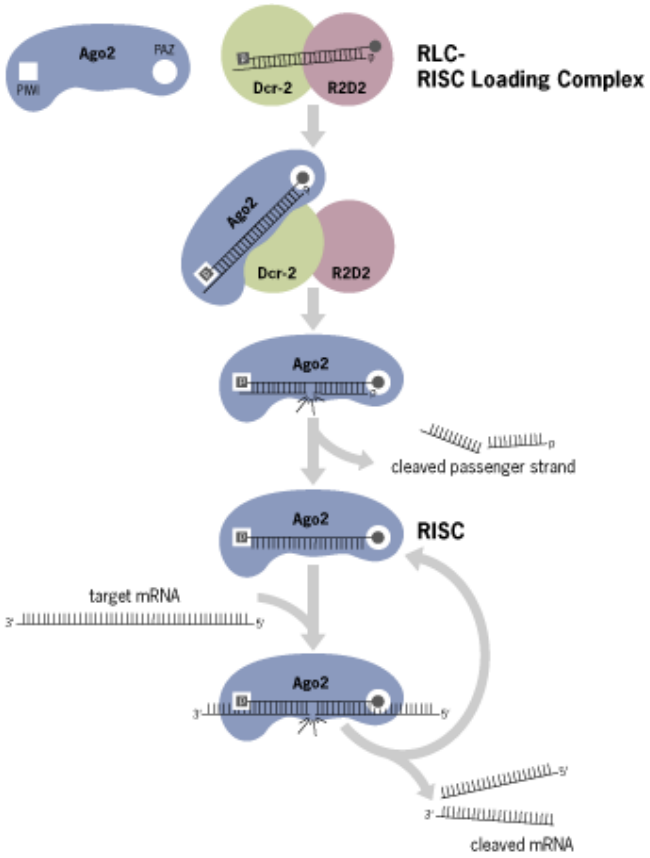

Figure 2.8: RISC Assemble and mRNA Cleavage (Ambion)

This is a general summary of current thinking about assembly of siRNA with RISC and mRNA cleavage activity. Only core components of the RISC loading complex (RLC) and RISC are depicted. RLC contains a Dcr-2/R2D2 heterodimer which binds the siRNA containing dinucleotide 3' overhangs. Core RISC component Ago2 displaces Dcr-2/R2D2. Duplex siRNA transfers to Ago2 by either concurrent or immediate Ago2-mediated cleavage of the passenger strand. ATP hydrolysis is required for RISC maturation to accelerate release of the cleaved passenger strands as it does for cleaved mRNA. Mature RISC includes only the guide strand of the siRNA, and can cleave multiple mRNA targets.

The recent study indicates that the thermodynamic property of each strand in mature siRNA duplex determines the selection of guide strand for RISC assembly. It seems likely the strands with less thermodynamic stability were preferred by RISC (Khvorova et al., 2003).

The details of catalytic reaction remain unclear, but it is known that the PIWI domain of Ago protein performs the cleavage of target mRNA at the site nucleotides 10 and 11 from 5' end of the guide strand of siRNA. The base paired siRNA-target mRNA duplex may contact with the conserved triad (Asp-Asp-His) in PIWI domain of Ago to form active catalytic centre, allowing the mRNA cleavage. The mismatches between siRNA and mRNA may sabotage the formation of the catalytic centre, leading to impaired mRNA degradation (Figure 2.4).

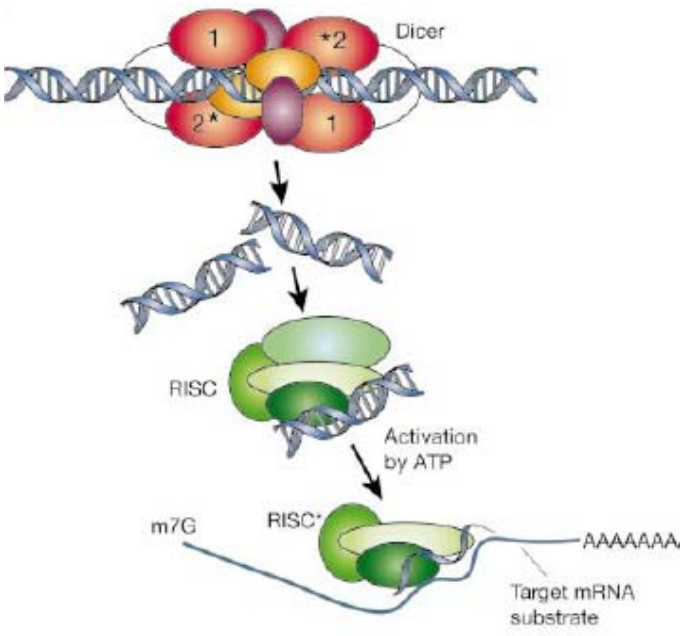

Figure 2.9: RNAi pathway (Hannon, 2002)

RNAi is initiated by the dimeric Dicer enzymes, which processes double stranded RNA into ~22 nucleotide small interfering RNAs. Cleavage into precisely sized fragments is determined by the fact that one of the active sites in each Dicer protein is defective (indicated by asterisk), shifting the periodicity of cleavage from 9-11 nucleotides to ~22 nucleotides in different speices. The siRNA are incorporated into a multicomponent nuclease RISC which activated by unwiding of siRNAs. The active RISC (indicated by asterisk) then uses the unwound siRNA as a guide for substrate selection.

Because of the remarkable potency of RNAi, an amplification step and spreading mechanism within the RNAi pathway were proposed. Multiple turnover effect of RISC induced RNA degradation mainly contributed to the amplification of the original RNAi signal: the cleaved mRNA targets offer new triggers to induce repeated cleavage cycle. Delivery of dsRNA or siRNA through plasmadesmata (cytoplasmic bridge) provides a possible explanation to the spreading of RNAi signal from cell to cell in a short range. The gene required for systemic silencing in *C.elegans* was identified, encoding transmembrane protein that may act as channel for silencing signal propagating.

2.3.2 Biological roles of RNAi

RNAi in plants is critical for the defending response to foreign genetic materials such as viruses or the protection against the self-propagation by transposons. It has been recognized as an adaptive immune system to the plant since the specific RNA-induced elimination of the foreign genetic materials could spread throughout entire organism from original encounter region. In some invertebrates such as Drosophila and *C. elegans*, RNAi is also involved in antiviral innate immunity to protect themselves from the invasion of pathogens. The virus-derived siRNA (viRNA) produced from viral genome induces the

specific silencing of virus gene through viRNA-guided effectors complexes. However, RNAi-mediated immunity in mammalian cells is poorly substantiated.

The major role of RNAi appears to be in gene regulation. A group of short RNA named microRNAs (miRNAs) was identified as critical gene regulators in various plants and animals. miRNAs are produced by Dicer through processing of primary microRNA (pri-miRNA) transcripts from non -coding regions in the genome. The endogenously expressed hairpin-like miRNAs are partially complementary to either UTR or coding sequences of mRNA molecules from one or more genes, inducing translational repression or mRNA degradation through the binding of miRNA to the mRNA. The translation machinery could be blocked by miRNA-mRNA complex while the mRNA degradation is conducted through a process similar to dsRNA-induced RNAi which is triggered by the formation of dsRNA between miRNA and target mRNA. Gene silencing mediated by miRNA is believed essential for wide variety of cellular functions including developmental processes, proliferation, differentiation and apoptosis. miRNA in plant was shown important to regulate almost entire gene network during development by direct modulating the expression of the key transcription factors. (Jackson and Standart, 2007)

Initially, RNAi was observed as a dsRNA-induced silencing at the post-transcriptional level by triggering the depletion of target mRNA without any effect on the rate of transcription. But accumulating evidence indicated that RNAi machinery affects gene functions at the level of genomic DNA through additional mechanisms including genomic methylation, chromatin remodeling, DNA elimination and even protein synthesis. RNA-induced DNA methylation (RdDM) is the first genomic modification discovered in RNAi world. In plants, dsRNA fragments that share sequence homology to the promoter region of the gene could trigger the promoter methylation, eventually leading to a transcriptional gene silencing (TGS) (Mette et al., 1999). Heterochromatin composed of degenerate retrotransposon sequences and tandem arrays of simple repeat unit has been long recognized as genetically inactive component in nuclei. Recently, the heterochromatic gene silencing and heterochromatin assembly was linked to RNAi in fission yeast (Noma et al., 2004). The dsRNA generated from tandem repeats and multiple copies of transposable elements in heterochromatin guided the histone methyltransferases to the homologous sites in chromatin to maintain the silenced state by modifying the heterochromatic proteins. The methylation of those proteins related to chromatin assembly facilitates the repression of transcription (Holmquist and Ashley, 2006).

RNAi has recently been implicated in DNA elimination in which the RNAi-mediated heterochromatin modification go further to discard the silenced chromatin, resulting in restructured genome. It is also believed that the RNAi pathway crosstalks with RNA editing which contribute to the diversity of gene products by altering the RNA sequences through post-transcriptional processing machinery. A-I RNA editing in which the adenosine residues were converted to inosine residues is most prevalent type in higher eukaryotes. The RNAi pathway may share the common dsRNA substrates with the A-I RNA-editing machinery, indicating A-I RNA-editing may be involved in RNAi-induced gene silencing of the genes (Nishikura, 2006).

2.3.3 RNAi application

RNAi has been applied in many organisms as a reverse genetic tool to characterize loss-of-function phenotypes. Increased understanding of mechanism and biological function of RNAi over last ten years leads to quick and significant improvements to the design algorithms of the artificial interfering RNA used in different systems.

Synthetic double-stranded RNA (dsRNA) has been used as a high-throughput approach in plants and invertebrates to achieve selective and efficient suppression of gene of interest (Schmid et al., 2002). But the application is precluded in mammalians since the introduction of long dsRNA over 30 nucleotides provokes general gene shutdown in most mammalian cell types. This nonspecific suppression caused by the exogenous dsRNA has been attributed to the antiviral interferon response which involves dsRNA-activated protein kinase pathway and dsRNA-dependent RNase activation, leading to general repression of translation and nonspecific RNA degradation (Billy et al., 2001). This problem has been resolved promptly by using synthetic short hairpin RNAs (shRNA) instead of long dsRNA (Paddison et al., 2002; Paul et al., 2002; Sui et al., 2002). The artificial shRNA successfully mimics innate small interfering RNA (siRNA) produced from the cleavage of dsRNA initiator, inducing transient sequence-specific gene silencing in mammalians. Accordingly, a system using DNA constructs for shRNA expression were soon developed to achieve RNAi mediated gene knockdown in a stable and long-term manner in both cultured cells and living organisms.

The effectiveness of siRNAs depends mainly on the sequence specificity, as single base pair mismatches between siRNA and target mRNA could drastically reduce the potency of silencing. But not all siRNAs with strict sequence specificity are effective. siRNAs targeting different sites on the same target mRNA show striking difference in silencing efficiency. This phenomenon could be explained by positional effect of the different accessibility of siRNAs to their target sites along the mRNA (Holen et al., 2002). Furthermore, gene silencing induced by siRNA could never be a gene knockout-----the most powerful siRNA results in reduction of target mRNA for at most 90% off.

2.3.3.1 Vector-based siRNA for gene silencing

For a long time, dsRNA and siRNA for gene silencing were synthesized chemically or produced by in vitro transcription. The delivery of dsRNA and siRNA into cells and organisms mainly rely on transfection and injection. The silencing effect could last for only a few days and does not appear to pass to the daughter cells.

Vector-based siRNA systems have been engineered to continually express shRNA, which could be processed in vivo into siRNA and then cooperate into RNAi pathway for gene specific silencing. This system has advantages in silencing longevity, delivery options and economy over synthetic siRNA strategy. It also makes the conditional and

inducible gene silencing possible by simply introducing corresponding control elements into the vector system. Reportedly, the silencing effect of RNAi mediated by lentiviral vector could persistent for several months in mouse brain (Makinen et al., 2006).

The initial designs of vector-based siRNA follow the same principle: The sequence encoding siRNA with 19-29 bases of homology to the target gene separated by a short spacer from its reverse complement part is synthesized as a double-stranded DNA oligonucleotide. The resulting insert was cloned into vector between a RNA polymerase III promoter and a 5-thymidine-in-a-row terminator (Figure 2.10). The RNA fragment produced by the promoters has defined start and naturally lack polyA tail. This transcript could fold back on itself to form a stem-loop structure with 3'-UU overhang which could be further processed into siRNA-like molecules, initiating the RNAi pathway.

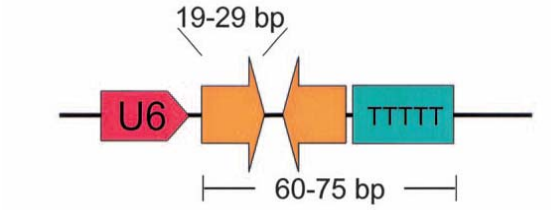

Figure 2.10 Schematic of vector-based siRNA expressing cassette (Paddison et al., 2002)

The sequence encoding siRNA with 19-29 bases of homology to the target gene separated by a short spacer from its reverse complement part is synthesized and annealled as a double-stranded DNA oligonucleotide. The resulting insert was cloned into vector between a RNA polymerase III promoter and a 5-thymidine-in-a-row terminator, which served as template for the siRNA transcription.

Promoters for siRNA transcription: Class III of RNase polymerase III (pol III) promoters H1 and U6 are most commonly used for siRNA transcription in vector-based siRNA system since they could produce small RNA transcripts lacking polyA tail that highly resemble to the active natural siRNA. The Pol III promoter transcribes 5s rRNA, tRNA and other small RNAs falling in the category of housekeeping genes required in all cell types. The transcription from Pol III is characterized with a well defined start and a termination signal consisting of a 5-thymidine stretch. Most importantly, the transcription does not rely on the sequences downstream of transcriptional start site, allowing the replacement of the original RNA gene with siRNA coding sequence. The transcriptional efficiency could be maintained in a high level to produce siRNA effectively both in vitro and in vivo. (Hannon et al., 1991) Moreover, those highly compected Pol III promoters with only a few cis-acting elements flanking through upstream of the start point for only 100-300 base pairs make them more acceptable to the space-limited viral vectors (Geiduschek and Kassavetis, 2001) (Myslinski et al., 2001).

In 2002, Sui and his colleague first demonstrated that siRNA expressed from mouse U6 RNA promoter in the vector can achieve robust and specific inhibition of endogenous target gene expression in multiple mammalian cell lines (Sui et al., 2002). Spontaneously,

another group developed a vector system based on human H1 RNA promoter for stable expressing siRNA to mediate persistent suppression of target gene in different mammalian cells (Brummelkamp et al., 2002).

Many constructs make use of RNA polymerase II promoters to drive the expression of long hairpin-like RNA which can be modified by Dicer into siRNAs to achieve gene downregulation. But the RNA fragment longer than 30nt transcribed from Pol II promoters will induce interferon response in mammalian cells, resulting in unspecific effect. The RNA polymerase II promoters need be converted to use small DNA template to synthesize hairpin-like siRNA fragments with the structural features close to active siRNAs. For instance, the modified cytomegalovirus (CMV) promoter has been adopted to drive siRNA transcription in the vector-based siRNA system to diminish expression of both exogenous and endogenous genes in vitro and in vivo (Xia et al., 2002).

Some elements could be introduced into the vector to add conditional, enhanced or inducible features to the gene silencing by vector-based siRNA. When an enhancer from CMV promoter was placed nearby to U6 promoter, the siRNA synthesis was increased and consequentially the silencing of the target gene was strengthen (Xia et al., 2003). Cre-loxP recombination system was used to provide spatial, temporal, cell-type specific or tissue-specific control over U6 promoter-driven siRNA expression (Kasim et al., 2004). Tetracycline-responsive repressor achieves conditional regulation to siRNA transcription (Matsukura et al., 2003) (Matthess et al., 2005).

Rational siRNA design for efficient RNAi: On the basis of the result from a systemic analysis of many siRNAs previously used for efficient knockdown, several groups have proposed a set of characteristics related to the function and efficiency of siRNA, including low GC content, a bias to low internal stability at the sense strand 3-terminus, lack of inverted repeats and sense strand base preference (Reynolds et al., 2004) (McIntyre and Fanning, 2006) (Taxman et al., 2006). The siRNA design incorporating those criteria significantly improves siRNA potency.

Design and construction of siRNA begins with the selection of target sites along the target mRNA. Since some regions of mRNA may be either highly structured or bound by regulatory proteins, the siRNA target sites has to be selected 50-100 downstream from the start codon of mRNA. 5’ and 3’ untranslated regions (UTRs) as well as exon-exon boundaries within the target mRNA must be excluded from the selection. Multiple target sites are necessary for one gene because siRNAs targeting different sites exhibit striking difference in silencing potency (Holen et al., 2002). Usually 3-4 siRNA vectors targeting different sites should be constructed for primary screening in vitro to single out the most efficient ones for further application.

The length of nucleotide sequence used as the stem of siRNA expression cassette ranges from 19 to 29nt, but the hairpin siRNAs with these various stem lengths all function well in gene silencing. siRNA with 2-4 Thymidine 3’ overhangs shows empirically most

efficient in knocking down target gene as the overhangs may play a role in protecting siRNA from exonuclease digestion. The addition of those unpaired overhangs to the siRNA duplexes does not show any obvious impairment in silencing effect and specificity (Miyagishi and Taira, 2002) (Harborth et al., 2003). Low G/C content (30-45%) in selected sequence is preferable for higher efficiency. The possible explanation is that the easier unwinding of hairpin structure with low G/C transcripts could facilitate processing the small hairpin RNA into active siRNA. U6 promoter requires an obligatory G (Guanosine) in the start point for initiating the transcription, whereas H1 promoter is highly permissive. Therefore the sequence starting with a G followed by 20 bases should be selected to obtain a total 21nt nucleotides sequence for constructing the U6 promoter-driven siRNA vector. Cluster of T residues should be strictly avoid when select the target sequence since the four or more T residues-stretch represents the termination signal to the Pol III promoters, leading to unexpected disturbance of siRNA production. To ensure the specificity of the RNAi, the BLAST research of the selected target sequences should be carried out within the corresponding genome database to exclude any homology to genes other than the target one.

siRNA achieves gene silencing in sequence-dependent manner. A single mismatch between the sequence of siRNA and the target sequence would drastically sabotage the inhibition of gene expression. But the insertion of mutations/bulges in the sense strand of hairpin-type siRNA is tolerable for the effective siRNA. As many as 7 mutations from C to T could be introduced in the sense strand to resolve the technical problem to sequence through hairpin region of siRNA construct, while gene silencing activity was fully retained (Miyagishi et al., 2004). To increase the thermal stability for high efficiency of RNAi, siRNA duplexes could be chemically modified by introducing phosphoiester or phosphorthioate linkages into the hairpin structure (Braasch et al., 2003).

Loop sequence and length are also critical to siRNA potency. siRNA transcripts produced in the nucleus from Pol III promoters remain inactive until they were efficiently processed to active form in cytoplasm. Loop motifs derived from natural microRNA were found helpful to improve the transportation of the siRNA transcripts from nucleus to cytoplasm and subsequentially promote the siRNA activation and gene knockdown efficiency (Chang et al., 2006) (Plasterk, 2006).

Appropriate control is necessary to validate the data obtained from the experiments. A siRNA with same nucleotide composition as the experimental siRNA but lacks sequence homology to the genome could be the best negative control.

Although vector-based siRNA has been proven a powerful tool to inhibit gene expression for better understanding of gene functions in many different cell lines and organisms, there are still limitations to this technology. First at all, the knockdown of the gene is transient even the vector-based system is relatively more resistant to RNA degradation than synthetic siRNA fragments. In the actively dividing cells, the silencing siRNA molecules transcribed from the vector were rapidly diluted to below the crucial

threshold which is necessary for gene inhibition. Moreover, the difficulty of plasmid transduction is another major obstacle for using vector-based siRNA in some cell lines and in living organisms. Recently, some viral vectors were developed as outstanding tool for easy delivery and persistent expression by integrating siRNA expressing unit into host genome (Michel et al., 2005).

2.3.3.2 Transgene-based RNAi

Reverse genetics is an important approach for understanding gene functions. The most powerful tool of reverse genetics in mammals is gene knockout technology by homologous recombination. But it is prohibitively complex, expensive and time-consuming to generate knockout animal lines with the conventional techniques. The other limitation is that the completely knockout of many genes may be lethal to the animal in early developmental stage. Recent progress has indicated that the vector-based siRNA could offer a time-saving and cost-effective alternative to generate transgenic lines by simply introducing linearized siRNA plasmid into ES cells. RNAi-induced gene knockdown effect can be transmitted for many generations in these transgenic animals. The lethal effect of gene knockout could be circumvented by generating partial and conditional transgenic siRNA animal lines (Xia et al., 2002; Kunath et al., 2003).

Transgenic mice having reduced expression of SOD1 mutant has been generated with modified siRNA targeting mutated Cu/Zn superoxide dismutase (SOD1) gene. These transgenic animals with improved phenotype of familial ALS disease caused by the mutant SOD1 proteins in CNS were very helpful to elucidate the function of SOD1 gene in neurons in mouse CNS. A genome-wide transgenic RNAi library with 22,279 transgenic lines covering 88% of the predicted protein-coding genes in Drosophila genome has been generated for conditional inactivation of gene function in the intact organism. The library offers systematical analysis of the genes in Drosophila with a spatial and temporal resolution (Saito et al., 2005; Xia et al., 2006; Dietzl et al., 2007).

2.3.3.3 Knockdown disease with RNAi

RNAi has rapidly developed into a highly promising approach for knocking down disease-related gene to alleviate disease pathology. siRNAs used therapeutically in whole animals was first reported on 2003. siRNA duplexes targeting the gene Fas encoding the Fas receptor were introduced into mice via intravenous injection to reduce Fas protein expression in mouse hepatocytes to protect the mice from Fas-mediated apoptosis which cause liver failure and fibrosis in autoimmune hepatitis (Song et al., 2003). From then on, the siRNA-based drug development has proceeded at an astonishing speed. Generally, all the disease-related genes and pathogens with known sequences could be the target of therapeutic siRNA. The siRNA drugs offer easier and faster approaches to get through the test in laboratory animals and clinical trial than other conventional small molecular drugs.

RNAi shows outstanding therapeutic advantages in several mouse models of human

neurological diseases. In the mouse model of spinocerebellar ataxia, siRNA targeting the mutant allele of ataxin-1 achieved a successful suppression of polyglutamine-induced neurodegeneration, altering disease phenotype by improving motor coordination, restoring cerebellar morphology and resolving ataxin-1 inclusions in Purkinje cells (Xia et al., 2004) (Bonini and La Spada, 2005). Those studies demonstrate the potential use of RNAi as powerful therapy fur dominant neurodegenerative disease. Vector-based siRNA also provides an especially well-suited mean for defending viral infections. Numerous examples illustrated that a wide range of viruses could be inhibited by RNA in vitro and in vivo (Dykxhoorn and Lieberman, 2006). Furthermore, the property of siRNA mimicking endogenous microRNA function make it valuable anticancer therapy because microRNAs are found very important in regulating cellular differentiation and proliferation which go wrong during cancer development.

The therapeutic application of RNAi is now approaching clinical trials. The sirna-027 developed by Sirna Therapeutics (Boulder, USA) as a potential drug for age-related macular degeneration (AMD) undergoes phase I clinical trial. AMD, resulted from macula damage, is the most common cause of blindness among the people over age of 55. So far there is no cure for AMD although laser surgery or photodynamic therapy may slow down the progression of the disease. Sirna-027 is a vector-based siRNA targeting to vascular endothelial growth factor receptor gene VEGFR-1 which stimulates the growth of new blood vessels, allowing to reduce the pathological angiogenesis associated with AMD. The chemically modified sirna-027 could be directly injected into the eyes. The phase I clinical trial shows a dose-dependent positive effect of this drug by stopping the deterioration in visual acuity. (SiRNA Therapeutics, News Release (11 July 2005), www.sirna.com) Moreover, PhaseI clinical trials examining siRNA-based drugs for treating respiratory syncytial virus (RSV) infection has finished without any report of untoward toxicity. Some nanoparticle-enabled siRNA-based anticancer therapies have begun human clinical trials.

To be useful as molecular tool for studing gene functions or as drugs, siRNAs need to be delivered into cytoplasm of cells where they were processed to active form for conducting target mRNA degeneration. Most of mammalian cells can not efficiently take up enough siRNAs to provoke gene silencing. Direct infusion or inhalation of naked siRNA could be used for the drug delivery to mucosal tissue such as the respiratory tract. Incorperating siRNA into specialized liposome or antibody pariticle facilitated the drug delivery to boarder range of cells and tissues. Viral vectors are now available as most powerful tools to breakthrough the obstacles of siRNA drug delivery. Among them, vectors derived from adenoviruses and adeno-associated viruses are most frequently used for siRNA expression in therapeutic strategies against chronic diseases and cancer since the vector could incorporate siRNA transgenes into cell genome by viral integration (Dykxhoorn and Lieberman, 2006) (de Fougerolles et al., 2007).

2.4 AAV vector delivery system

Adeno-associated Virus (AAV) is a small (approximately 25nm in diameter) linear single-stranded DNA virus that belongs to the family *Parvoriridae*. The first adeno-associated virus was isolated in early 1960's as a contaminant of adenovirus but latterly identified as a replication-defective dependovirus which requires helper virus to facilitate its productive infection and replication. AAV infection results in the establishment of latent integration of viral DNA in the nucleus of the cells, while the wild type AAV can enter the productive cycle in the presence of helper viruses such as adenovirus (Ad), herpes simplex virus (HSV) or papillomavirus (HPV), leading to the replication of viral DNA and packaging of viral particles with pre-assembled capsids (Goncalves, 2005).

AAV serotypes*:* To date, totally 11 AAV serotypes with over a hundred AAV variants have been isolated. 8 serotypes, AAV-1 to AAV-8, have been identified in primates. All of the known serotypes of AAV can infect multiple diverse tissue types in many species. The tissue and cell tropism range for each AAV serotype is determined by the surface topologies of virions which account for the interactions between capsid proteins and cellular components of the host cells. Structural and functional correlation of the AAV capsid has been extensively studied for better understanding of the mechanisms underlying their diverse tissue tropisms. The crystal structure of AAV-2 has been determined with X-ray crystallography, whereas the structures of AAV4 and AAV5 have been reconstructed using cryoelectron microscopy. The analyses on the structures of other AAV serotypes are currently in progress (Grimm et al., 2003).

AAV2 presents its natural tropism towards murine skeletal muscles, neurons and hepatocytes. Among all of the AAV Serotypes, AAV-2 has been the most extensively and intensively examined one. The docking site for AAV-2 binding has been identified as heparin sulfate proteoglican (HSPG) which functions as a primary receptor while the other three, hepatocyte growth factor receptor (HGFR), integrin $a_V\beta_5$ and fibroblast growth factor receptor 1(FGFR-1) act as co-receptor to enable the endocytosis for AAV uptake (Wu et al., 2006).

Although AAV-2 is the most popular serotype in various AAV-based applications, it has been discovered that other serotypes can be more effective in gene delivery in certain circumstances respecting to their tropic binding to receptors. AAV-6 shows much strong infection to respiratory epithelial cells. AAV-7, AAV1 as well as AAV5 present high transduction efficiency to skeletal muscle cells and vascular endothelial cells, whereas AAV-8 shows especially powerful effect in transducing hepatocytes. AAV-3 is superior for the transduction of megakaryocytes. As a hybrid of AAV1 and AAV2, AAV-6 has lower immunogenicity than others. Utilization of the AAV vectors derived from different serotypes for gene delivery to different tissues not only reduces the vector load due to higher tissue specific transduction efficiency, but also helps to circumvent the humoral immune response to natural infection or prior exposure of certain AAV vectors. Based on

the results from the mutagenesis study of molecular structures of the parvoviruses and the capsid, the structural proteins of the virions could be manipulated to change tissue tropism to different cell types for expanding usage of AAV vectors. (Wu et al., 2006)

AAV structure: AAV genome is built of either positive-sensed or negative-sensed single-stranded DNA of approximately 4.7 kb long flanked by two inverted terminal repeats (ITRs). The complete nucleotide sequence of the genome of adeno-associated virus 2 (AAV2) has been determined. The single-stranded genome of AAV-2 is 4,675 nucleotides in length flanked by two ITRs of 145 nucleotides each. The ITRs are the only cis-acting elements needed for effective replication, encapsidation and integration of the AAV (Grimm, 2002).

Two open reading frames (ORFs): rep (replication) and cap (capsid) were discovered in AAV genome, which direct the synthesis of 6 major RNA species by 3 different transcriptional promoters and alternative splicing signals in the mRNAs. The former ORF is composed of four genes encoding four nonstructural proteins Reps required for AAV life cycle and the latter one contains genes encoding for three structural proteins VPs which constitute viral capsid.

In the first ORF rep, two overlapping mRNAs of different length were transcribed from promoter p5 and p19, respectively. Each of mRNAs contains an intron, giving rise to totally four various proteins translated from the two mRNAs by different splicing. The proteins are named according to their sizes in kilodaltons as Rep 78, Rep 68, Rep 52 and Rep40. Rep78 and its splicing variant Rep 68 transcribed by p5 participate in viral DNA replication, transcriptional control and site-specific integration through the interaction with Rep-binding element (RBE) and terminal resolution site (Trs) sequences located in the ITRs of the viral genome. Rep52 and its splicing variant Rep40 transcribed by p19 play essential roles in accumulation of single-stranded progeny genomes for packaging. AAV genome displays economic genetic organization of the virus with such overlapping arrangement of multiple genes (Goncalves, 2005).

The transcription of capsid proteins VP1, VP2 and VP3 were all controlled by one promoter named p40 in the second ORF cap but the translations of three proteins have different initiation codons or alternative splicing sites in the single mRNA. Usually in the presence of helper virus adenovirus, the longer intron excision is dominant, resulting the 2.3kb mRNA. The 2.6kb mRNA encoding VP1 protein is produced by shorter intron splicing. VP2 is translated from the noncanoical start codon ACG, while VP3 is translated from conventional start codon AUG in the shorter mRNA transcript. Apparently, VP1, VP2 and VP3 in molecular masses of 87, 72 and 62KD differ from each other only on their progressively reduced N terminus. The VP1, VP2 and VP3 proteins are assembled in certain molecular ratio to form mature characteristic icosahedral empty AAV virion in the nucleus of host cells (Figure 2.11).

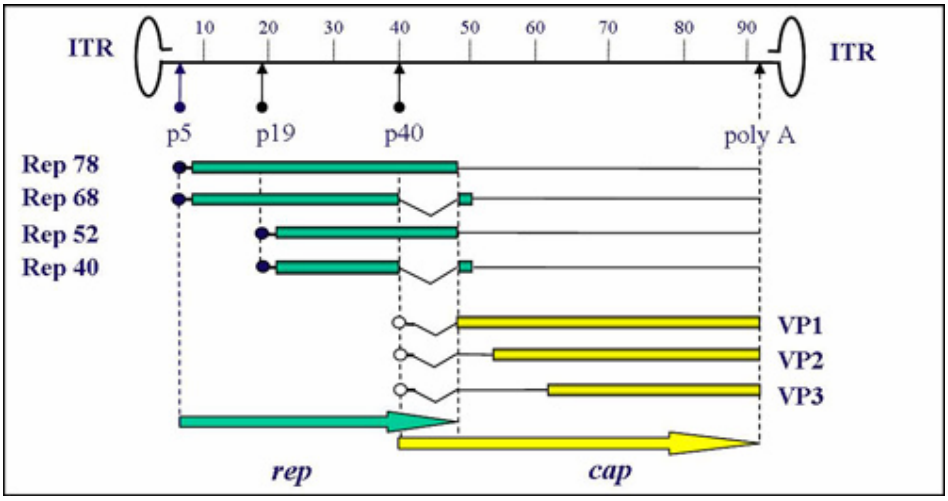

2.11: AAV Genome (by Anna Salvetti)

AAV genome contains two open reading frames (ORFs): rep (replication) and cap (capsid), which directs the synthesis of 6 major RNA species by matching 3 different transcriptional promoters and alternative splicing signals in the mRNAs. The former ORF is composed of four genes encoding four nonstructural proteins Reps required for AAV life cycle and the latter one contains genes encoding for three structural proteins VPs which constitute viral capsid. The transcription of capsid proteins VP1, VP2 and VP3 were all controlled by one promoter named p40 in the second ORF cap but the translations of three proteins have different initiation codons or alternative splicing sites in the single mRNA. The 2.6kb mRNA encoding VP1 protein is produced by shorter intron splicing. (Figure) VP2 is translated from the noncanoical start codon ACG, while VP3 is translated from conventional start codon AUG in the 2.3Kb mRNA transcript. VP1, VP2 and VP3 in molecular masses of 87, 72 and 62KD differ from each other only on their progressively reduced N terminus. The VP1, VP2 and VP3 proteins are assembled in certain molecular ratio to form mature characteristic icosahedral empty AAV virion in the nucleus of host cells

The AAV virions have an icosahedral capsid consisting of 60 copies of three structural proteins VP1, VP2 and VP3 at a ration of 1:1:18. VP1, VP2 and VP3 share the common C-terminal region called VP3 unit which comprises a conserved eight-stranded antiparallel beta-barrel motif. The large loops inserted between the strands of beta-barrel are therefore presented on the surface of protein to enable the characteristic profiles of AAV serotypes.

***Infection cycle of AAV*:** From infecting a cell to producing new infectious viral particles, the AAV infection cycle involves the following steps: First the AAV attachs to the host membrane by binding to specific receptors and coreceptors, followed by the endocytosis to enter the host cells. The AAV then goes through endosomal trafficking and finally translocates into the nucleus of the host where the viral genome forms the double-stranded DNA genome. The replication-defective AAV exists in latency form by integrating site-specifically into host genome DNA in the absence of helper virus. Upon the co-transfection with helper virus, AAV genome is rescued to enter a lytic productive phase where the single-stranded AAV DNA genome is synthesized and encapsidated into a 20nm diameter capsid pre-assembled by the VP1 toVP3 proteins. The capsid assembly is confined in the nucleoli of the host cells. Fully assembled AAV capsids enter the nucleoplasm in a Rep-dependent manner where the selective DNA encapsidation is directed by the interaction of empty capsid and Rep proteins with the virus genome. Then,

the complete virions are finally released from the host cell. Although the overall pattern of virus assembly and encapsidation is identified, the biochemical mechanisms in these processes remain unknown. (Snyder and Flotte, 2002) (Seisenberger et al., 2001) (Figure 2.12)

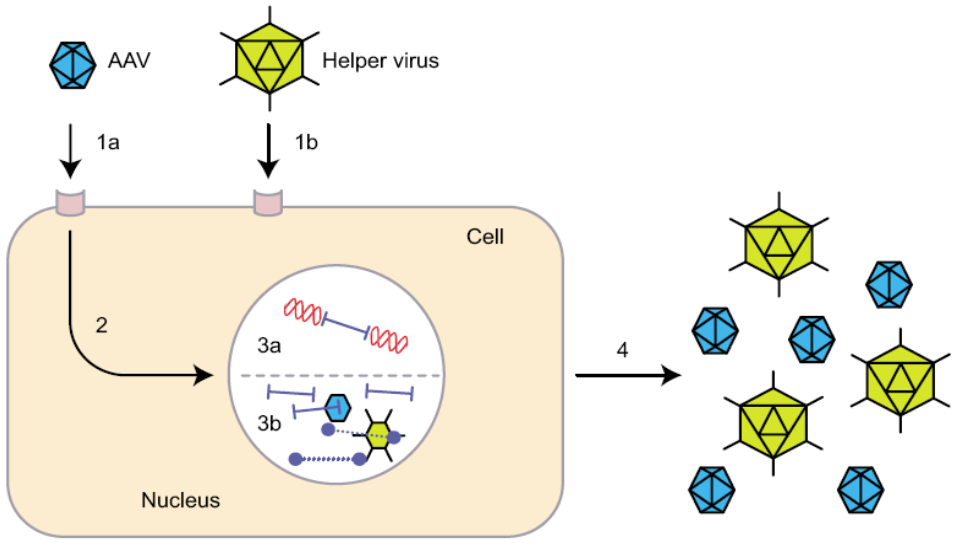

Figure 2.12: Life cycle of AAV (by Boris Blechacz and Stephen J. Russell)
AAV first attachs to the host membrane by binding to specific receptors and coreceptors and enters the host cells through endocytosis **(1)**. The AAV then goes through endosomal trafficking and finally translocates into the nucleus of the host where the viral genome forms the double-stranded DNA genome **(2)**. The replication-defective AAV exists in latency form by integrating site-specifically into host genome DNA. Upon the activation, AAV genome is rescued to enter a lytic productive phase where the single-stranded AAV DNA genome is synthesized and encapsidated into a 20nm diameter capsid pre-assembled by the VP1 toVP3 proteins **(3)**. Fully assembled AAV capsids enter the nucleoplasm where the selective DNA encapsidation is directed by the interaction of empty capsid and Rep proteins with the virus genome. Finally, the complete virions are released from the host cell **(4)**.

AAV Vector*:* Following the establishment of the first infectious clone ofAAV-2 in 1982, the use of adeno-associated virus (AAV) as a gene transfer vector has been steadily increased over the past years mainly because it offers sustained gene expression in a board range of host cells both in vitro and in vivo. The extended tropism of AAV covering primate, canine, murine and avian cell types could be explained by the use of ubiquitous HSPG as primary docking sites for infection. The stable and lasting expression of the transgene is achieved by a stable integration of the transgene between two ITRs into host genome with a special predilection for a region on chromosome in both dividing cells and non-dividing cells. Prolonged in vivo expression of transgenes transduced by AAV-2 vectors has been observed in liver, brain, skeletal muscle and lung of different animal models.

The structural genes (cap) and the packaging genes (rep) are delivered *in trans*, which makes AAV an efficient recombinant vectors for gene delivery. Recombinant AAV vectors are derived from the wild type virus by replacing almost complete genomic sequence (96%) of rep and cap genes by the transgenes combined with transcriptional control elements. Limited cloning capacity of AAV vector can be resolved by using the

unique feature of ITRs to join multiple in dependent rAAV genomes by intermolecular recombination (Grimm, 2002; Goncalves, 2005).

The minimal set of the adenoviral genes required for efficient generation of progeny AAV particles has been identified, allowing the new methods of helper-free recombinant AAV production which do not require helper virus co-infection into the cells. (Grimm et al., 2003)The elements required for AAV packaging and Adenovirus helper functions could be combined on a single helper plasmid to co-transfect with rAAV plasmids for high-titer rAAV production in the absence of helper viruses. Since the only wild-type sequences remained in the recombinant viral genome are the AAV ITRs, the immunogenicity and direct cellular toxicity caused by viral proteins and contaminating helper viruses can be completely avoided. Direct administration of rAAV vectors results in persistent transduction of cells with mild humoral immune response which could be overcome by transient immune suppression (Zolotukhin, 2005).

AAV vectors for gene therapy*:* To be clinically applicable, the viral vectors should be replication-defective, non-immunogenic, non-toxic but still able to deliver transgenes efficiently into nucleus of the host cells. The non-pathogenic character, lack of viral genes, lack of cellular toxicity, the ability to confer long-term gene expression, ability to generate high titer vector preparation and board range of tissue tropism makes AAV a very appealing candidate for creating viral vector for safe gene therapy in human. Despite approximately 80% of human population is seropositive for AAV-2, so far no human disease has been related to AAV. The cloning and manipulation of rAAV vector could be carried out in ordinary laboratory in Biological Safety Class I level. Additionally, AAV is particular suitable to clinical use due to its apparent limited capacity to provoke immune response in human, thus reducing the risk of any immune-associated pathology. Since the transgene flanked by the two ITRs could be integrated into host genome with a special predilection for a region on chromosome 19 in human to achieve stable and lasting expression, multiple administrations are not necessary. Besides, ability of efficiently transduce highly differentiated postmitotic cells such as neurons allows recombinant AAV vector a valuable alternative to other gene delivery systems in CNS and PNS which have very low accessibility for other delivery methods (Ruitenberg et al., 2002) (Kaspar et al., 2002) (Paterna and Bueler, 2002).

Recombinant AAV-2 vectors have been examined in preclinical studies for a variety of diseases such as hemophilia and Duchenne muscular dystrophy. Over 10 different AAV-2 based vectors have been administered in patients in clinical trials as therapeutic drugs. The AAV-mediated treatment of hemophilia B has resulted in very promising therapy in the clinical trial (Tenenbaum et al., 2004).

However the AAV-2 vectors show rather limited efficiency in infecting a number of clinically relevant cells of therapeutic interest, such as liver and muscle cells. Another inherent drawback hampering the gene transfer by AAV2 vectors is that the majority of human population has been prevalently exposed to AAV2, thus carrying the neutralizing

antibodies against vectors derived from AAV-2. Those problems could be resolved either by using other naturally occurring serotypes of AAV such as AAV1, 4, 5 and 6 or by changing tissue/cellular specificity through modification of vector genomes and capsid proteins. The mosaic virion is generated by using the helper constructs which encodes mixing capsid subunits from different serotypes. The mosaic rAAV1/2 generated from helper plasmid expressing capsid proteins from AAV1 and AAV2 has more comprehensive infection panel which combines characteristic tropisms of the two serotypes. Chimeric rAAV is such kind of hybrid vectors containing capsid proteins that has been engineered by exchanging domain or amino acid between different serotypes. Specific capsid domains such as surface loops which are vital for determining tissue tropism could be replaced from one serotype to another, resulting in gain or loss of certain tissue specificity. Those pseudotyped vectors have shown improved potency and broadened tropism of AAV vector (Thomas et al., 2003).

To further improve the recombinant AAV delivery system, different cellular promoters were used to drive the transgene in the vector for different expressing pattern. For instance, PDGF promoter used in AAV vectors offering higher neuron specificity than CMV promoter was used in mouse brain. Conditional and inducible features of the transgenes could also be realized by corresponding transcriptional elements (Kugler et al., 2001) (Ehrengruber et al., 2001).

Gene silencing through small interfering RNAs (siRNAs) is rapidly becoming a powerful tool for genetic analysis of mammalian cells. Recently, recombinant AAV vectors have achieved a successful siRNA delivery in mammalian cells, which overcomes the problem of poor transfection efficiency of the plasmid-based siRNA systems. High specificity and efficiency of the rAAV-siRNA delivery system make it a promising tool for gene therapy in human by knocking down disease-related genes (Tomar et al., 2003).

In an attempt to search for potent AAV vectors with enhanced performance profiles, molecular techniques were used for the identification and isolation of endogenous AAVs from a variety of primate tissues. A family of novel primate AAVs consisting of 110 non-redundant species of proviral sequences was discovered and turned to be prevalent in 18-19% of the tissues evaluated. Initial evaluation of vectors based on these novel AAVs for tissue tropism and gene transfer potency in mouse models led to the discovery of vectors with improved gene transfer efficiency to different target tissues. Gene therapies with novel AAV vectors have achieved long term phenotypic corrections in several animal models. Vectors based on new primate AAVs could become the next generation of efficient gene transfer vehicles for various gene therapy applications.

III. Materials and Methods

3.1 Construction of parent vectors

3.1.1 pBlueU6

The promoter of the mouse U6 RNA gene (GenBank access number: X06980, -315~0) was isolated by PCR using a genomic DNA template from BL6 mouse with the sense primer 5'-GCGGATCC *(BamH I)*GACGCCATCTCTA-3' and the antisense primer 5'-GCTCTAGA*(Xba I)*GCGTTAAC*(Hpa I)*AAGGCTTTT- CTCCAAGG-3'. The resulting PCR product digested with RE *BamH I* and *Xba I* was cloned into a pBluescript II SK(+) vector (Stratagene) to form pBlueU6 (Figure 3.1). The *Hpa I* and *Xba I* sites introduced by the antisense primer allow the insertion of the siRNA sequence into the transcriptional frame under the mouse U6 RNA promoter.

If not specified, the restriction endonucleases (REs) used in this project are products from New England Biolabs (NEB). The rapid DNA ligation kit (Roche applied sciences) was used for fast and efficient cloning. A PCR purification kit, Gel extraction kit, Plasmid Maxiprep and Miniprep kit allowed easy purification of the PCR products, DNA fragments and ultrapure plasmid DNA.

3.1.2 pBlue-hU6

The promoter of the human U6 RNA gene (GenBank access number: X07425, -250~0) was isolated by PCR using a genomic DNA template from a human skin sample (kindly provided by Dr. Sabine Wenner's Lab, Cell. Biol. Inst., ETH) with the sense primer 5'-GCCTCGAG *(Xho I)* AGAGGGCCTATT- TCCCATGA-3' and antisense primer 5'-CCCAAGCTT *(Hind III)*AAAAAGGTGTTTCGT- CCTTTCCAC-3'. The resulting PCR fragment digested with Xho I and Hind III was cloned into a pBluescript II SK(+) vector to obtain pBlue-hU6.

3.1.3 pBlue-hH1

The promoter of the human H1 RNA gene (GenBank access number: S68670, -97~0) was isolated by PCR using genomic DNA template from a human skin sample with the sense primer 5'-GCCTCGAG*(Xho I)*ATTTGCATGTCG- CTATGTGT-3' and antisense primer 5'-CCCAAGCTT*(Hind III)*AAAAAG- GGGAAAGAGTGGTCTCATA-3'. The resulting PCR fragment digested with Xho I and Hind III was cloned into a pBluescript II SK (+) vector to create pBlue-hH1.

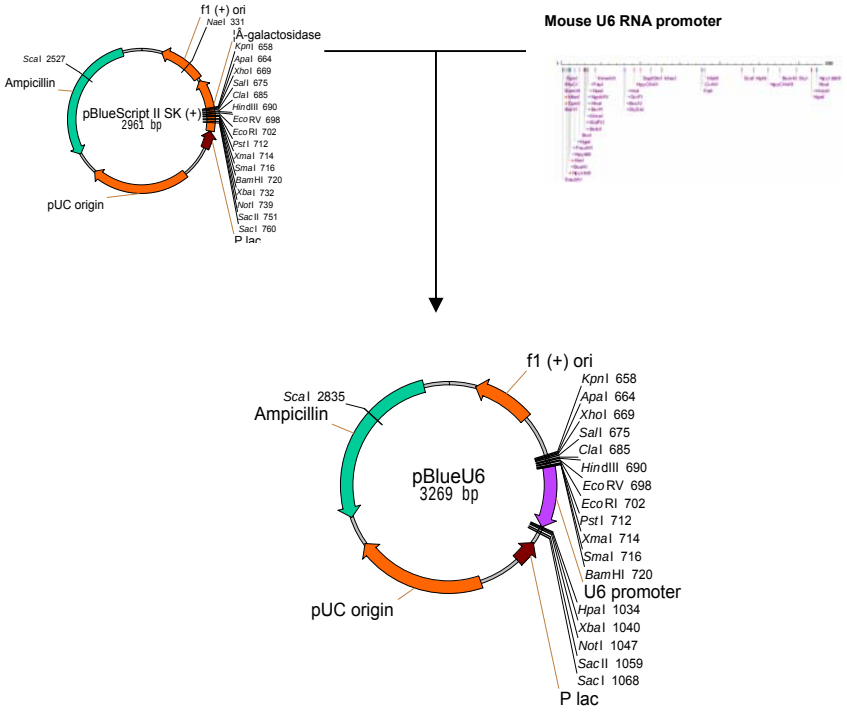

Figure 3.1: Construction of the vector containing the mouse U6 RNA promoter

The promoter of the mouse U6 RNA gene was isolated by PCR using a genomic DNA template from BL6 mouse with primers. The resulting PCR product digested with RE BamH I and Xba I was cloned into a pBluescript II SK (+) vector. The Hpa I and Xba I sites introduced by the antisense primer allow the insertion of the siRNA sequence into the transcriptional frame under the mouse U6 RNA promoter.

3.1.4 Construction of an AAV vector containing an EGFP marker

The psubAAV2-CBA-WPRE vector (kindly provided by Dr. Hansruedi Bueler's lab, Inst. Mol. Biol, Uni. of Zurich) was digested with Kpn I and Hpa I to remove the CBA-WPRE promoter-enhancer sequence. The CMV promoter conducted EGFP expression cassette was obtained by digesting pEGFP-N1 (ClonTech.) with Afl II and Afl III (1630bp fragment). The vector and fragment blunted with Klenow (Roche) were ligated together to form psubAAV2-CMV-EGFPN1. The resulting plasmids were identified and characterized by RE analysis and transfected into HEK293T cells to detect green fluorescence.

3.1.5 Construction of an AAV vector expressing calsyntenin-1

The 3200bp fragment resulting from the digestion of pcDNA3.1-mmCst1 (kindly provided by Dr. Peter Sonderegger's Lab, Biochem. Inst. Uni. of Zurich) with *Sac I* was blunted with Klenow and then cloned into a psubAAV-CMV-EGFPN1 vector linearized and blunted at *Nhe I* and *Hpa I* sites to form the psubAAV2-CMV-Cst1 construct.

3.1.6 Construction of an AAV vector containing the EGFP-2A fusion frame

Using pEGFP-N1 vector as template, the EGFP sequence was amplified by a two-round nest-PCR with the forward primer 5'-CTAGCTAGC*(Nhe I)*ATGGTGAGCAAGGGCGAGGAGC-3' and two reverse primers containing the 2A sequence derived from the foot and mouth disease virus (FMDV) gene 5'-TCCCGCAAGCTTAAGAAGGTCAAAATTCTTGTACAGCTCGTCCATGCCGAG-3', 5'-GGTGTACA(*BsrG I*)GGGCCC(*Apa I*)AGGGTTGGACTCGAC-GTCTCCCGCAGGCTTAGGAAGG-3'.

The resulting PCR product containing the EGFP-2A fusion gene cassette was cloned into a psubAAV2-CMV-EGFPN1 vector between the *Nhe I* and *BsrG I* sites to form the psubAAV2-CMV-EGFP2A construct. The *Apa I* and *BsrG I* sites were introduced with a second antisense primer to facilitate the cloning of coding sequences to express 2A linked EGFP fusion protein in the genes of interest. Upon translation, the 16aa FMDA 2A peptide (NFDLLKLAGDVESNPG) mediates self-cleavage on its own C-terminus to give rise to an EGFP marker fused with a 2A tag and the intacting target protein (Figure 3.2).

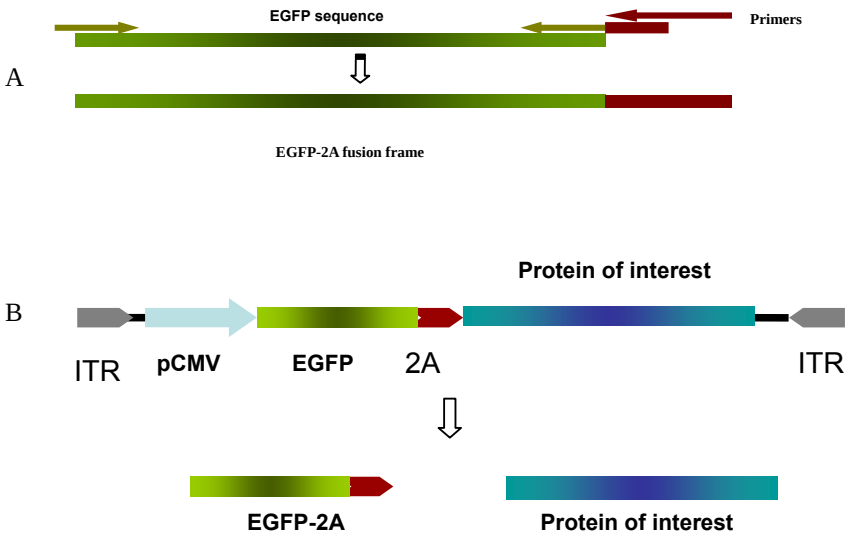

Figure 3.2: Schematic illustration of the construction of the 2A linked EGFP fusion protein

A: Nest PCR amplification to construct the EGFP-2A fusion frame: Using pEGFP-N1 vector as template, the EGFP sequence **(green)** was amplified by a two-round nest-PCR with the primers which contains 2A sequence **(red)** in the antisense primers.
B: The self-cleavage of the fusion protein by the FMDV 2A peptide: Upon translation, the FMDA 2A peptide mediates self-cleavage on its own C-terminus to give rise to an EGFP marker fused with a 2A tag and the intacting target protein **(blue)**.

3.2 Design and Cloning strategies for constructing siRNA expression vectors

3.2.1 Hairpin-type siRNA

The general strategy for constructing hairpin-type siRNA vector involves the design, synthesis, annealing of two complementary oligonucleotides into a double-stranded DNA insert, and subsequent cloning of the insert into a siRNA expression vector.

The insert is designed such that it specifies a 19nt sequence derived from the open reading frame of the target gene, separated by a 9nt spacer from its 19nt reverse complementary sequence plus a termination signal consisting of five thymidines in a row. The insert provides a template for the RNA polymerase III RNA promoter to produce hairpin RNA transcripts. For each target site, one pair of complementary oligonucleotides is chemically synthesized and annealed to form a double-stranded DNA insert with overhangs that could be cloned into the pBlueU6 vector linearized with Hpa I and Xba I (Figure3.3).

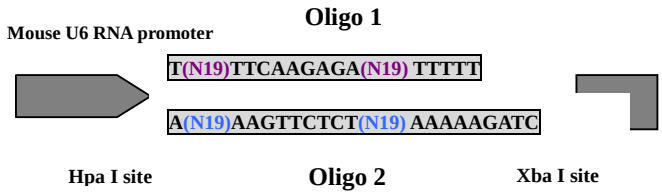

Figure 3.3: Design and cloning of the oligonucleotides

Two complementary oligonucleotides are chemically synthesized and annealed to form a double-stranded DNA insert with overhangs. The resuting insert is cloned into the pBlueU6 vector linearized with Hpa I and Xba I.

Annealing oligos with a PCR apparatus: The oligos (SIGMA 0.05 µmole scale, purified by HPLC) were dissolved in ddH_2O to give a final concentration of 3µg/µl. The two oligos were mixed in equal molar ratio in annealing buffer (100 mM potassium acetate, 30 mM Hepes-KOH pH 7.4, 2 mM Mg-acetate) and incubated at 95°C for 5 minutes, 70°Cfor 10 minutes, then slowly cooled down to 4°C. The resulting products can be stored long term at -20°C.

Phosphorylation of annealed insert: The inserts were treated with polynucleotide kinase (T4 PNK kit, Roche) for 30 minutes at 37°C then incubated for 10 minutes at 70°C in a heating block to deactivate PNK. Ligation (Roche rapid ligation kit): PNK treated oligo inserts were mixed with pBlueU6 vector linearized with Hpa I and Xba I in a molar ratio 2:1 in ligation buffer, incubated at RT for 30 minutes. Small amount of the resulting ligation mixture was used to transform bacterial competent cells (E.coli. XL-Blue, prepared according to the Super-competent Cell Protocol provided by Dr. Jingxuan Yang, ETH. Cell Biology Institute). The bacterial colonies were screened and identified with RE analysis and sequencing for desired clones (Figure 3.4).

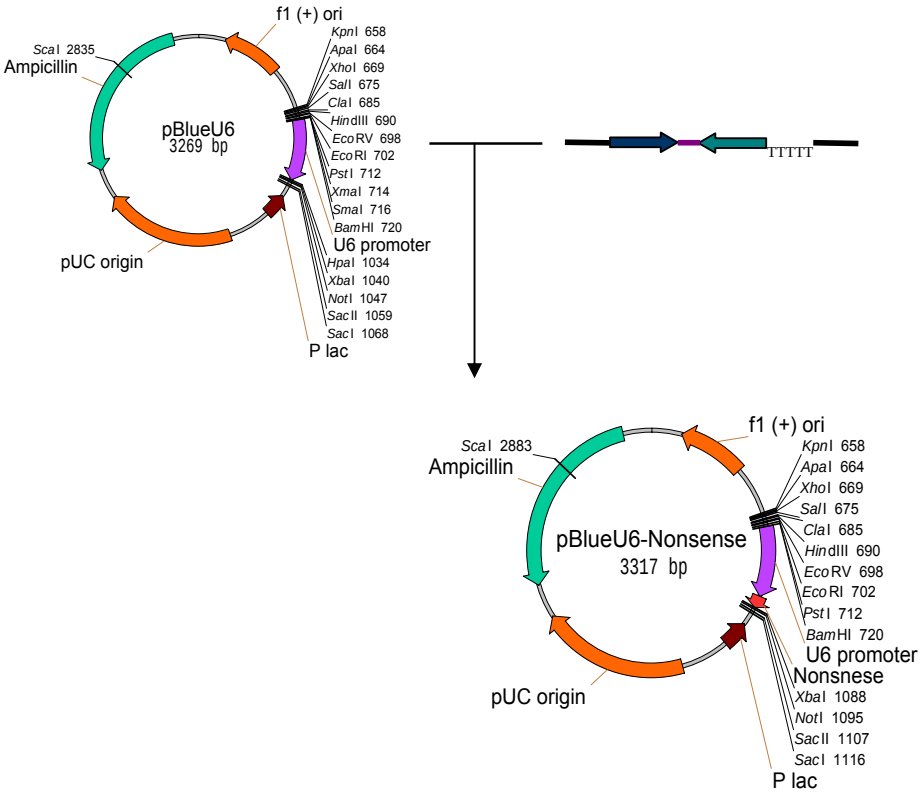

Figure 3.4: Construction of hairpin-type nonsense siRNA expression vector with pBlue-mU6

PNK treated nonsense siRNA inserts were cloned into pBlueU6 vector linearized with Hpa I and Xba I to form the hairpin-type nonsense siRNA expression vector.

3.2.2 Tandem-type siRNA

The tandem-type siRNA expression vector employs two independent mouse U6 promoter cassettes to produce sense and antisense RNA transcripts of the target sequence simultaneously. After the transcription of the individual single-stranded RNA, these two complementary transcripts could anneal for further processing to form an active siRNA duplex.

Using the mouse U6 promoter sequence serving as template, two independent PCR reactions were conducted with two reverse primers containing sense and antisense siRNA sequence respectively. The resulting PCR products containing the mouse U6 promoter conducted sense and antisense siRNA expressing cassettes were digested with corresponding restriction enzymes and then cloned into pBluescript.II SK(+) (Figure 3.5).

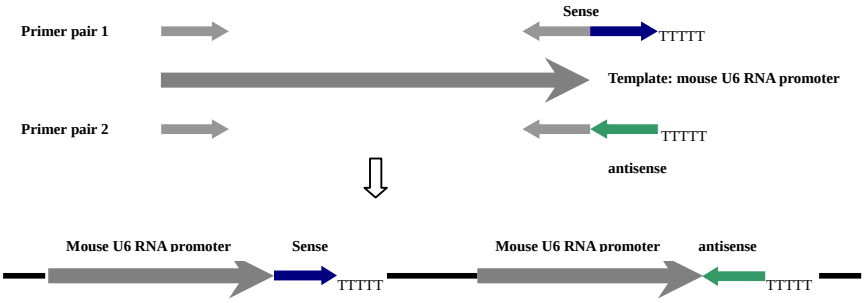

Figure 3.5: Construction of a tandem type siRNA expression vector

Using the mouse U6 promoter sequence serve as template, two independent PCR reactions were conducted with two sets of reverse primers containing sense and antisense siRNA sequence respectively. The resulting PCR products containing the mouse U6 promoter conducted sense and antisense siRNA expressing cassettes were digested with corresponding restriction enzymes and then cloned into pBluescript.II SK(+). The resulting vector produces two individual complementary transcripts which could anneal to each other to form the active siRNA duplexes.

3.2.3 PCR approach for constructing hairpin type siRNA expression vector

Using the human U6 RNA gene and its 3' flanking sequence on a pBlue-hU6 vector as templates, two PCR fragment was amplified with two pairs of primers that contain sense and antisense siRNA sequences within their reverse primer and forward primer, respectively.

The resulting PCR products were digested with corresponding enzymes and cloned into pBluescript.II SK (+) independently. After sequencing identification, the fragment containing the antisense siRNA sequence from one plasmid was cloned into another plasmid containing the sense siRNA sequence to form a human U6 promoter-conducted hairpin type siRNA expressing cassette.

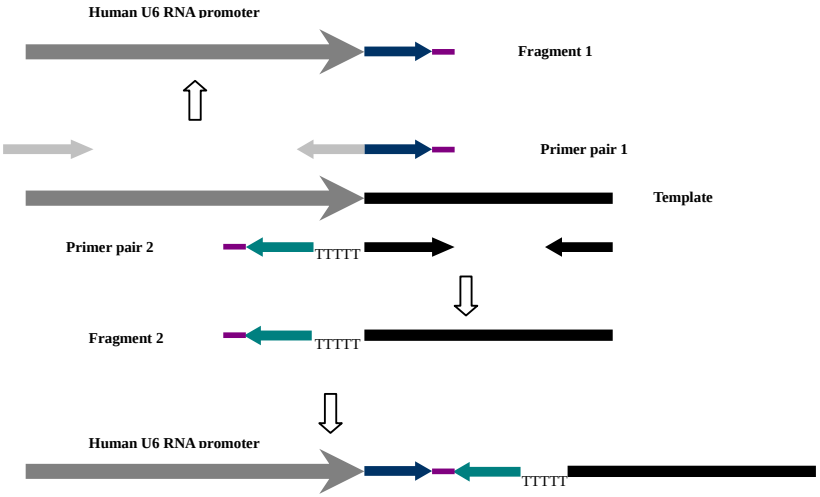

Figure 3.6: PCR approach for constructing a hairpin type siRNA expression vector.

Using the human U6 RNA gene and its 3' flanking sequence on a pBlue-hU6 vector as templates, two PCR fragment was amplified with two pairs of primers that contain sense and antisense siRNA sequences within their reverse primer and forward primer, respectively. The resulting PCR products digested with corresponding enzymes were cloned into pBluescript.II SK (+) independently. After sequencing identification, the fragment containing the antisense siRNA sequence from one plasmid was cloned into another plasmid containing the sense siRNA sequence to form a human U6 promoter-conducted hairpin type siRNA expressing cassette.

3.3 Cell culture

3.3.1 The NG108-15 cell line

The NG108-15 cell line is a hybrid dividing culture resulting from the fusion of mouse neuroblastoma and glioma, which still expresses many neuronal properties. NG108-15 cells were cultured in DMEM medium (Gibco: 21969-035. Invitrogen) supplemented with 10% FCS, 4 mM L-glutamine, HAT (100 µM hypoxantine, 1 µM aminopterin, 16 µM thymidine), 100 U/ml penicillin-streptomycin (Gibco 15140-122) in the incubator at 37°C with 5% CO_2. Cells were seeded at 1:5 onto fresh culture plates when reaching confluence. Cells with more than 5 passages were seeded onto a 12-well-plate (Nunclon, Nunc) at a concentration of 1 X 10^5 cells/well 24 hours before experiments,

3.3.2 The HEK 293T cell line

The cells were cultured in DMEM medium (Gibco: 21969-035 Invitrogen) supplemented with 10% FCS, 5 mM L-glutamine, 0.1 mM sodium-pyruvate, 100 U/ml penicillin-streptomycin in the incubator at 37°C with 5% CO2. Cells were diluted at 1:10 in fresh culture when reaching confluence. Cells with more than 5 passages were used for transfection.

3.3.3 Primary hippocampal neuronal cultur:

(Modified from P. Sonderegger's Lab protocol developed by Renato Frischknecht and Anna Fejtova)

A pregnant mouse was killed by cervical dislocation and the E18 embryos were taken out from the uterus. The heads of embryos were collected in Petri dishes containing ice-cold HBSS+ (Gibco:14025-050 Invitrogen). After removing the skin, skull and meninges with forceps, the hippocampi were dissected out from the brain with fine scissors and washed twice with HBSS- (Gibco: 14175-053 Invitrogen). To disassociate the cells, the hippocampi were incubated 5 minutes at 37°C n 0.25% trypsin (Gibco 25090-028 Invitrogen). Pouring off the solution carefully, the tissue clump was washed with plating medium (DMEM Gibco: 31053-028 supplemented by 10% FCS, 1 mM sodium pyruvate, 5 mM glutamine, 0.5 mg/ml albumax). The tissue was triturated in plating medium carefully by pipetting several times. Cells were counted with a microscope counting chamber and diluted to the desired concentration with plating medium.

Culturing the primary neuronal cells on cover slips: The 20mm round glass coverslips (Deckgläser, Germany) were incubated with 99% ethanol for 10 minutes at RT, followed by washing three times with sterile ddH_2O. After the overnight incubation in coating buffer (0.5 mg/ml poly-L-lysine, 150 mM sodium borate, pH 8.4, sterilized by filtering through a 0.45 um filter) at 37°C, coated coverslips were washed three times with sterile water, and dried in the laminar flow hood.

100 µl of the cell suspension were plated on coated coverslips, incubated for 1 hour in a 37°C incubator with a 5% CO_2 supply, then transferred onto coverslips to a 12-well-plate containing 1 ml culturing medium of DMEM (Gibco:31053-029) supplemented with 10% FCS, 1 mM sodium pyruvate, 5 mM glutamine, 0.5 mg/ml albumax, 2% B27 (Gibco:17504-44). The cytosine arabinoside (AraC, Calbiochem: 251010) was added to a final concentration of 15 µM to prevent the outgrowth of glial cells. The cells were fed by adding 100µl of culturing medium every 10 days.

To grow the cells on plastic culture plates, the same protocol was used except that the coating concentration of poly-L-lysine was 20µg/ml. For low density culture, a glial feeder layer was pre-established on the poly-L-lysine coated culture dishes to support the growth and differentiation of neurons.

The glial feeder cells were prepared from postnatal 1 day mouse: Cortexes were collected in HBSS and trypsinized with 0.25% trypsin. Tissue was triturated and diluted in neuron plating medium (as described above) to the desired concentration. Cells were cultured in Petri dishes until they reached confluence. Glial feeder cells were resuspended by trypsinization and plated on the culture plates (Nunc) at a density of 0.5×10^5 cells/cm^2. The cover slips with primary neuronal culture were placed on the plates upside down, so the neuron side faced the bottom of the dishes.

The Paraplast Tissue Embedding Medium (Sherwood medical:8889-501007) was

heated to 150°C until it was in the melted state, then three drops of the melted embedding medium were deposited on the plates with a glass pipette providing support for the cover slips when it became solid.

3.4 Transient transfection of NG108-15 and HEK 293T cells using the lipofectamine 2000 reagent (Invitrogen)

For adherent HEK 293T and NG108-15 cells, cells were seeded 24 hours before transfection at a concentration of 1 x 10^5 cells /ml. The plasmids were diluted with OptiMEM medium I (Gibco: 31985-047, Invitrogen) to 10 µg/ml in Eppendorf tubes. The lipofectamine reagent was diluted to 10% (V/V) with OptiMEM medium. The plasmid and lipofectamine solutions were mixed together and incubated 30 minutes at RT to form the plasmid-lipofectamine complex. The mixture was added dropwise to cell culture dishes. Changing the medium was not necessary. 24 hours later, the transfected cells could be used for further experiments.

3.5 Stoppini type hippocampal slice culture

(Modified from the Cold Spring Harbor protocol developed by Leah Fuller and Michael E. Dailey)

Post-natal 6 days C57BL/6 mice were killed by quick decapitation with scissors. The heads were dissected with fine tip surgical scissors to expose the brain. Cerebrums were collected in Petri dishes filled with ice-cold dissection solution GBSS++ (Gibco Hank's balanced salt solution, supplemented with 6mg/ml glucose), then the hippocampus were excised from the brain with blunt spatula and fine forceps.

The hippocampus was cut into transverse sections at an interval of 300 µm with a tissue chopper. The slices were separated and plated on Millicell-CM Organotypic Cell Culture Inserts (Millipore: 0.4 µm) in a 6-well-plate filled with 1 ml culture medium (48.5% BME, 25% HBSS, 25% heat-inactivated horse serum supplemented with 4 mM L-glutamine and 6 mg/ml glucose. pH: 7.2-7.4.) The slices on the membrane were maintained in the interface between the atmosphere and medium in the incubator at 35°C, 5% CO2, 95% humidity. The medium was changed every 3 days.

3.6 Introducing plasmid DNA into hippocampal slice cultures via electroporation

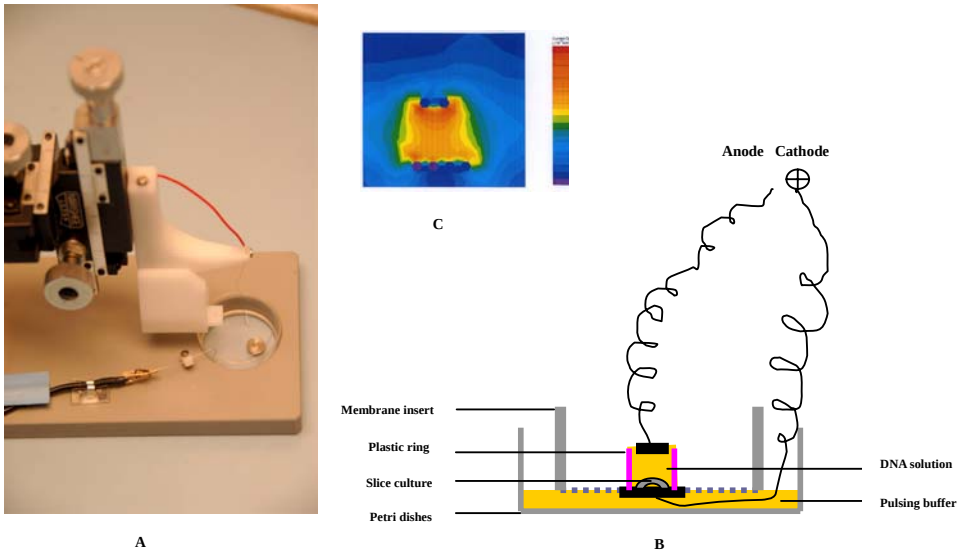

Figure 3.7 Electroporation in organotypic cultures

A: Self-made electroporation device
B: Schematic illustration of the electroporation setup: The slice cultures are placed between two parallel electrodes. The chamber is filled with DNA solution and the electric field is applied to introduce DNA into slice culture.
C: Current density measurement and distribution between paired electrodes

The experiment was conducted under sterile conditions in a laminar flow hood. The Millicell membrane insert (Millipore: 0.4 μm hydrophilic PTFE) carrying the hippocampal slices was transferred into the Φ3.5 mm sterile Petri dishes filled with 2 ml pulsing buffer (Gibco HBSS supplemented with 20 mM HEPES, pH 7.2). The Petri dishes were mounted in the electroporation device such that the target slice was positioned between the two parallel electrodes. A 2 mm-high plastic ring (Φ4.0 mm inner diameter, cut from polyethylene tube with a razor blade, flame polished) was placed so as to enclose part of the slice culture. The chamber formed by the ring was filled with a 1.0 μg/ul DNA solution diluted with pulsing buffer. The cathode was attached to the membrane from the bottom of the membrane insert and the anode was placed on top of the plastic ring to make contact with the DNA solution.

The electric field was generated by an ECM830 electroporator (BTX). The electroporation parameters were optimized to a voltage of 125 V, a pulse number of 6, a pulse length of 50 ms, and a pulse interval of 1s to minimize damage to the slices. The insert was washed with medium to remove the debris and pulsing buffer before it was returned to the culture plate for further culturing (Figure 3.7).

3.7 Counting EGFP positive cells with Flow Cytometry

24 hours after the transfection, the NG108-15 cells were trypsinized and collected by centrifugation, then resuspended with PBS containing 0.2 % Triton X-100 at RT for 20-30 minutes. After washing with PBS, cells were collected and equilibrated with 0.5 ml flow cytometry buffer (PBS supplemented with 2% FCS, 1 mM $MgCl_2$ and 1 mM $CaCl_2$).

A Beckmann-Coulter EPICS XL bench-top instrument and System II Data Acquisition & Display software were used to count the green fluorescent cells. The emission was measured at FL3 (long pass filter 670 nm) to determine the region for live cells. Detection was set at the FL1 channel (525 nm band pass filter) to measure the emission of green fluorescence from EGFP positive cells. The data on scatter parameters and histograms were recorded in log mode until 10,000 events were evaluated. The peak value obtained from the histograms represents the fluorescent intensity of the sample.

3.8 AAV preparation and purification

3.8.1 Packaging of AAV particles:

(Modified after the Grimm protocol, Human Gene Therapy, 9.2745-2760).

In general, to produce adenovirus-free rAAV particles, 293T cells are transiently co-transfected with rAAV vector plasmid and helper plasmid pDG, which contains adenovirus helper and all elements involving AAV packaging function.

HEK 293T cells were seeded on 20 culture plates (Φ15 cm, Cellstar: 639160) with 1.5 $x10^7$ cells per plate. The cell density reached about 70% confluence after 24 hours. Cells were transferred to fresh medium without antibiotics and incubates for 2~3 hours. The mixture of rAAV plasmid and helper plasmid pDG was prepared in an equal molar ratio according to the formula: Y µg rAAV plasmid = (1000 µg pDG helper X length in Kb of rAAV plasmid.)/21.8kb

The plasmids were mixed with 3.0 ml 2.5 M $CaCl_2$ buffer (2.5 M $CaCl_2$ in H_2O, stored at -20°C in 20 ml aliquots), then diluted with sterile ddH_2O to a final volume of 25 ml.
10 polystyrene snap cap tubes (Falcon, 12ml) were prepared with 2.5 ml HeBs buffer (NaCl, HEPES, Na_2HPO_4 in H_2O, pH adjusted to 7.12 with NaOH, stored at -20°Cin 50 ml aliquots.) in each tube. 2.5 ml of DNA/$CaCl_2$ mixture was added dropwise into each tube, mixed by gently tapping and incubated for 5 minutes at room temperature.

2.5 ml of the mixture was divided dropwise into each cell culture plate and mixed gently. After incubating overnight at 37°C, 5% CO_2, cells were cultured in 25 ml fresh medium containing antibiotics (100U/ml penicillin-streptomycin). 48~52 hours after the transfection, cells were collected into sterile 50 ml Falcon tubes with plastic cell spatula and centrifuged at 1200 rpm for 5 minutes at 4°C.

To prepare the cell lysate, the cell pellet was resuspended in resuspension buffer (0.15 M NaCl, 50 mM Tris-HCl, pH: 8.5) to a final volume 15 ml. The cells were frozen and thawed two times by transferring tubes between liquid nitrogen and a 37°C water bath. The tubes were vortexed at full speed for 1 minute after each thawing to dissolve cell clumps. the mixture wa passed through a 21 G needle using a 10 ml syringe to further remove cell clumps.

3.8.2: Purification with iodixanol gradients

(Modifed after the Grimm protocol. Human Gene Therapy, 9.2745-2760).

Benzonase (Sigma-Aldrich) was added into the cell lysate to a final concentration of 50 U/ml and the mixture was incubated for 30 minutes at 37°C.

The clear lysate was obtained by centrifugation at 7000 rpm for 20 minutes at 15°C in a SS-34 rotor (Beckman) to remove cell debris. The supernatant was transferred to a 50 ml Falcon tube and filled to a final volume of 15 ml with the resuspension buffer (as describe above).

The 25 x 89 Beckman Ultraclear quick-seal tubes were loaded with lysate and iodixanol gradient medium with a long needle fitted to a syringe or peristaltic pump. The gradient (from top to bottom) consisted of 15 ml cleared lysate; 9 ml 15% iodixanol in a PBS-MK-high salt buffer; 6 ml 25% iodixanol in PBS-MK buffer supplemented with 15 µl 0.5% Phenored (red); 5 ml 40% iodixanol in PBS-MK buffer; 5 ml 57% iodixanol in PBS Supplemented with 12.5 µl 0.5% Phenored (red).

The tubes were balanced with fluid until the difference between tubes was less than 0.08 g. The tubes were sealed with tube sealer (Beckman 357442). The tubes were centrifuged in a Type 70i Beckman fixed-angle rotor at 55,000 rpm for 90 minutes at 18°C.

Tubes were wiped with 70% ethanol followed by puncturing from the side with a 20 G needle connected to a 5 ml syringe at a level 1-2 mm above the boundary between 40% and 57% iodixanol gradient zones. Then, a 23 G needle was used to puncture the top of the tube to allow air to enter the tube. The clear 40% iodixanol fraction containing rAAV particles was slowly aspirated into the syringe.

The rAAV solution was concentrated to 1 ml with a Biomax-100K NMWL filter device (Millipore UFC910024) by centrifugation. After washing three times with PBS, the concentrated rAAV solution aliquots were stored at -80°C

The stock solution used in the gradient:

2 x PBS-MK-high salt buffer: 2 M NaCl, 20 mM Na_2PO_4, 20 mM NaH_2PO_4, 2 mM $MgCl_2$, 5 mM KCl

10 x PBS-MK buffer: 1.37 M NaCl, 100 mM Na_2PO_4, 100 mM NaH_2PO_4, 10 mM $MgCl_2$, 25 mM KCl

3.8.3 Purification with heparin affinity chromatography

(Modifed after the SSCP method from the Wilson Lab, Human Gene Therapy 12:71-76.2001)

The cell lysate (15 ml) was incubated with 0.1 mg DNase I and RNase A (Roche) 30 mintues at 37°C, cleared by centrifugation at 3000 rpm for 15 minutes at 4°C. Deoxycholic acid was added to the lysate to a final concentration of 0.5% and incubated at 37°C for 30 minutes. Then the lysate was passed through 5μm and 0.45μm pore-size filters sequentially to remove debris.

8 ml of the heparin agarose suspension was loaded into the 2.5-cm-diameter glass column equipped with a Luer Lock. The matrix was equilibrated with 25 ml PBS, pH 7.4.

The cleared lysate was passed through the heparin agarose column at a flow speed of 1 drop/second. The matrix was washed with 15 ml of low-salt PBS (PBS supplemented with 0.1 M NaCl, pH 7.4) twice. The AAV particles were eluted with 15 ml high-salt PBS (PBS supplemented with 0.4 M NaCl. pH 7.4) and concentrated to the desired volume with a Biomax-100K NMWL filter device (Millipore UFC910024) by centrifugation. After washing three times with PBS, the concentrated rAAV solution aliquots were stored at -80°C

Titers of the rAAV were determined by optical density measurement (Molecular Therapy: vol.7, No.1 Method). The UV absorbance at 260 nm and 280 nm of the denatured rAAV samples were measured with a spectrometer (Ultrospec 2000, Pharmacia Biotech). The molar extinction coefficients of the combined capsid proteins were determined empirically by amino acid analysis; the absorbance at 260 nm and the 260nm/280nm ratio were used to calculate the concentration of the rAAV vector genome according to the formula: Vector genome/ml = $4.47 \times 10^{19} (A_{260}-0.59A_{280})/MW_{DNA}$

3.9 PAGE and immunoblot

A reducing SDS-PAGE system with 7.5% or 10% polyacrylamide gel was used to evaluate protein samples from cell extracts.

***Protein sample preparation**:* Cell extracts were prepared by resuspending and incubating cells in lysis buffer (50 mM Tris, 150 mM NaCl, 2 mM EDTA, 1% Triton-100) for 30 minutes at RT. Protein concentration was determined by Lowry's method (1951).

Protein samples used for SDS-PAGE were prepared by incubating the lysate at 95°Cfor 10 minutes, with loading buffer (6 x buffer: 0.2M Tris-HCl, 48% glycerol, 4% SDS, 2% β-mercaptoethanol, 0.2% bromophenol blue, pH 6.8).

***Electrophoresis**:* Samples were run in 7.5% and 10.0% SDS polyacrylamide gel at a constant current of 20mA/gel with an electrophoresis system (BioRad MiniProtean II) according to the Laemmli method (1970). Pre-stained protein standards (Bio-Rad 161-0318) were used to monitor the protein separation during electrophoresis, which

indicated the efficiency of protein transfer to the membrane in the following immunoblots.

Immunoblots: The proteins in the gel were blotted on a PVDF membrane pre-treated with 95% methanol. The blotting was conducted overnight at constant voltage 20V/gel in 4°Ccold room in blotting buffer (25 mM Tris, 192 mM glycine, 20% Methanol) with a wet blot system (BioRad TransBlotCell)

.

After the transfer, the PVDF membrane was blocked by rinsing in 95% methanol for 10 seconds, dried for 30minutes at RT, and then incubated in primary antibody solution (1.5% TopBlock reagent (VWR AG. Switzerland) in TBST containing 20 mM Tris, 150 mM NaCl and 0.1% Tween-20, pH 7.4) overnight at 4°C. Polyclonal antibodies R140 and R85 against mouse calsyntenin-1 were diluted at 1:500 or 1:1000 for Western blots.

R85 antibodies recognizing the cadherin domain in the extracellular part were produced by immunizing rabbits with the recombinant peptide containing 43-295 residues of murine calsyntenin-1. R140 antibodies were raised against several peptides from the cytoplasmatic part of murine calsyntenin-1. The anti-alpha-actin antibody (sigma) was used in Western blots to detect alpha-actin as a loading control. After washing 3 times with TBST at RT, the PVDF membrane was incubated in a secondary antibody solution (1.5% TopBlock reagent in TBST, HRP-conjugated goat-anti-rabbit IgG diluted at 1:20,000) for 1 hour at RT.

Detection of secondary antibody-bound protein was achieved with the Enhanced Chemiluminescent (ECL) substrate kit (SuperSignal WestPico, Pierce) or with a freshly prepared home-made HRP-ECL substrate. The home-made substrate was prepared by mixing Buffer A (0.25 mM Luminol/DMSO, 0.05 mM p-Cormaric acid/DMSO in 0.1 M Tris-HCl, pH 8.5) with Buffer B (0.02% H_2O_2 in 0.1 M Tris.Cl pH 8.5) in equal volumes. The PVDF membrane was incubated in the mixture for 10 minutes. The ECL emission was visualized and processed with a Fuji cooled CCD camera in Stella unit (Raytest, Germany) and combined software package.

3.10 Immunocytochemistry

Cells grown on coverslips were fixed for 10 minutes with 4% paraformaldehyde (PFA) in PBS (pH 7.4) containing 4% sucrose at RT, pre-incubated for 1 hour in blocking PBS supplemented with 10% FCS and 0.1% glycine at RT. The coverslips were exposed overnight to well-characterized primary antibodies diluted with PBS supplemented with 3% FCS and 0.1% saponin at RT. (R140 diluted at 1:100, GM 130 diluted aqt 1:500). After washing with PBS containing 0.1% Tween-20, the cells were incubated in secondary antibodies in PBS supplemented with 3% FCS, 0.1% saponin for 1 hour at RT in dark. Secondary antibody G&R-Fitc/ D&G-Fitc/D&R-cy3/D&M-cy5 (Jackson Immuno-Research Laboratories) were diluted in 1:300 to 1:500. The coverslips were washed with PBS and mounted on glass slides with fluorescent mounting medium (DakoCytomation).

3.11 Immunohistochemistry on organotypic slices culture

The cultures were washed 3 times with PBS, fixed with 4% PFA in 0.1 M PB buffer for 10 minutes. After three washes with PBS, the cultures were incubated overnight at 4°C in 0.1 M PB buffer supplemented with 30% sucrose solution and 12% glycerol. The cultures were frozen and thawed in dimethylbutane at -40~-50°C to increase the permeability to the antibodies. Then the cultured slices were removed from the cover slips or membranes with a brush. From then on, the culture was freely floating in the solution.

The cultures were blocked in 10% horse serum in PBS for 1 hour and then incubated 5 days in primary antibody solution (10% horse serum, 0.3% Triton-100, 1% NaN3 in PBS, antibody R140 diluted at 1:100.) at 4°C with a cold room shaker. After washing with PBS, the cultures were transferred into secondary antibody solution (10% horse serum, 0.3% Triton-100) and incubated overnight with a 4°C shaker. The cultures were thoroughly washed with PBS for 2 days with a 4°C shaker and then mounted onto glass slides with fluorescent mounting medium (DakoCytomation) and cover slips.

3.12 Fluorescent microscopy

Fluorescence of cells on coverslips was viewed with a fluorescent microscope (Axiophot, Carl Zeiss). Images were captured with a Zeiss camera AxioCam or Leica confocal microscope TCS-SP1. DAPI and Hoechst fluorescence of nuclei was captured by excitation at 330-380 nm with a 440 nm barrier filter. Cy3 fluorescence was visualized by excitation at 510-550 nm, with a barrier of 590 nm. Cy5 fluorescence was detected by excitation at 590-650 nm, with a barrier of 700 nm. FITC/GFP fluorescence was visualized by excitation at 470-490 nm, with a barrier of 520-580 nm.

3.13 Morphological analysis

Primary hippocampal neurons were plated at low density in $2x10^4$cells/ml for morphological analysis. 10 days after the AAV infection, the cells were fixed in 4% PFA in PBS containing 4% sucrose for 10 minutes. After rinsing with PBS, coverslips were mounted onto glass slides with fluorescent mounting medium (DakoCytomation).

For each treatment, 10 green fluorescent neurons were randomly selected from the microscopic fields and images were captured with a CCD video camera. The numbers of primary dendrites originating from neuronal soma and the secondary dendrite branches were counted to evaluate dendritic development.

3.14 NMDA-induced excitotoxicity in primary neuronal culture

Primary neuronal cells infected with calsyntenin-1 overexpressing or down-regulating rAAV vectors were cultured on 12-well plates for more than 10 days before they were used for excitotoxic studies. The excitotoxic stress was induced by exposing the cells to 100 μM NMDA for 30 minutes. To assess apoptotic responses of the cells to NMDA excitotoxicity, Hoechst staining assays were conducted 24 hours after the NMDA exposure to indicate nuclear condensation in apoptotic cells and apoptotic-like cells.

IV. Results and Discussion

The most common method to study a new gene is to achieve and characterize loss-of-function and gain-of-function. Recently, vector-based siRNA has become a popular tool to investigate genes through the powerful and specific suppression of a particular gene.

RNA polymerase III promoters have been widely used in DNA plasmid vectors to drive the expression of siRNAs to enable long-term gene inhibition of a targeted gene in mammalian cells.

4.1 RNA polymerase III promoters isolated from mouse and human genomic DNA by PCR

Among the RNA polymerase III promoters, the U6 and the H1 promoters are the best characterized, with the U6 promoter stretching several hundred base pairs but the H1 promoter having a relatively short length of 100 base pairs. These two promoters give different patterns of amount and sub-cellular location of siRNAs expression in different cell types.

The essential elements in mammalian U6 and H1 promoters are highly conserved so that human promoters can induce siRNA production efficiently in mouse cell lines. We cloned vectors with the mouse U6 promoter and additionally with human U6 and H1 promoters.

4.1.1 Mouse U6 promoter:

GCGGATCCGACGCCGCCATCTCTAGGCCCGCGCCGGCCCCCTCGCACAGACT
TGTGGGAGAAGCTCGGCTACTCCCCTGCCCCGGTTAATTTGCATATAATATTTCC
TAGTAACTATAGAGGCTTAATGTGCGATAAAAGACAGATAATCTGTTCTTTTTAATA
CTAGCTACATTTTACATGATAGGCTTGGATTTCTATAAGAGATACAAATACTAAATTA
TTATTTTAAAAAACAGCACAAAAGGAAACTCACCCTAACTGTAAAGTAATTGTGTG
TTTTGAGACTATAAATATCCCTTGGAGAAAAGCCTTGTTAACGCTCTAGAGC

4.1.2 Human U6 Promoter:

GCCTCGAGAGGGCCTATTTCCCATGATTCCTTCATATTTGCATATACGATACAAGG
CTGTTAGAGAGATAATTAGAATTAATTTGACTGTAAACACAAAGATATTAGTACAAA
ATACGTGACGTAGAAAGTAATAATTTCTTGGGTAGTTTGCAGTTTTTAAAATTATGT
TTTAAAATGGACTATCATATGCTTACCGTAACTTGAAAGTATTTCGATTTCTTGGCT
TTATATATCTTGTGGAAAGGACGAAACACCTTTTTTAAGCTTGGG

4.1.3 Human H1 promoter:

GCCTCGAGATTTGCATGTCGCTATGTGTTCTGGGAAATCACCATAAACGTGAAAT
GTCTTTGGATTTGGGAATCTTATAAGTTCTGTATGAGACCACTCTTTCCCTTTTTA
AGCTTGGG

Previous studies (Seppo.YH, J.Gene.Med 2006) showed that the U6 promoter is more efficient than the H1 promoter in gene silencing in mouse cells *in vitro* and *in vivo*. Our siRNA vector construction was based mainly on the vector containing the mouse U6 promoter.

4.2 Summary of siRNA constructs against EGFP and mouse calsyntenins

In the hairpin-type siRNA construct, the RNA polymerase III promoter U6 produces small transcripts extending from a well-defined start to a 5T–in-row terminal. Once the siRNA is transcribed, its reverse complementary part folds back immediately to bind tightly to the sense fragment, giving rise to a hairpin structure, which mimics the natural RNA intermediate in the RNA interference pathway and eventually induces a sequence-dependent transcriptional inhibition mediated by RISC (Figure 4.1).

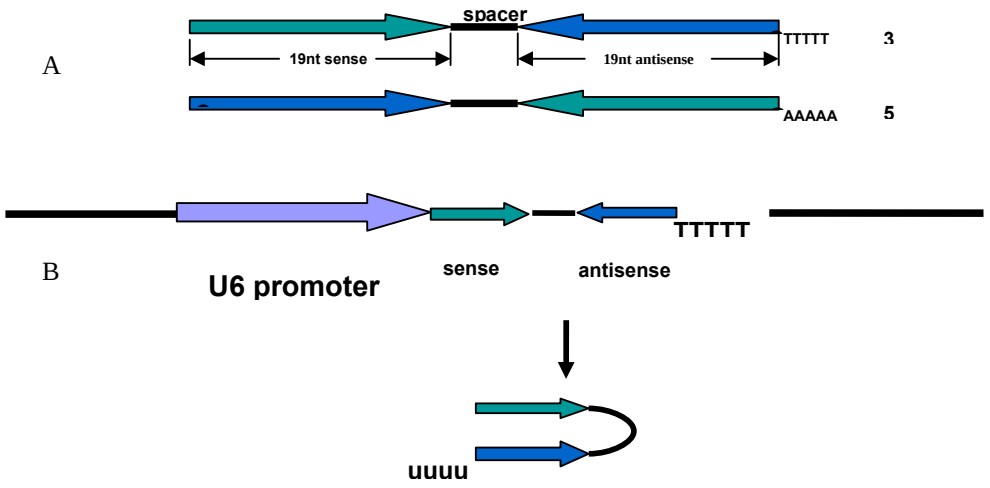

Figure 4.1: Schematic illustration of a hairpin-type siRNA transcribed from a U6-driven vector

A: Design of two complimentary oligonucleotides

B: siRNA generated by a hairpin-type siRNA cassette: The siRNA transcripts fold back to bind tightly with the complementary sequences to form hairpin structure, which mimic the natural RNA intermediate in the RNA interference pathway.

GCGGATCCGACGCCGCCATCTCTAGGCCCGCGCCGGCCCCCTCGCACAGACT
TGTGGGAGAAGCTCGGCTACTCCCCTGCCCCGGTTAATTTGCATATAATATTTCCTAG
TAACTATAGAGGCTTAATGTGCGATAAAAGACAGATAATCTGTTCTTTTTAATACTAGCT
ACATTTTACATGATAGGCTTGGATTTCTATAAGAGATACAAATACTAAATTATTATTTTAA
AAAACAGCACAAAAGGAAACTCACCCTAACTGTAAAGTAATTGTGTGTTTTGAGACTA
TAAATATCCCTTGGAGAAAAGCCTTGTTT(GGAGCTGTTCACCGGGGTG)TTCAAGAG
A(CACCCCGGTGAACAGCTCC)TTTTTTAACGCTCTAGAGC
pBlueU6-siEGFP.1 targeting EGFP gene 18-37bp

(GCCCACCCTCGTGACCACC)TTCAAGAGA(GGTGGTCACGAGGGTGGGC)TTTTT
pBlueU6-siEGFP.2 targeting EGFP gene 173-192bp

(GCGTGCAGCTCGCCGACCA)TTCAAGAGA(TGGTCGGCGAGCTGCACGC)TTTTT
pBlueU6-siEGFP.3 targeting EGFP gene 536-545bp

(GGTGAACGACGTGAACGAG)TTCAAGAGA(GTCGTTCACGTCGTTCACC)TTTTT
pBlueU6-siCst1.1 targeting mouse calsyntenin-1 458-476bp

(GGCTGTCTTCCCGAGCATC)TTCAAGAGA(GATGCTCGGGAAGACAGCC)TTTTT
pBlueU6-siCst1.2 targeting mouse calsyntenin-1 842-860bp

(GGACCCGTCTGAGGAGAG)TTCAAGAGA(CTCTCCTCAGACGGGTCC)TTTTT
pBlueU6-siCst1.3 targeting mouse calsyntenin-1 1298-1316bp

The vector pBlueU6-siNonsense, producing siRNA transcripts that do not target any mammalian gene, is designed as a control to validate the specificity of the RNA interference.
(GGCATACCGCCCCGGGATG)TTCAAGAGA(CATCCCGGGGCGGTATGCC)TTTTT
The target sequence of nonsense siRNA is derived from rice genome (Oryza sativa: EF576615.1).

siRNA targeting different sites of the same gene demonstrates strikingly different gene silencing efficiency. This positional effect may relate to the different accessibility of the siRNA to target sites on mRNA. Up to now, no clear correlation between target sequence and siRNA potency has been revealed except for a slight bias to lower GC content (about 40%) within the target sequence. Multiple sites were usually selected randomly along the target gene sequence to construct a pool of siRNA plasmids, which was then screened for the most effective one. Statistically, only one fourth of siRNA plasmids against a particular gene result in significant reduction in gene expression.

The specificity of the siRNA is exclusively sequence dependent, which means single nucleotide mutations in siRNA sequence may abolish the gene silencing effect. To ensure the specificity of the siRNA, potential target sites were screened with an appropriate

genome database www.ncbi.nlm.nih.gov/BLAST to avoid homology to other functional coding sequences. Moreover, all of the siRNA plasmids were proofread repeatedly by PCR sequencing.

Unfortunately, in many cases chromatography shows that the sequencing reaction was quelled at the start region of the siRNA sequence. This can be explained by the fact that the strong secondary structure in the siRNA hairpin is extremely difficult to sequence by the PCR sequencing method. (Figure 4.2)

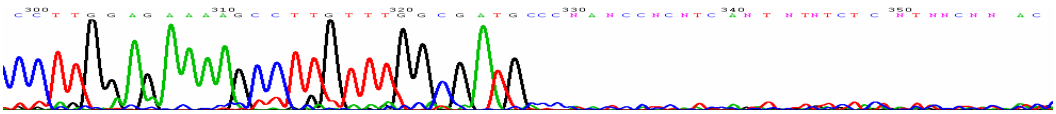

ACCTTGGAGAAAAGCCTTGTTTGCGTGCAGCTCGCCGACCAttcaagagaTGGTCGGC
GAGCTGCACGC)TTTTT

Figure 4.2: Sequencing quelled at siRNA region

We have had success in breaking through the siRNA hairpin regions by using a combination of addition of DMSO to a final concentration of (v/v) 10% and pre-denaturation of template DNA at 96°C for 5 minutes before PCR sequencing. But both the addition of DMSO and the pre-denaturation impaired the performance of the DNA polymerase in the reaction system, leading to inaccurate base identification and even total shut down of the reaction.

To circumvent these sequencing obstacles, tandem-type siRNA constructs were designed and cloned. In this system, no strong secondary structure was formed between the sense and antisense sequence of the siRNAs since they were cloned separately and under the control of different RNA polymerase III promoters. The individually transcribed RNA strands were predicted to bind to each other to form double-stranded RNA, which could be further transformed in the RNA interference pathway, leading to target gene silencing. (Figure 4.3)

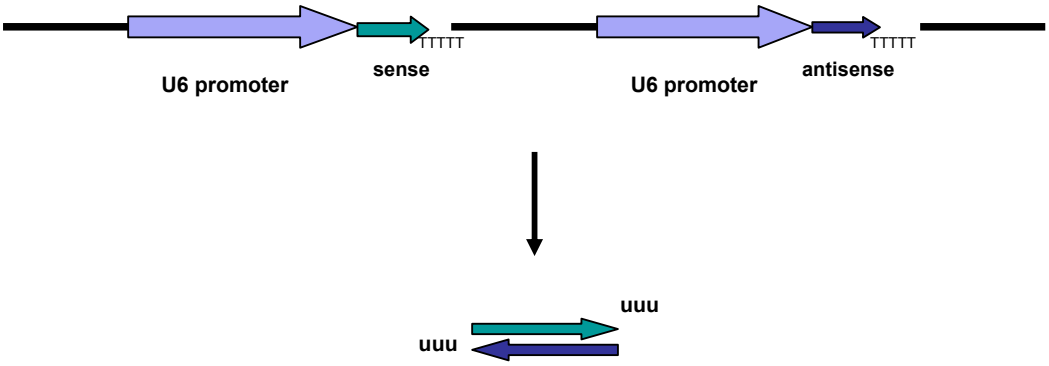

Figure4.3: Schematic illustration of siRNA generated by the U6-driven tandem-type siRNA vector

In tandem-type siRNA system, no strong secondary structure was formed between the sense and antisense sequence of the siRNAs since they were cloned separately and under the control of different RNA polymerase III promoters. The individually transcribed RNA strands anneal to each other to form active siRNA duplex, which could be transformed in the RNA interference pathway, leading to target gene silencing.

One tandem type siRNA construct pBlueU6-siEGFP-T was cloned to target the EGFP gene at 173-192bp.

GCCCACCCTCGTGACCACCTTTTTT sense strand

GGTGGTCACGAGGGTGGGCTTTTT antisense strand

4.3 Testing with EGFP

Initially, a series of siRNA vectors against enhanced green fluorescent protein (EGFP) were designed and constructed to validate our vector-based siRNA system in mammalian cells. siRNA vectors against the EGFP gene, such as pBlueU6-siEGFP.1 etc. were co-transfected with EGFP expressing vector pEGFP-N1 into HEK293T cells using the lipofactamine 2000 reagent. The intensity of green fluorescence provided a direct evaluation of the EGFP expression level when visualized with fluorescent microscopy.

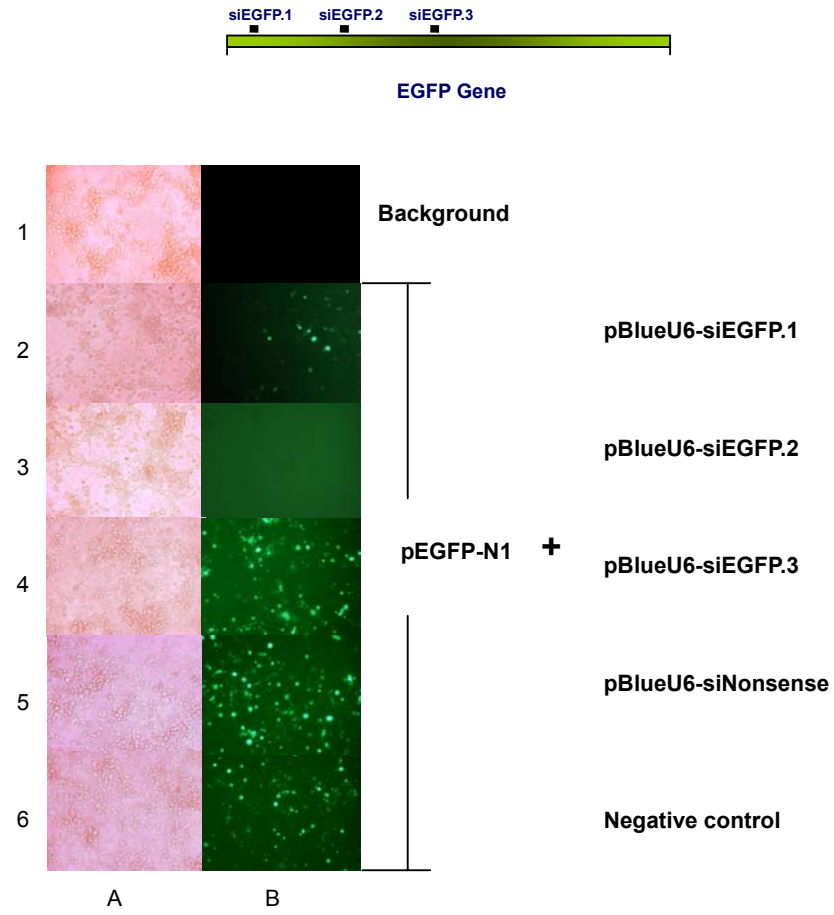

Figure 4.4: Silencing co-transfected EGFP expression in HEK293T cell lines by siEGFP gene transfer

siRNA plasmids targeting the EGFP gene were co-transfected with EGFP expressing vector pEGFP-N1 into HEK293T cells using the lipofactamine 2000 reagent. The intensity of green fluorescence provided a direct evaluation of the EGFP expression level when visualized with fluorescent microscopy.
A: normal light
B: green fluorescent: The intensity of green fluorescence indicates the EGFP expression level which is negatively proportional to knockdown efficiency of the corresponding siRNA plasmid.

As shown in figure 4.4, the reduction of green fluorescence intensity indicated that

EGFP expression was down-regulated by all three siEGFP constructs at different levels when normalized with green fluorescence intensity in the siNonsense control, which showed no obvious interference of EGFP expression. The pBlueU6-siEGFP2 targeting EGFP gene 173-192bp demonstrated the most efficient EGFP reduction. (Figure 4.4)

The lipofectamine 2000 reagent could achieve 97% transfection efficiency in NG108-15 cells when determined by flow cytometry, offering a powerful tool to deliver plasmid DNA into cell lines. The hairpin-type construct pBlueU6-siEGFP.2, its derivative pBlue6-siEGFP-m that has a single nucleotide mutation in siRNA sequence, and the tandem-type construct pBlueU6-siEGFP-T were co-transfected with the EGFP-expressing vector pEGFP-N1 into NG108-15 cells, respectively. (Figure 4.5)

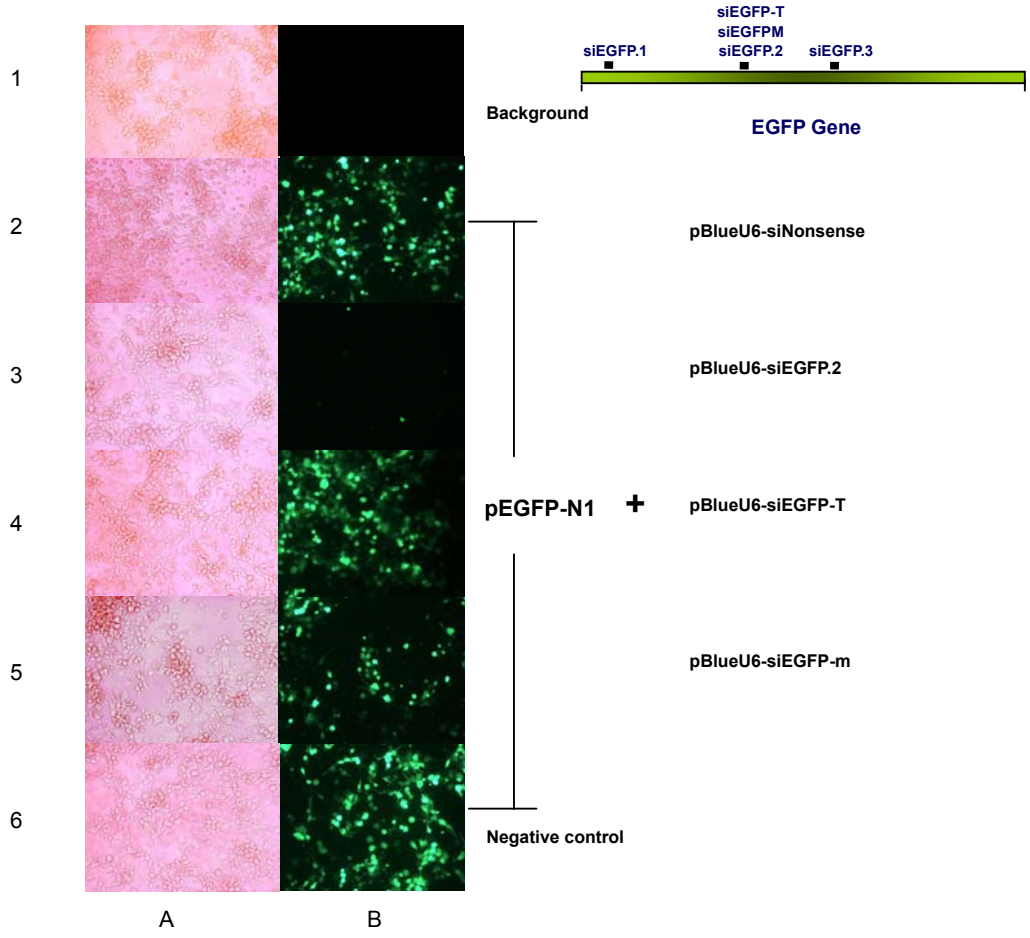

Figure 4.5: Silencing EGFP expression in the NG-108 cell line by siEGFP gene transfer

siRNA plasmids targeting the EGFP gene were co-transfected with EGFP expressing vector pEGFP-N1 into NG-108 cells using the lipofactamine 2000 reagent. The intensity of green fluorescence provided a direct evaluation of the EGFP expression level when visualized with fluorescent microscopy.
A: normal light
B: green fluorescence: The intensity of green fluorescence indicates the EGFP expression level which is negatively proportional to knockdown efficiency of the corresponding siRNA plasmid.

Even derived from the same target sequence, the hairpin-type siEGFP suppressed EGFP expression more efficiently than the tandem-type siEGFP in this case. The mutant derivative pBlueU6-siEGFP-m shows significant sabotaged ability of target gene silencing compared with the fully-sequence-matched pBlueU6-siEGFP.2, suggesting the strict sequence dependent specificity of the siRNA system.

To exclude the possibility that the EGFP reduction is due to the interference during gene transfection, the cultures transfected with pBlueU6-siEGFP.2 were examined with over-exposure at 3000 ms to detect the reduced green fluorescence. The results demonstrated that the transfection of EGFP-expressing vector pEGFP-N1 was successful. EGFP expression was generally suppressed in the cells by siEGFP (Figure 4.6).

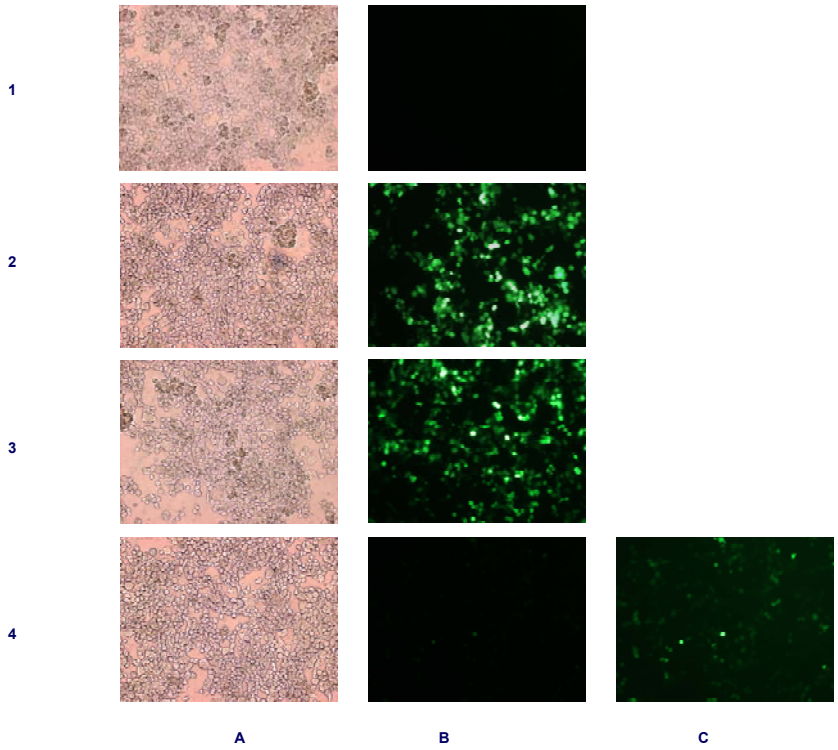

Figure 4.6: Silencing EGFP expression in the NG-108 cell line by siEGFP gene transfer.

siRNA plasmids targeting the EGFP gene were co-transfected with EGFP expressing vector pEGFP-N1 into NG-108 cells using the lipofactamine 2000 reagent. The intensity of green fluorescence provided a direct evaluation of the EGFP expression level when visualized with fluorescent microscopy.
A: Normal light; **B**: Green fluorescence (30 ms);
C: Green fluorescence overexposure (3000 ms)
The intensity of green fluorescence indicates the EGFP expression level which is negatively proportional to knockdown efficiency of the corresponding siRNA plasmid.
1: control;
2: pEGFP-N1 transfection;
3: Co-transfection of pEGFP-N1 and pBlueU6-Nonsense;
4: co-transfection of pEGFP-N1 and pBlueU6-siEGFP-2

The efficiency of EGFP suppression by siRNA was determined with flow cytometry. The percentage of EGFP positive cells was recorded and calculated, giving a 60% reduction of EGFP positive cells with pBlueU6-siEGFP.2 when normalized to the control pBlueU6-siNonsense (Figure 4.7).

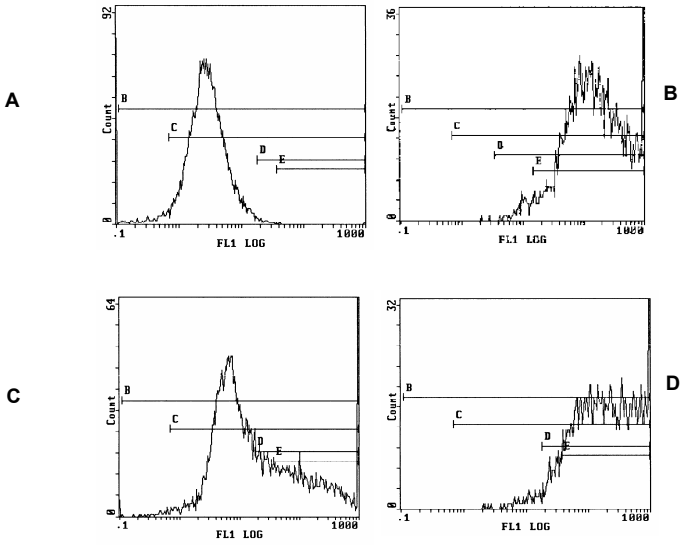

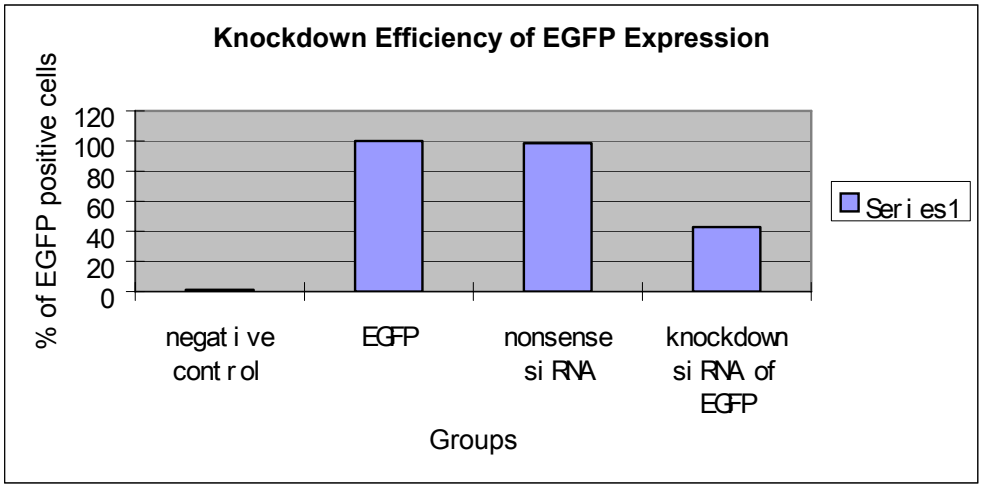

:

Figure 4.7: Determining silencing efficiency of EGFP expression with flow cytometry

The efficiency of EGFP suppression by siRNA was determined with flow cytometry. The percentage of EGFP positive cells was recorded, calculated and normalized with pBlueU6-nonsense control.
A: Background control
B: EGFP expression
C: siRNA against EGFP
D: Nonsense siRNA control

4.4 Down-regulating co-transfected calsyntenin-1 expression in the NG108-15 cell line

siRNA constructs against calsyntenin-1 were tested in the NG-108 cell line by co-transfection with the calsyntenin-1 over-expressing vector pcDNA3.1-mmCst1. Immunoblotting with the polyclonal antibody R140 recognizing the cytoplasmic part of calsyntenin-1 revealed that co-transfected calsyntenin-1 expression was suppressed to undetectable levels by pBlueU6-siCst1.1 (Figure 4.8).

The specificity of the knockdown was validated with the nonsense control pBlueU6-siNonsense, which did not show obvious interference to calsyntenin-1 expression. The data were normalized to endogenous housekeeping gene alpha-actin expression as aninternal control to validate the experiment.

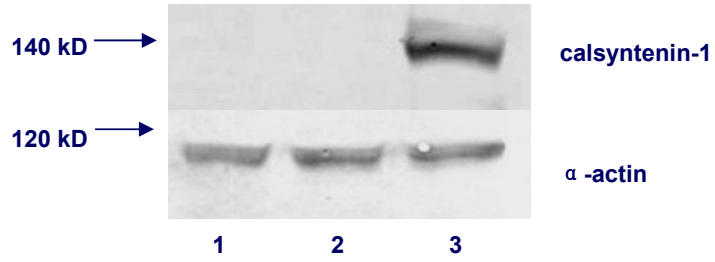

Figure 4.8: Down-regulation of co-transfected calsyntenin-1 by the corresponding siRNA in the NG-108 Cell Line

1: control
2: pcDNA3.1-cst1 co-transfected with pBlueU6-siCst1-1
3: pcDNA3.1-cst1 co-transfected with pBlueU6-nonsense

Endogenous calsyntenin-1 and 3 expressions in NG108-15 cells were detected at the transcriptional level with RT-PCR. Calsyntenin-2 expression could not be detected with this method. But the expression level of calsyntenin-1 and 3 in this cell line is very low and beyond the sensitivity of immunoblotting detection.

A semi-quantitative RT-PCR method was developed to examine calsyntenin down-regulation using mRNA normalized to the housekeeping gene GAPDH. However, many highly variable factors involved in the method could affect the accurate reflection of gene activity, resulting in unstable and irreproducible readouts (data not shown).

To date, the factors affecting the potency of the vector-based siRNA system to knock down endogenous calsyntenin remain unclear. In the future, quantitative real-time RT-PCR, a well-established and sensitive approach to quantify specific mRNA abundance, could be used to evaluate siRNA-mediated calsyntenin silencing at the mRNA level.

4.5 Primary hippocampal neuronal culture

Cultured neurons develop both morphologically and functionally in dissociated primary neuronal culture, providing a simplified and easily accessible *in vitro* model to investigate the properties and functions of neurons. The highly preserved key phenotypic features such as polarity and synaptic connections represent advantages over continuous neuronal cell lines for this type of research.

The hippocampus is the most commonly used structure in preparing neuronal cultures since its well-defined structure can be easily isolated from the brain and its relatively simple cell populations, with a vast majority of pyramidal cells dominating over many fewer interneurons, giving a relatively homogenous culture. Over several decades, intensive studies have provided a comprehensive understanding of the many features of hippocampal neurons in the culture, offering helpful guidelines to new experiments.

Dissociated neuronal cultures were prepared from hippocampi of embryonic 18-day-old mouse. Cells were cultured on poly-L-lysine coated coverslips in chemically defined medium. Low-density cultures with widely spaced cells are ideal for imaging and morphological studies. High-density cultures are often prepared for biochemical anaylsis such as immunoblotting and immunopercipitation (Figure 4.9).

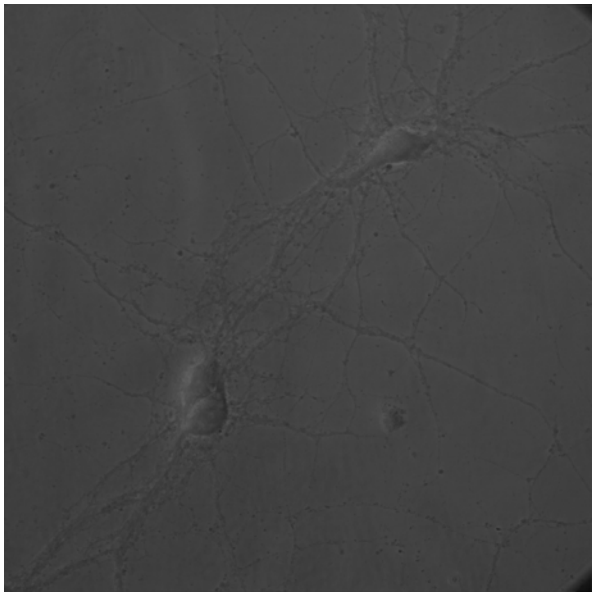

Figure 4.9: Dissociated primary hippocampal neuronal culture growing on coated coverslips at a low-density

The dissociated primary hippocampal neuronal culture prepared from E17-18-day-old mouse which grow on the poly-L-lysine coated coverslips for 14 days, exhibiting preserved morphological features.

Consistent calsyntenin-1, -2 and -3 expressions were detected with RT-PCR in mouse primary hippocampal neuronal culture (Figure 4.10).

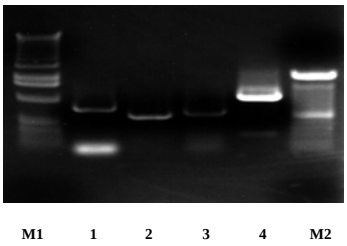

M1: marker 1
1: Calsyntenin-1
2: Calsyntenin-2
3: Calsyntenin-3
4: GAPDH
M2: marker 2

Figure 4.10: RT-PCR for calsyntenin expression profile with total RNA prepared from mouse primary hippocampal neuronal culture

Calsyntenin-1, -2,-3 are expressed in mouse primary hippocampal neuronal cultures

4.6 Organotypic hippocampal slice culture

The organotypic culture is an *in vitro* system in which differentiated cells closely resemble their *in vivo* counterparts, offering a possibility to establish easy-to–manipulate and biologically meaningful 3-dimensional models with well-preserved structure and function in a native-like configuration. The principle neuronal populations, pyramidal neurons and granule cells, are well-characterized in hippocampal slice cultures. Also, the connectivity of the neurons in culture has been well characterized in previous studies. Therefore, the hippocampal slice culture has been widely used to investigate many aspects of neuronal function, such as neuronal development, electrophysiological properties and pathology.

Following the method developed by Stoppini et al in 1991, hippocampal slice cultures were prepared from postnatal 6-day-old neonates and maintained on semi-permeable membranes in culture at the interface of a humidified atmosphere and medium. When plated, the slices spontaneously attach to the membrane and flatten down to about 100 µm in thickness from the original 300 µm within a few days. In Nissl-stained culture, sub-regions such as the dentate gyrus (DG), CA1 and CA3 are highly distinguishable from each other, demonstrating histological preservation and integrity (Figure 4.11).

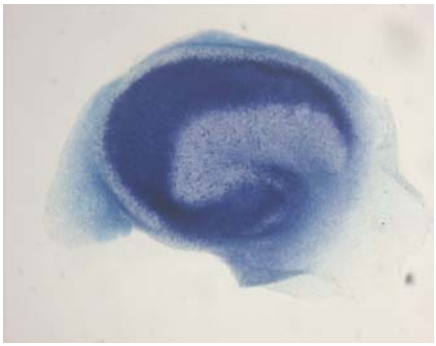

Figure 4.11: Nissl-stained organotypic hippocampal slice culture

The Nissl-stained hippocampal slice culture shows histological preservation and integrity.

Immunoflorenscence staining with the antibody R140 and the neuronal marker NeuN reveals the calsyntenin-1 expression profile in mouse hippocampal slice culture, with the neurons in CA3 region showing the strongest calsyntenin-1 distribution (Figure 4.12).

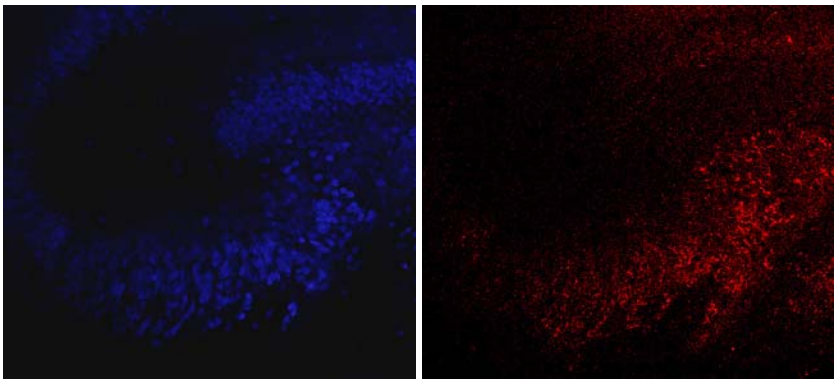

Figure 4.12 Calsyntenin-1 expressions in mouse organotypic hippocampal slice culture

Blue: NeuN neuronal marker that stains the nuclei of neurons
Red: Mouse calsyntenin-1 detected with the R140 antibody

4.7 The attempts to transduce neurons in primary neuronal culture and organotypic slice culture

To deliver the siRNA cassettes into neurons in culture, we first tried several nonviral approaches, which are considered less time-consuming and do not require complicated molecular biological facilities for their application.

It is well known that the post-mitotic, terminally differentiated neurons are among the most difficult cell types to be transduced by foreign genetic materials. The routinely used non-viral methods for cell transfection such as liposome reagents, electroporation, biolistics (gene gun) all encountered significant problems in neurons, resulting in poor efficiency of gene delivery. We followed a protocol for transfection with the lipofectamine 2000 reagent at a low concentration, which has been reported to achieve high throughput gene delivery consistently in primary neurons. Transfection efficiency was evaluated 3 days later when the transfected cells were indicated by the green fluorescence of the EGFP marker. In our experience, Lipofectamine 2000 achieved only 10% transfection efficiency within the surviving cells, and the lifespan of the transduced neurons was drastically reduced to about 1 week. In addition, obvious morphological disruption, such as reduced neuronal dendritic branching, was observed in most of the neurons (Figure 4.13).

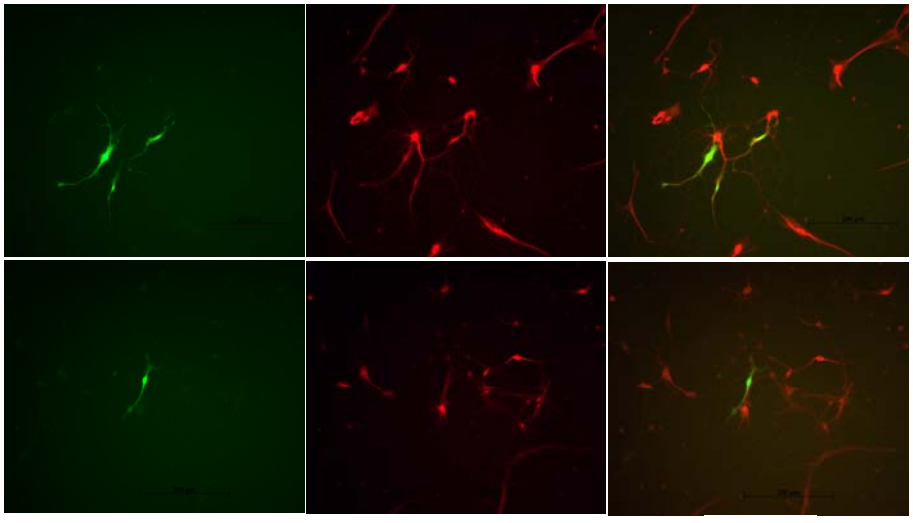

EGFP R140 Merge

Figure 4.13: Lipofectamine 2000 transfection in primary hippocampal neuronal culture

Lipofactamine 2000 achieves very low transfection efficiency in primary neuronal cultures. Obvious morphological disruption such as reduced neuronal dendritic branching was observed in most of the cells.

Electroporation is a mechanical delivery approach that works by transiently increasing the permeability of the cell membrane with externally applied electrical current. In the strong pulsing electrical field, the plasma membrane is temporarily disturbed, allowing the foreign compounds to enter the cell.

Based on the description of the electroporation device that have been used to successfully transfer DNA into mouse brain tissues (Weaver, 1995), we set up an electroporation system with a pair of home-made plate-like electrodes and a pulse generetor (BTX products). A constant and evenly distributed electrical field was generated between the parallel electrodes when current was applied (Figure 4.14).

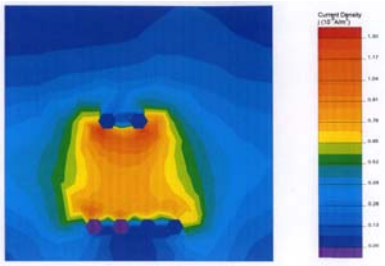

Figure 4.14: Measurement of electrical field distribution and density

After pulsing hundreds of slices, we found that the method is not applicable for organotypic cultures because of its low efficiency, poor reproducibility and unclear cellular specificity. In our experience, only few cells, mainly located in the marginal region of the slice culture, were transduced (Figure 4.15).
Additionally, cell damage and even tissue rupture were observed frequently after electroporation.

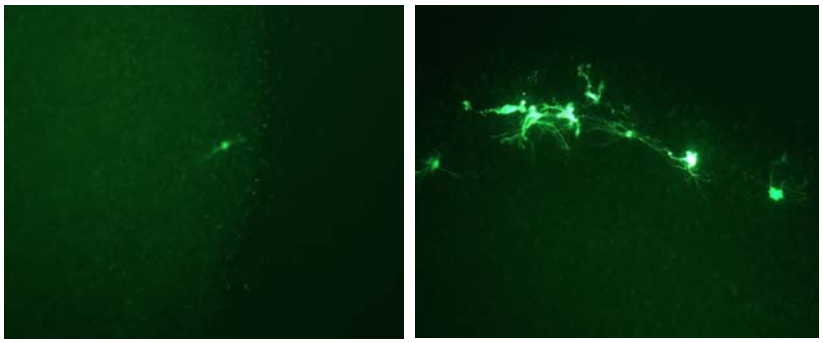

Figure 4.15: Electroporation in an organotypic hippocampal slice culture
Electroporation achieves very low efficiency and poor reproducibility in tranducing hippocampal slice cutures. Only few cells located in the margin eare were transduced without any cellular specificity. Cell damage and tissue rupture were generally observed after the manipulation.

Recently, advanced electroporation techniques such as the cellaxess CX1 capillary have become commercially available as a potential tool offering higher competency to introduce genes into cells in organotypic slice cultures.

4.8 Recombinant adeno-associated virus vector

Frustrated by the electroporation and liposome delivery system, we switched our efforts to setting up a viral vector system, which may allow better transduction in neurons. Compared with other viral vectors being used in gene delivery, recombinant adeno-associated vector (rAAV) is distinguished by its outstanding efficiency to transduce post-mitotic neurons long-term efficacy, safety and, most importantly, the minimal disturbance of the host gene expression profile. The stable integration of the AAV vector into the host genome allows persistent transgenic expression. The fact that the AAV vector is not associated with human pathology because it cannot replicate allows all the experiments to be conducted in ordinary laboratory settings. Additionally, rAAV vectors and the methods of preparation are well-established, permitting straightforward implementation of the technique.

Briefly, the generation of recombinant AAV vectors employs the complete replacement of the wild type AAV genome with genes of interest flanked by two 145bp viral ITR (Inverted Terminal Repeats) sequences that contain signals for packaging. When the recombinant AAV plasmids were co-transfected with the helper plasmid pDG, which contains genes encoding AAV structural capsid proteins and other proteins necessary for viral packaging, the ITR could be specifically recognized and recruited by the viral capsid, leading to efficient packaging of the transgene into the infectious virus. The cloning capacity of the AAV subtype 2 vector is limited to approximately 5.0kb of DNA.

ITR sequences also carry the signals involved in virus integration, allowing the transgene cloned between the two ITRs integrated into the host genome to achieve stable long-lasting expression.

4.8.1 AAV infection of hippocampal slice cultures

We tested the efficiency of AAV infection in slice cultures by simply adding the solution containing a recombinant AAV vector carrying an EGFP maker into the medium immediately after the preparation of the slices. 10 days after the infection, large numbers of green fluorescent cells were detectable (Figure 4.16).

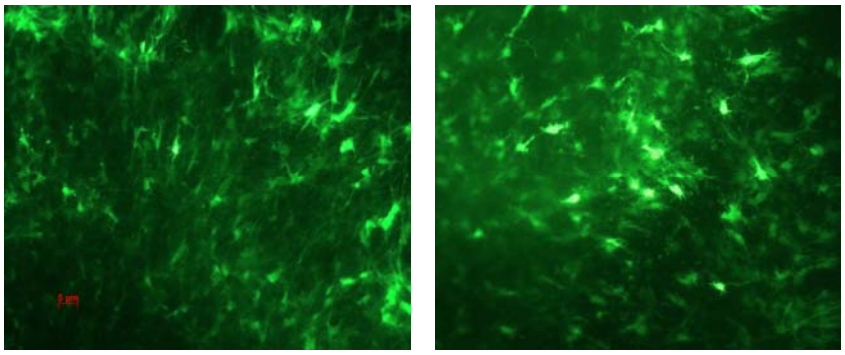

CA1 region **CA3 region**

Figure 4.16: AAV infection in a hippocampal slice culture.
AAV vector carrying EGFP reporter shows promising transfection efficiency in subregions CA1 and CA3 of hippocampal slice culture.

To evaluate cell tropism associated with AAV infection in slice cultures, an antibody against the neuronal marker NeuN was used for immunofluorescence staining to identify neurons. As shown below, only few NeuN positive cells overlapped with EGFP fluorescent cells, suggesting that most of AAV infected cells are not neurons (Figure 4.17).

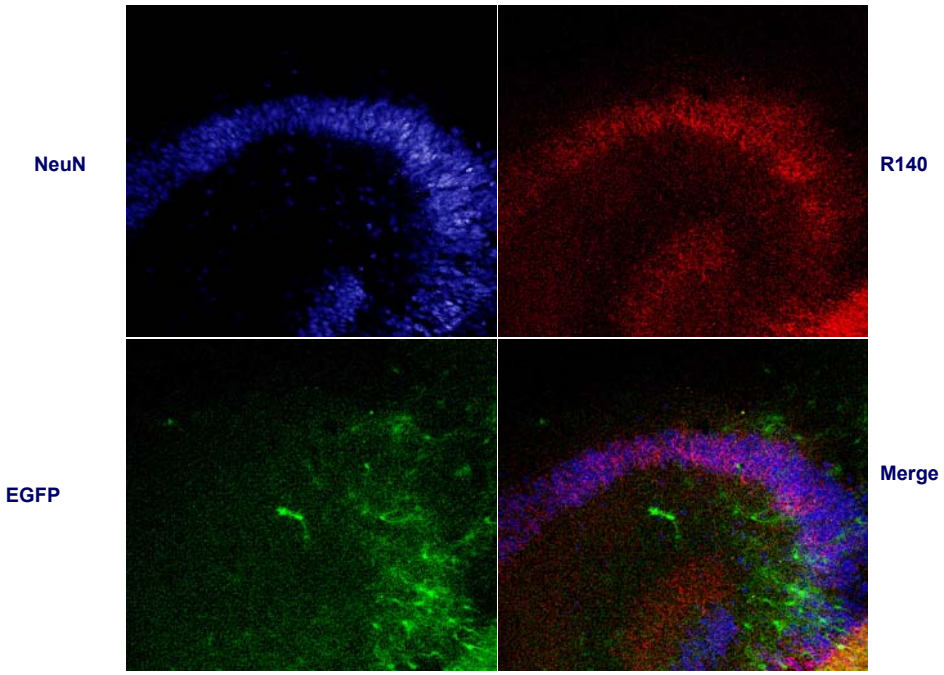

Figure 4.17: AAV infection in a hippocampal slice culture
Neurons indicated by neuronal marker NeuN do not show much overlap with the cells expressing AAV-introduced EGFP reporter. Calsyntenin-1 indicated by R140 antibody is mainly expressed in pyramidal neurons.

A previous study (Ehrengruber, M.U., 2001) of a vector derived from Semliki forest virus (SFV) demonstrated high transduction of neurons in hippocampal slice cultures, but the method can only be used for short-term studies since the viability of infected cells was drastically reduced because of virus-induced cytotoxicity at 7 days after the infection.

In addition, the Biolistic technique (biological ballistics) has been used successfully to deliver DNA into neurons in organotypic slice cultures by shooting DNA-coated gold particles directly into cells (McAllister.A.K, 2000). But this approach is limited by its low cellular specificity and the requirement of costly instruments.

4.8.2 AAV infection in primary neuronal cultures

Fortunately, the AAV approach demonstrated very promising infection patterns in primary hippocampal neuronal cultures when tested with the AAV-CMV-EGFP vector. In optimized conditions, the transfection efficiency could reach as high as 90%.

AAV was applied to the medium immediately after the neurons were plated. The green fluorescent cells could be detected under the microscope at 7 days after infection. The high-grade EGFP expression was sustained for 6 weeks until neurons in the culture died (Figure 4.18).

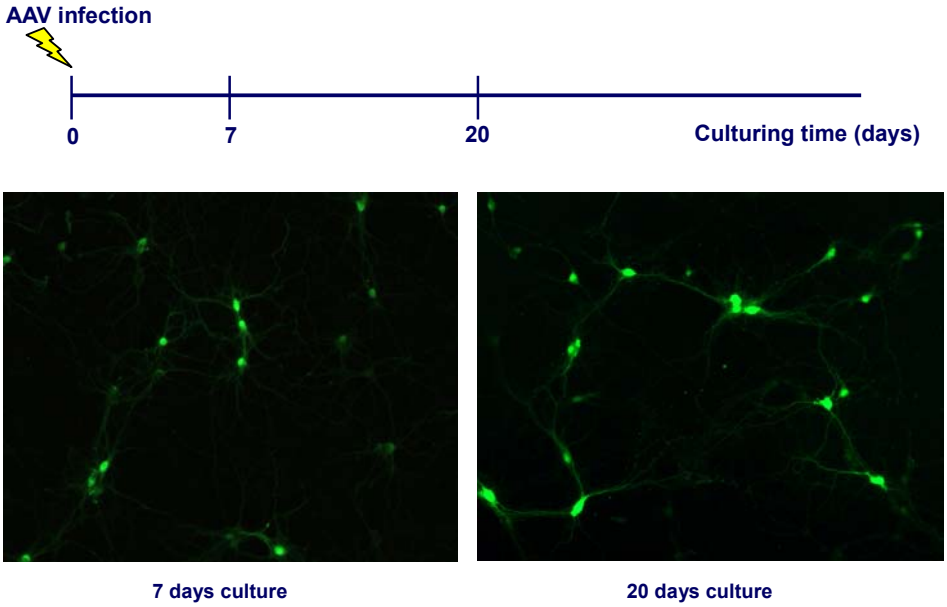

Figure 4.18: AAV infection in primary hippocampal neuronal cultures

Green fluorescence of EGFP reporter can be detected in primary hippocampal neuronal culture 7 days after infection.

]

In our experience, rAAV proved to be a highly versatile transfection vector in primary neuronal cultures resulting in stable and long-term expression after a single administration.

4.8.3 Construction of an AAV-siRNA vector with an EGFP marker

The parent vector psubAAV2-CMV-WPRE was used to construct the AAV vectors to express siRNAs.

First, the cassette for EGFP expression was isolated from pEGFP-N1 and subsequently cloned into the AAV vector, giving a marker for infected cells. The resulting psubAAV2-CMV-EGFPN1 plasmids were screened with RE analysis and further analyzed by transfection into HEK293T. Green fluorescence was detectable at 24 hours after transfection.

AAV particles were produced according to the preparation and purification methods described above. The HEK293T cells infected with AAV particles AAV-CMV-EGFPN1 efficiently expressed EGFP, which was detectable with fluorescent microscopy at 72 hours after infection, demonstrating that the AAV particles we prepared were active and infectious. (Figure 4.19)

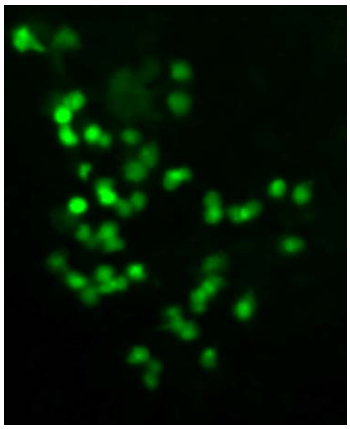

Figure 4.19: HEK293T cell infected with AAV2-CMV-EGFPN1
HEK293T cells offer a quick and easy testing for the infectiosity and activity of recombinant AAV carrying EGFP reporter. Green fluorescence of EGFP reporter can be detected 72 hours after infection.

Next, siRNA cassettes were transferred from previous pBluescript-based siRNA constructs into AAV vectors to form the AAV vector-based siRNA constructs. In this vector, EGFP expression is regulated by the CMV promoter while siRNA transcription is controlled independently by U6 promoter. (Figure 4.20)

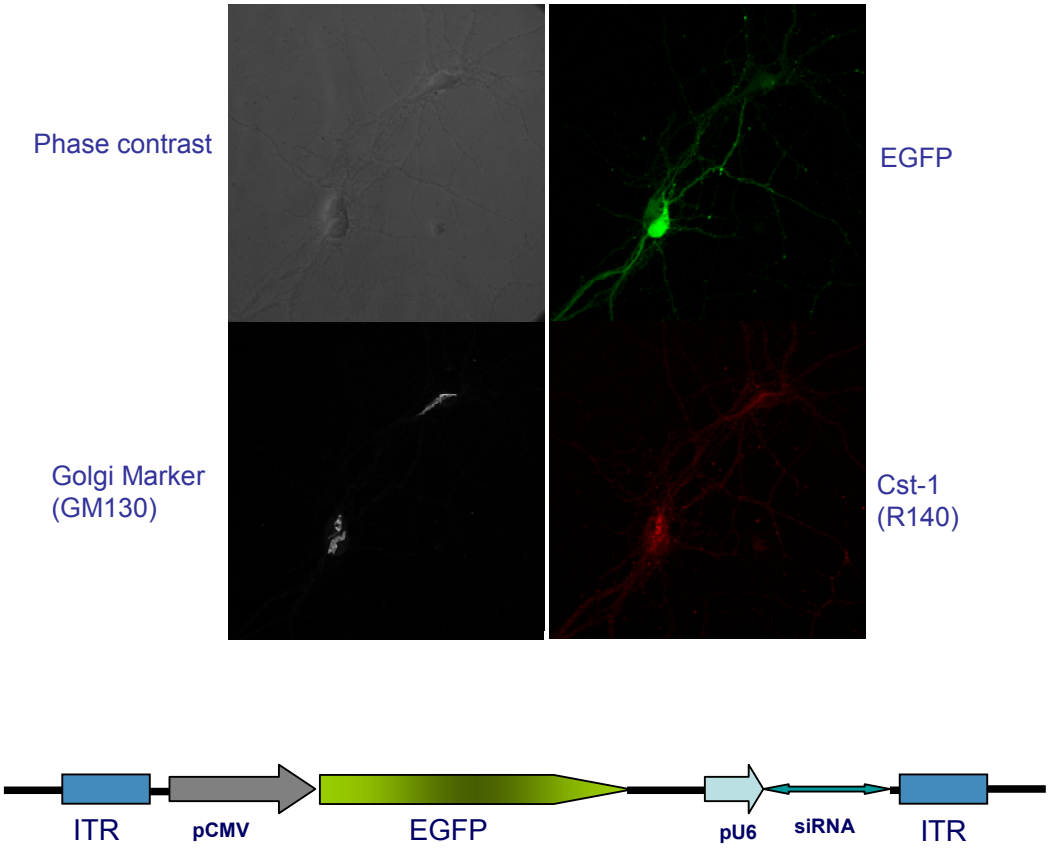

Figure 4.20: AAV-siRNA vector containing an EGFP marker

AAV vector containing EGFP marker shows successful infection in the neurons in primary neuronal culture. Golgi marker serves as the indicator of the cell body of the neurons. The cartoon schematically outlines U6 promoter driven siRNA expression AAV vector carrying the CMV promoter driven EGFP marker.

4.8.4 AAV vector containing the EGFP-2A fusion frame

The major disadvantage of the rAAV vector is the limited cloning capacity, which allows only approximately 5.0kb of transgenic DNA to be packaged into the viral genome. When we tried to obtain calsyntenin and EGFP marker co-expression in the AAV vector, it became problematic because the two transcription units exceeded the limitation of AAV packaging ability.

The usage of the 2A sequence derived from the foot and mouse disease virus (FMDV) allows the bi-cistronic transcription from a single ORF (Open Reading Frame) unit encompassing the coding sequence of both peptides linked by the short sequence-encoding 2A peptide. Once translated, the 2A peptide leads to the separation of the two proteins by self-cleavage on its own C-terminal. The 2A sequence is rather short extending only for 48nt, which makes it extremely suitable for cloning multiple genes into the AAV vector.

ATGGTGAGCAAGGGCGAGGAGCTGTTCACCGGGGTGGTGCCCATCCTGGTCG
AGCTGGACGGCGACGTAAACGGCCACAAGTTCAGCGTGTCCGGCGAGGGCGA
GGGCGATGCCACCTACGGCAAGCTGACCCTGAAGTTCATCTGCACCACCGGCA
AGCTGCCCGTGCCCTGGCCCACCCTCGTGACCACCCTGACCTGGGGCGTGCA
GTGCTTCAGCCGCTACCCCGACCACATGAAGCAGCACGACTTCTTCAAGTCCG
CCATGCCCGAAGGCTACGTCCAGGAGCGCACCATCTTCTTCAAGGACGACGGC
AACTACAAGACCCGCGCCGAGGTGAAGTTCGAGGGCGACACCCTGGTGAACC
GCATCGAGCTGAAGGGCATCGACTTCAAGGAGGACGGCAACATCCTGGGGCAC
AAGCTGGAGTACAACTACATCAGCCACAACGTCTATATCACCGCCGACAAGCAG
AAGAACGGCATCAAGGCCAACTTCAAGATCCGCCACAACATCGAGGACGGCAG
CGTGCAGCTCGCCGACCACTACCAGCAGAACACCCCCATCGGCGACGGCCCC
GTGCTGCTGCCCGACAACCACTACCTGAGCACCCAGTCCGCCCTGAGCAAAGA
CCCCAACGAGAAGCGCGATCACATGGTCCTGCTGGAGTTCGTGACCGCCGCC
GGGATCACTCTCGGCATGGACGAGCTGTACAAGAATTTTGACCTTCTTAAGCTT
GCGGGAGACGTCGAGTCCAACCCTGGGCCC(Apa I)GC

The coding sequences of calsyntenins will be cloned downstream to the 2A sequence by insertion into the Apa I site.

4.9 Knockdown of endogenous calsynetnin-1 in primary neuronal cultures

When evaluated by immunoblotting, all three AAV vectors expressing siRNA directed against mouse calsyntenin-1 gene successfully reduced the endogenous calsyntenin-1 expression in primary neuronal cultures. The gene knockdown is specific as validated by expression of the housekeeping gene alpha-actin as a loading control.

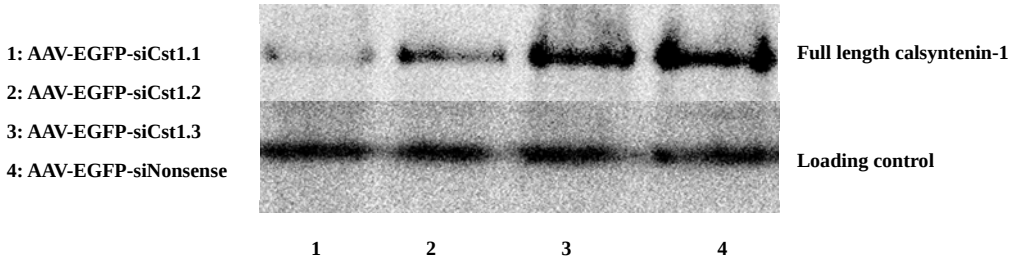

Figure 4.21: Screening of AAV-EGFP-siCst1 vectors for calsyntenin-1 silencing in primary neuronal cultures

AAV vector containing different siRNA cassette targeting calsyntenin-1 shows distinguishable difference in the knockdown efficiency of calsyntenin-1 expression. The AAV-EGFP-siCst1.1 achieves the excellent target gene silencing effect while AAV-EGFP-siCst1.2 AAV-EGFP-siCst1.3 shows moderate or slight inhibition of calsyntenin-1 expression.

The AAV-EGFP-siCst1.1 which targets the calsyntenin-1 gene at 458-476bp achieved the most striking target gene silencing effect, while the AAV-EGFP-siCst1.3 targeting at 1298-1316bp showed slight inhibition. That siRNA vectors targeting different sites along the calsyntenin-1 gene achieved gene knockdown of different levels can be explained by the positional effect of siRNA (Figure 4.21).

The calsyntenin-1 expression levels in AAV infected cultures were assessed by immunoblotting, followed by quantitative measurement with densitometry (ImageJ software, http://rsb.info.nih.gov/ij/).

Relative mouse calsyntenin-1 expression in recombinant AAV infected primary neuronal cultures was normalized against the loading control alpha-actin. Taking the calsyntenin-1 level in control virus AAV-EGFP-siNonsense treated culture as 100%, the expression levels of the full length and the stump of calsyntenin-1 in AAV-EGFP-siCst1.1-treated cultures were reduced to 19.2% and 35.9%, respectively (Figure 4.22).

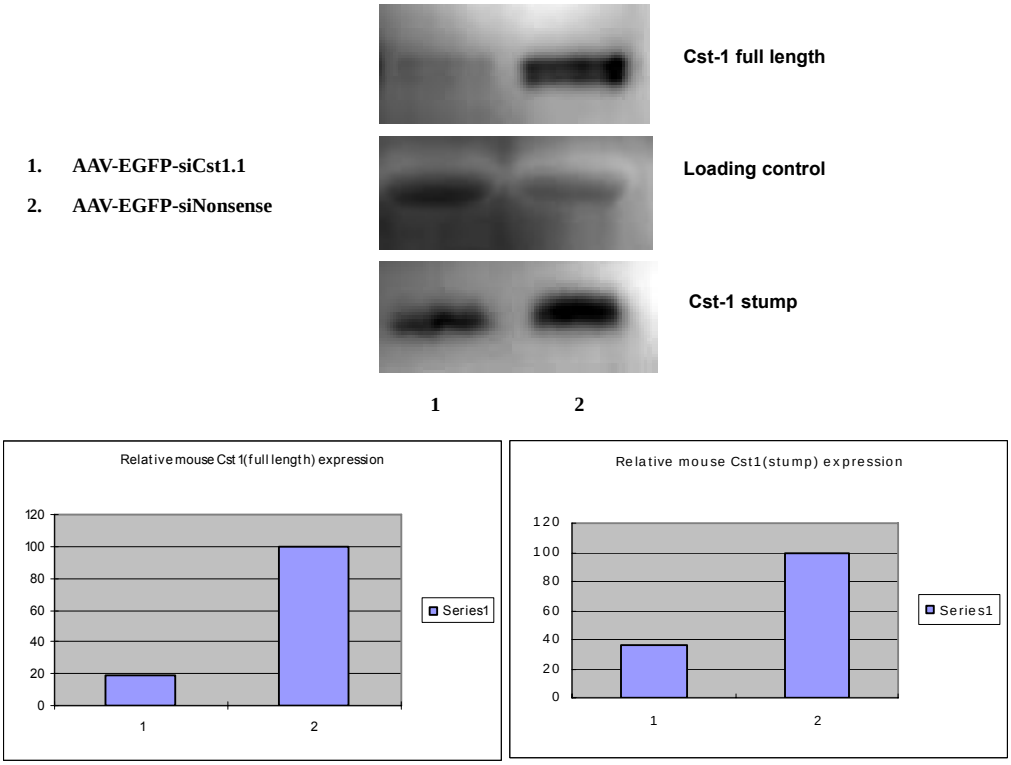

Figure 4.22: Efficiency of calsyntenin-1 knockdown in primary neuronal cultures with AAV-EGFP-siCst1.1

AAV vector AAV-EGFP-siCst1.1 achieves target gene silencing effect in primary neuronal culture. The efficiency of calsyntenin-1 knockdown was evaluated by immunoblotting, showing the expression level of full length and the stump of calsyntenin-1 were reduced to 19.2% and 35.9% respectively.

In order to further improve the knockdown potency of siRNAs, the loop sequence could be replaced by the one derived from endogenously expressed miRNA, which could facilitate the export of siRNA from the nucleus to the cytoplasm to form an active siRNA duplex (Haibin.X, 2004).

Moreover, modified promoters derived from RNA polymerase type III or type II promoters such as the tetracycline-responsive H1 promoter and the enhanced CMV promoter, enable more effective or conditional siRNA suppression of target genes.

Calsyntenin knockdown in primary neuronal cultures infected with targeting rAAV-siRNA vectors was further assessed with immunofluorescence. Our results indicate significantly suppressed calsyntenin-1 expression in AAV-EGFP-siCst1 infected neurons when general gene expression was normalized to Golgi Marker expression (Figure 4.23).

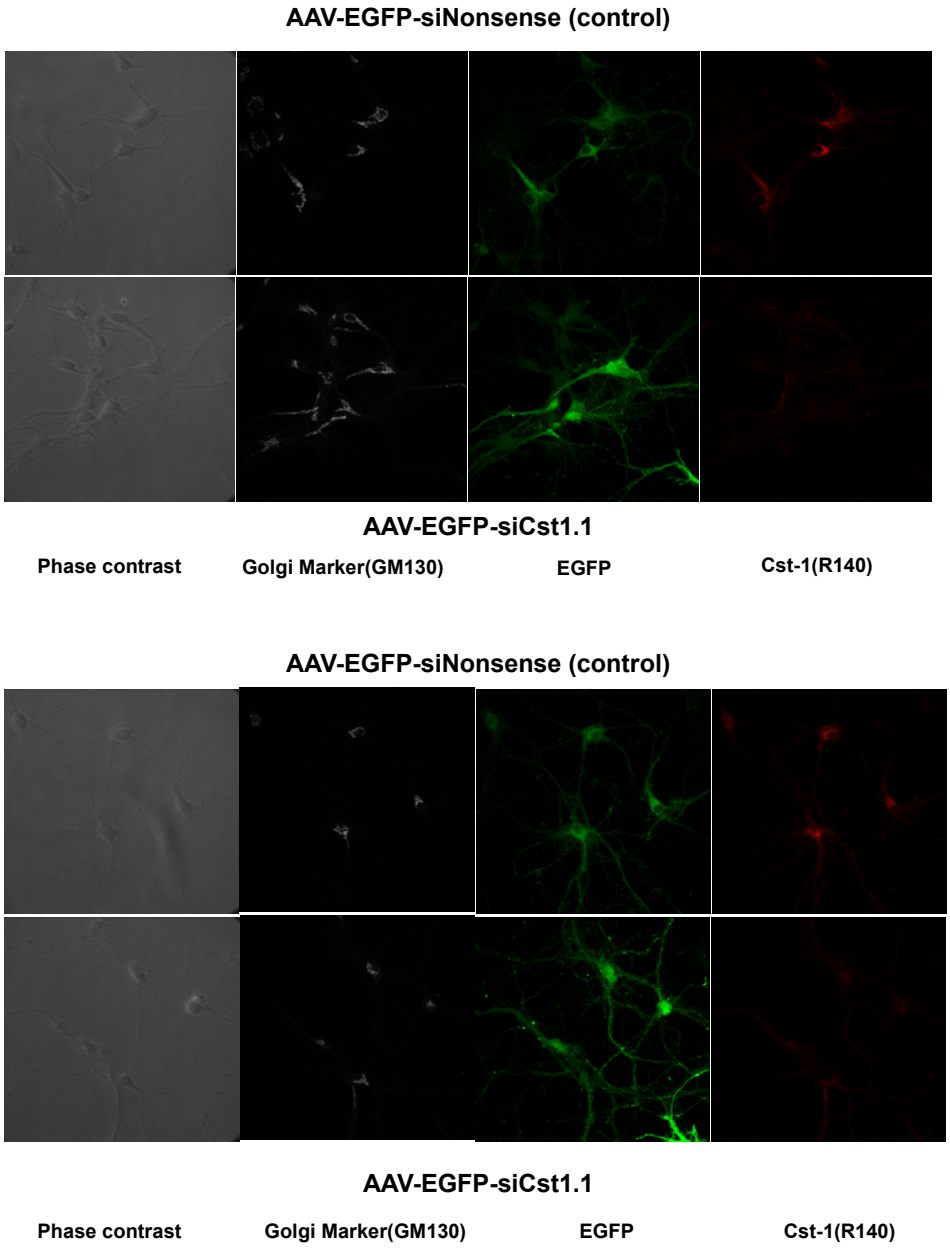

Figure 4.23: Calsyntenin-1 knockdown in primary neuronal cultures with AAV-EGFP-siCst1.1

AAV vector AAV-EGFP-siCst1 significantly suppressed calsyntenin-1 expression in primary hippopcampal neuronal culture when the calsyntenin-1 expression levels were assessed with immunofluorescence and normalized to Golgi Marker levels.

After repeated experiments and time-course studies, we came to the conclusion that

calsyntenin-1 down-regulation in primary hippocampal neuronal cultures are specific, stable, long-lasting and highly reproducible.

4.10 Preliminary morphological studies

rAAV treated neurons were fixed and visualized with fluorescent microscopy 15-20 days after the AAV infection. 9 neurons with at least 4 primary dendrites arising from the soma were randomly selected from 6 cover-slips in each group. The number of primary dendrites for each neuron were counted and recorded. For statistical analysis, the average primary dendritic number was calculated for each group and subsequently used to perform a T-test with Microsoft Excel software to compare the formation of primary dendrites. Correlations were calculated by linear regression analysis. A P value < 0.05 was considered significant. The results demonstrated that the AAV-EGFP-siCst1 infection did not induce significant changes in primary dendrite generation when compared with the control group treated with AAV-EGFP-siNonsense (Figure 4.24).

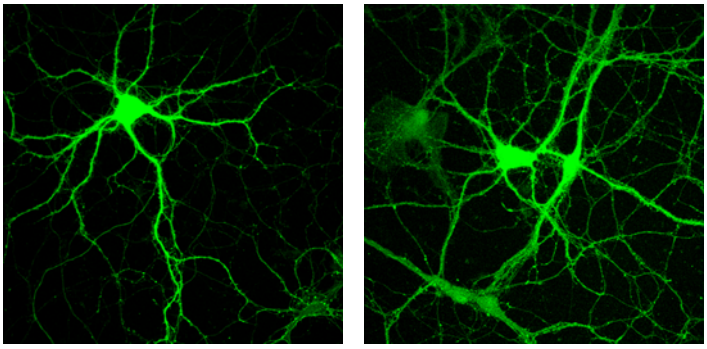

AAV-EGFP-siCst1.1 **AAV-EGFP-siNonsense**

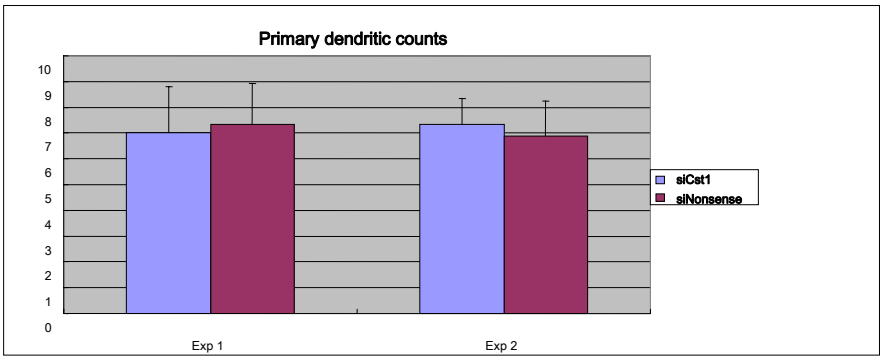

Figure 4.24: Assessment of primary dendrite number in neurons

AAV vector AAV-EGFP-siCst1 which significantly suppressed calsyntenin-1 expression in primary hippopcampal neuronal culture doesn't show detectable changes in primary dendritic generation when compared with the control vector AAV-EGFP-nonsense.

Dentritic branching patterns have great impact on neuronal function, representing a major aspect of neuronal morphology. Neurons make two types of neuronal extensions: axons that send outputs to other neurons, and dendrites, that are specialized for receiving and processing inputs. The morphological pattern of the dendrites is quite variable from one type of neuron to another, permitting differential contributions to informational processing. Moreover, morphological changes often reflect functional disorders.

4.11 Calsyntenin and excitotoxic neuronal death in vitro

To answer the question whether calsyntenins are involved in excitotoxicity, a NMDA-induced apoptotic and necrotic neuronal death model was used to study the consequences of excitotoxic stress when applied to calsyntenin knockdown cultures.

Mouse primary hippocampal neuronal cells infected with calsyntenin-1 down-regulating vector AAV-EGFP-siCst1 were cultured on a 12-well plate for more than 10 days before they were used for experiments. The excitotoxic stress was induced by exposing the cells to 100 μM NMDA for 30 minutes. To assess neuronal cell death, Hoechst staining assays were conducted at 24 hours after NMDA exposure to indicate nuclear condensation in apoptotic cells and necrotic cells as small bright dots (Figure 4.25).

Neurons from 10 randomly selected separate fields from 4 cover-slips in each group were counted, giving the percentage of apoptotic plus necrotic cells in total cells. Using Prism software, One-way Analysis of Variance (ANOVA) was performed to compare the percentage of apoptotic and necrotic cells. Correlations were calculated by linear regression analysis. A P value < 0.05 was considered significant.

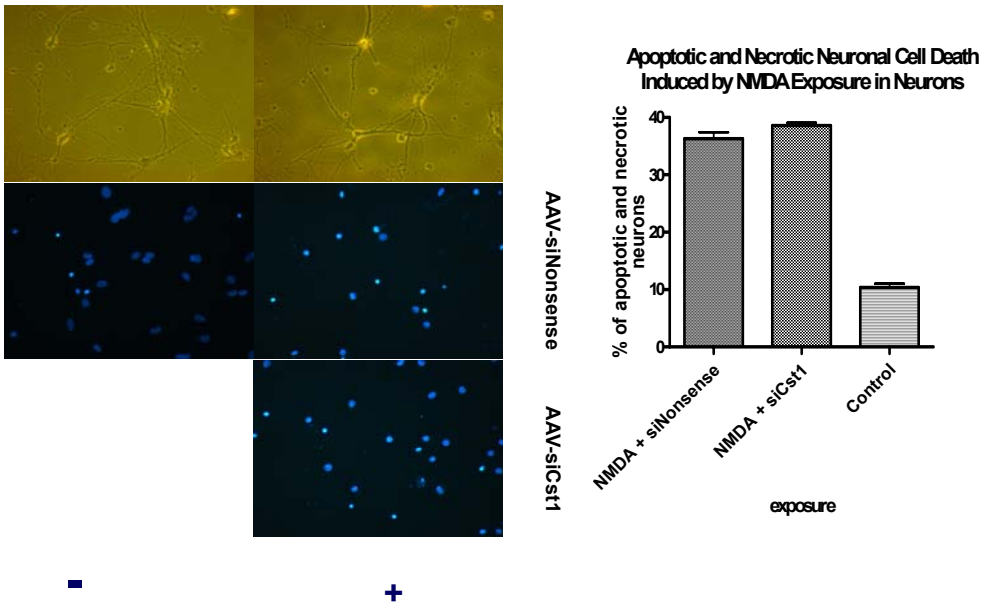

Figure 4.25: Assessment of NMDA-induced apoptotic and necrotic cell death in primary neuronal cultures

Assessed with Hoechst staining for apoptotic and necrotic neuronal cell death, the neurons transduced by AAV-EGFP-siCst1 do not show significant difference in the reaction to the NMDA induced excitotoxicity compared with the neurons transduced by AAV-EGFP-siNonsense control vector.

Preliminary data show that there is no significant difference in the reaction to the excitotoxic insult between calsyntenin-1 knockdown neurons and Nonsense control neurons ($p = 0.09, > 0.05$).

The data obtained from calsyntenin-1 knockdown experiments are insufficient by far to conclude that calsyntenins do not play a role in excitotoxicity. Most probably the calsyntenins may exhibit functional compensation amongst each other. Further extensive studies will be done when triple knockdowns of all three calsyntenins are achieved in neuronal culture.

V. Conclusions and Outlook

We successfully set up a DNA vector-based small interfering RNA system, which has been proven to achieve specific and long-lasting gene down-regulation in several cell lines and in primary neuronal cultures.

An AAV vector delivery system was established providing efficient gene transduction into neurons in primary neuronal cultures to achieve specific gene knockdown or over-expression.

Co-transfected and endogenous calsyntenin-1 expression has been significantly down-regulated in cell lines and in primary neuronal culture, allowing studies of loss-of-function of specific genes.

Preliminary data have been collected from morphological and functional studies providing a basic characterization of calsyntenin-1. The calsyntenin-1 knockdown did not show a notable influence on dendrite formation when evaluated by analyzing primary dendritic number. No impact of calsyntenin-1 on excitotoxic stress was detected in a NMDA-induced excitotoxic neuronal death model.

The data obtained from these calsyntenin-1 knockdown experiments are insufficient to conclude that calsyntenins do not play a role in excitotoxicity. The calsyntenin members share highly conserved structures, suggesting potential functional compensation amongst each other. Extensive studies will be done when triple knockdown of all three calsyntenins is achieved by a vector containing siRNA cassettes against calsyntenin-1,2 and 3.

Further morphological investigation such as the measurement of total dendritic length, secondary dendrite branching, and synaptic density will be conducted to give a more comprehensive understanding of the role which calsyntenins play in neuronal cell development.

Calsyntenin suppression and over-expression *in vitro* and *in vivo* will be realized in the future with the rAAV vehicle. Reversible focal cerebral ischemia induced by temporary middle cerebral artery occlusion may serve as a useful model to answer the question whether the calsyntenins modulate excitotoxic neuronal cell death *in vivo*.

The application of our vector-based siRNA system can be extended to study any other genes of interest by achieving loss-of-function. The system could be further modified to attain higher efficiency by replacing the loop sequence derived from

natural miRNA to improve export from the nucleus to the cytoplasm. Moreover, inducible elements could be introduced into the vector to achieve conditional knockdown of the target gene, which would help in avoiding the lethal effect associated with the deletion of certain genes.

Reference

Araki Y, Tomita S, Yamaguchi H, Miyagi N, Sumioka A, Kirino Y, Suzuki T (2003) Novel cadherin-related membrane proteins, Alcadeins, enhance the X11-like protein-mediated stabilization of amyloid beta-protein precursor metabolism. J Biol Chem 278:49448-49458.

Arundine M, Tymianski M (2003) Molecular mechanisms of calcium-dependent neurodegeneration in excitotoxicity. Cell Calcium 34:325-337.

Bano D, Nicotera P (2007) Ca2+ signals and neuronal death in brain ischemia. Stroke 38:674-676.

Berliocchi L, Bano D, Nicotera P (2005) Ca2+ signals and death programmes in neurons. Philos Trans R Soc Lond B Biol Sci 360:2255-2258.

Bernstein E, Denli AM, Hannon GJ (2001a) The rest is silence. Rna 7:1509-1521.

Bernstein E, Caudy AA, Hammond SM, Hannon GJ (2001b) Role for a bidentate ribonuclease in the initiation step of RNA interference. Nature 409:363-366.

Berridge MJ, Lipp P, Bootman MD (2000) The versatility and universality of calcium signalling. Nat Rev Mol Cell Biol 1:11-21.

Berridge MJ, Bootman MD, Roderick HL (2003) Calcium signalling: dynamics, homeostasis and remodelling. Nat Rev Mol Cell Biol 4:517-529.

Billy E, Brondani V, Zhang H, Muller U, Filipowicz W (2001) Specific interference with gene expression induced by long, double-stranded RNA in mouse embryonal teratocarcinoma cell lines. Proc Natl Acad Sci U S A 98:14428-14433.

Bonini NM, La Spada AR (2005) Silencing polyglutamine degeneration with RNAi. Neuron 48:715-718.

Braasch DA, Jensen S, Liu Y, Kaur K, Arar K, White MA, Corey DR (2003) RNA interference in mammalian cells by chemically-modified RNA. Biochemistry 42:7967-7975.

Brummelkamp TR, Bernards R, Agami R (2002) A system for stable expression of short interfering RNAs in mammalian cells. Science 296:550-553.

Burgoyne RD (2007) Neuronal calcium sensor proteins: generating diversity in neuronal Ca2+ signalling. Nat Rev Neurosci 8:182-193.

Burgoyne RD, Weiss JL (2001) The neuronal calcium sensor family of Ca2+-binding proteins. Biochem J 353:1-12.

Chang K, Elledge SJ, Hannon GJ (2006) Lessons from Nature: microRNA-based shRNA libraries. Nat Methods 3:707-714.

Clapham DE (1995) Calcium signaling. Cell 80:259-268.

Clapham DE (2007) Calcium signaling. Cell 131:1047-1058.

Dawson VL, Dawson TM (1998) Nitric oxide in neurodegeneration. Prog Brain Res 118:215-229.

de Fougerolles A, Vornlocher HP, Maraganore J, Lieberman J (2007) Interfering with disease: a progress report on siRNA-based therapeutics. Nat Rev Drug Discov 6:443-453.

Dietzl G, Chen D, Schnorrer F, Su KC, Barinova Y, Fellner M, Gasser B, Kinsey K, Oppel S, Scheiblauer S, Couto A, Marra V, Keleman K, Dickson BJ (2007) A genome-wide transgenic RNAi library for conditional gene inactivation in Drosophila. Nature 448:151-156.

Dykxhoorn DM, Lieberman J (2006) Knocking down disease with siRNAs. Cell 126:231-235.

Ehrengruber MU, Hennou S, Bueler H, Naim HY, Deglon N, Lundstrom K (2001) Gene transfer into neurons from hippocampal slices: comparison of recombinant Semliki Forest Virus, adenovirus, adeno-associated virus, lentivirus, and measles virus. Mol Cell Neurosci 17:855-871.

Elbashir SM, Harborth J, Lendeckel W, Yalcin A, Weber K, Tuschl T (2001) Duplexes of 21-nucleotide RNAs mediate RNA interference in cultured mammalian cells. Nature 411:494-498.

Fire A, Xu S, Montgomery MK, Kostas SA, Driver SE, Mello CC (1998) Potent and specific genetic interference by double-stranded RNA in Caenorhabditis elegans. Nature 391:806-811.

Geiduschek EP, Kassavetis GA (2001) The RNA polymerase III transcription apparatus. J Mol Biol 310:1-26.

Goncalves MA (2005) Adeno-associated virus: from defective virus to effective vector. Virol J 2:43.

Grimm D (2002) Production methods for gene transfer vectors based on adeno-associated virus serotypes. Methods 28:146-157.

Grimm D, Kay MA, Kleinschmidt JA (2003) Helper virus-free, optically controllable, and two-plasmid-based production of adeno-associated virus vectors of serotypes 1 to 6. Mol Ther 7:839-850.

Guo S, Kemphues KJ (1995) par-1, a gene required for establishing polarity in C. elegans embryos, encodes a putative Ser/Thr kinase that is asymmetrically distributed. Cell 81:611-620.

Haeseleer F, Imanishi Y, Sokal I, Filipek S, Palczewski K (2002) Calcium-binding proteins: intracellular sensors from the calmodulin superfamily. Biochem Biophys Res Commun 290:615-623.

Hannon GJ (2002) RNA interference. Nature 418:244-251.

Hannon GJ, Chubb A, Maroney PA, Hannon G, Altman S, Nilsen TW (1991) Multiple cis-acting elements are required for RNA polymerase III transcription of the gene encoding H1 RNA, the RNA component of human RNase P. J Biol Chem 266:22796-22799.

Harborth J, Elbashir SM, Vandenburgh K, Manninga H, Scaringe SA, Weber K, Tuschl T (2003) Sequence, chemical, and structural variation of small interfering RNAs and short hairpin RNAs and the effect on mammalian gene silencing. Antisense Nucleic Acid Drug Dev 13:83-105.

Hintsch G, Zurlinden A, Meskenaite V, Steuble M, Fink-Widmer K, Kinter J, Sonderegger P (2002) The calsyntenins--a family of postsynaptic membrane proteins with distinct neuronal expression patterns. Mol Cell Neurosci 21:393-409.

Holen T, Amarzguioui M, Wiiger MT, Babaie E, Prydz H (2002) Positional effects of short interfering RNAs targeting the human coagulation trigger Tissue Factor. Nucleic Acids Res 30:1757-1766.

Holmquist GP, Ashley T (2006) Chromosome organization and chromatin modification: influence on genome function and evolution. Cytogenet Genome Res 114:96-125.

Ivings L, Pennington SR, Jenkins R, Weiss JL, Burgoyne RD (2002) Identification of Ca2+-dependent binding partners for the neuronal calcium sensor protein neurocalcin delta: interaction with actin, clathrin and tubulin. Biochem J 363:599-608.

Jackson RJ, Standart N (2007) How do microRNAs regulate gene expression? Sci STKE 2007:re1.

Kasim V, Miyagishi M, Taira K (2004) Control of siRNA expression using the Cre-loxP recombination system. Nucleic Acids Res 32:e66.

Kaspar BK, Vissel B, Bengoechea T, Crone S, Randolph-Moore L, Muller R, Brandon EP, Schaffer D, Verma IM, Lee KF, Heinemann SF, Gage FH (2002) Adeno-associated virus effectively mediates conditional gene modification in the brain. Proc Natl Acad Sci U S A 99:2320-2325.

Ketting RF, Haverkamp TH, van Luenen HG, Plasterk RH (1999) Mut-7 of C. elegans, required for transposon silencing and RNA interference, is a homolog of Werner syndrome helicase and RNaseD. Cell 99:133-141.

Khvorova A, Reynolds A, Jayasena SD (2003) Functional siRNAs and miRNAs exhibit strand bias. Cell 115:209-216.

Konecna A, Frischknecht R, Kinter J, Ludwig A, Steuble M, Meskenaite V, Indermuhle M, Engel M, Cen C, Mateos JM, Streit P, Sonderegger P (2006) Calsyntenin-1 docks vesicular cargo to kinesin-1. Mol Biol Cell 17:3651-3663.

Kugler S, Meyn L, Holzmuller H, Gerhardt E, Isenmann S, Schulz JB, Bahr M (2001) Neuron-specific expression of therapeutic proteins: evaluation of different cellular promoters in recombinant adenoviral vectors. Mol Cell Neurosci 17:78-96.

Kunath T, Gish G, Lickert H, Jones N, Pawson T, Rossant J (2003) Transgenic RNA interference in ES cell-derived embryos recapitulates a genetic null phenotype. Nat Biotechnol 21:559-561.

Liu J, Carmell MA, Rivas FV, Marsden CG, Thomson JM, Song JJ, Hammond SM, Joshua-Tor L, Hannon GJ (2004) Argonaute2 is the catalytic engine of mammalian RNAi. Science 305:1437-1441.

Makinen PI, Koponen JK, Karkkainen AM, Malm TM, Pulkkinen KH, Koistinaho J, Turunen MP, Yla-Herttuala S (2006) Stable RNA interference: comparison of U6 and H1 promoters in endothelial cells and in mouse brain. J Gene Med 8:433-441.

Matranga C, Tomari Y, Shin C, Bartel DP, Zamore PD (2005) Passenger-strand cleavage facilitates assembly of siRNA into Ago2-containing RNAi enzyme complexes. Cell 123:607-620.

Matsukura S, Jones PA, Takai D (2003) Establishment of conditional vectors for hairpin siRNA knockdowns. Nucleic Acids Res 31:e77.

Matthess Y, Kappel S, Spankuch B, Zimmer B, Kaufmann M, Strebhardt K (2005) Conditional inhibition of cancer cell proliferation by tetracycline-responsive, H1 promoter-driven silencing of PLK1. Oncogene 24:2973-2980.

McIntyre GJ, Fanning GC (2006) Design and cloning strategies for constructing shRNA expression vectors. BMC Biotechnol 6:1.

Mette MF, van der Winden J, Matzke MA, Matzke AJ (1999) Production of aberrant promoter transcripts contributes to methylation and silencing of unlinked homologous promoters in trans. Embo J 18:241-248.

Michel U, Malik I, Ebert S, Bahr M, Kugler S (2005) Long-term in vivo and in vitro AAV-2-mediated RNA interference in rat retinal ganglion cells and cultured primary neurons. Biochem Biophys Res Commun 326:307-312.

Miyagishi M, Taira K (2002) U6 promoter-driven siRNAs with four uridine 3' overhangs efficiently suppress targeted gene expression in mammalian cells. Nat Biotechnol 20:497-500.

Miyagishi M, Sumimoto H, Miyoshi H, Kawakami Y, Taira K (2004) Optimization of an siRNA-expression system with an improved hairpin and its significant suppressive effects in

mammalian cells. J Gene Med 6:715-723.

Myslinski E, Ame JC, Krol A, Carbon P (2001) An unusually compact external promoter for RNA polymerase III transcription of the human H1RNA gene. Nucleic Acids Res 29:2502-2509.

Napoli C, Lemieux C, Jorgensen R (1990) Introduction of a Chimeric Chalcone Synthase Gene into Petunia Results in Reversible Co-Suppression of Homologous Genes in trans. Plant Cell 2:279-289.

Nishikura K (2006) Editor meets silencer: crosstalk between RNA editing and RNA interference. Nat Rev Mol Cell Biol 7:919-931.

Noma K, Sugiyama T, Cam H, Verdel A, Zofall M, Jia S, Moazed D, Grewal SI (2004) RITS acts in cis to promote RNA interference-mediated transcriptional and post-transcriptional silencing. Nat Genet 36:1174-1180.

Paddison PJ, Caudy AA, Bernstein E, Hannon GJ, Conklin DS (2002) Short hairpin RNAs (shRNAs) induce sequence-specific silencing in mammalian cells. Genes Dev 16:948-958.

Pal-Bhadra M, Bhadra U, Birchler JA (1997) Cosuppression in Drosophila: gene silencing of Alcohol dehydrogenase by white-Adh transgenes is Polycomb dependent. Cell 90:479-490.

Paterna JC, Bueler H (2002) Recombinant adeno-associated virus vector design and gene expression in the mammalian brain. Methods 28:208-218.

Paul CP, Good PD, Winer I, Engelke DR (2002) Effective expression of small interfering RNA in human cells. Nat Biotechnol 20:505-508.

Plasterk RH (2006) Micro RNAs in animal development. Cell 124:877-881.

Rand TA, Petersen S, Du F, Wang X (2005) Argonaute2 cleaves the anti-guide strand of siRNA during RISC activation. Cell 123:621-629.

Reynolds A, Leake D, Boese Q, Scaringe S, Marshall WS, Khvorova A (2004) Rational siRNA design for RNA interference. Nat Biotechnol 22:326-330.

Romano N, Macino G (1992) Quelling: transient inactivation of gene expression in Neurospora crassa by transformation with homologous sequences. Mol Microbiol 6:3343-3353.

Ruitenberg MJ, Eggers R, Boer GJ, Verhaagen J (2002) Adeno-associated viral vectors as agents for gene delivery: application in disorders and trauma of the central nervous system. Methods 28:182-194.

Saito Y, Yokota T, Mitani T, Ito K, Anzai M, Miyagishi M, Taira K, Mizusawa H (2005) Transgenic small interfering RNA halts amyotrophic lateral sclerosis in a mouse model. J Biol Chem 280:42826-42830.

Sattler R, Tymianski M (2000) Molecular mechanisms of calcium-dependent excitotoxicity. J Mol Med 78:3-13.

Schmid A, Schindelholz B, Zinn K (2002) Combinatorial RNAi: a method for evaluating the functions of gene families in Drosophila. Trends Neurosci 25:71-74.

Seisenberger G, Ried MU, Endress T, Buning H, Hallek M, Brauchle C (2001) Real-time single-molecule imaging of the infection pathway of an adeno-associated virus. Science 294:1929-1932.

Snyder RO, Flotte TR (2002) Production of clinical-grade recombinant adeno-associated virus vectors. Curr Opin Biotechnol 13:418-423.

Song E, Lee SK, Wang J, Ince N, Ouyang N, Min J, Chen J, Shankar P, Lieberman J (2003) RNA interference targeting Fas protects mice from fulminant hepatitis. Nat Med 9:347-351.

Song JJ, Smith SK, Hannon GJ, Joshua-Tor L (2004) Crystal structure of Argonaute and its

implications for RISC slicer activity. Science 305:1434-1437.

Sui G, Soohoo C, Affar el B, Gay F, Shi Y, Forrester WC, Shi Y (2002) A DNA vector-based RNAi technology to suppress gene expression in mammalian cells. Proc Natl Acad Sci U S A 99:5515-5520.

Susin SA, Lorenzo HK, Zamzami N, Marzo I, Snow BE, Brothers GM, Mangion J, Jacotot E, Costantini P, Loeffler M, Larochette N, Goodlett DR, Aebersold R, Siderovski DP, Penninger JM, Kroemer G (1999) Molecular characterization of mitochondrial apoptosis-inducing factor. Nature 397:441-446.

Tabara H, Sarkissian M, Kelly WG, Fleenor J, Grishok A, Timmons L, Fire A, Mello CC (1999) The rde-1 gene, RNA interference, and transposon silencing in C. elegans. Cell 99:123-132.

Taxman DJ, Livingstone LR, Zhang J, Conti BJ, Iocca HA, Williams KL, Lich JD, Ting JP, Reed W (2006) Criteria for effective design, construction, and gene knockdown by shRNA vectors. BMC Biotechnol 6:7.

Tenenbaum L, Chtarto A, Lehtonen E, Velu T, Brotchi J, Levivier M (2004) Recombinant AAV-mediated gene delivery to the central nervous system. J Gene Med 6 Suppl 1:S212-222.

Thomas CE, Ehrhardt A, Kay MA (2003) Progress and problems with the use of viral vectors for gene therapy. Nat Rev Genet 4:346-358.

Tomar RS, Matta H, Chaudhary PM (2003) Use of adeno-associated viral vector for delivery of small interfering RNA. Oncogene 22:5712-5715.

Vogt L, Schrimpf SP, Meskenaite V, Frischknecht R, Kinter J, Leone DP, Ziegler U, Sonderegger P (2001) Calsyntenin-1, a proteolytically processed postsynaptic membrane protein with a cytoplasmic calcium-binding domain. Mol Cell Neurosci 17:151-166.

Won SJ, Kim DY, Gwag BJ (2002) Cellular and molecular pathways of ischemic neuronal death. J Biochem Mol Biol 35:67-86.

Wu Z, Asokan A, Samulski RJ (2006) Adeno-associated virus serotypes: vector toolkit for human gene therapy. Mol Ther 14:316-327.

Xia H, Mao Q, Paulson HL, Davidson BL (2002) siRNA-mediated gene silencing in vitro and in vivo. Nat Biotechnol 20:1006-1010.

Xia H, Mao Q, Eliason SL, Harper SQ, Martins IH, Orr HT, Paulson HL, Yang L, Kotin RM, Davidson BL (2004) RNAi suppresses polyglutamine-induced neurodegeneration in a model of spinocerebellar ataxia. Nat Med 10:816-820.

Xia XG, Zhou H, Xu Z (2006) Transgenic RNAi: Accelerating and expanding reverse genetics in mammals. Transgenic Res 15:271-275.

Xia XG, Zhou H, Ding H, Affar el B, Shi Y, Xu Z (2003) An enhanced U6 promoter for synthesis of short hairpin RNA. Nucleic Acids Res 31:e100.

Zamore PD, Tuschl T, Sharp PA, Bartel DP (2000) RNAi: double-stranded RNA directs the ATP-dependent cleavage of mRNA at 21 to 23 nucleotide intervals. Cell 101:25-33.

Zolotukhin S (2005) Production of recombinant adeno-associated virus vectors. Hum Gene Ther 16:551-557.

SIDE PROJECT: Danio rerio Calsyntenin-1

(By the helpf of *Dr.* Melody (Ying-yu) Huang from *Prof.Dr.* Stephan Neuhauss group)

Figure 1: General expression profile of calsyntenin-1 in telencephalon, diencephalon, midbrain, hindbrain, spinal cord, cranial ganglia, pharyngeal pouches, lateral line and nose.
Prim15 to Prim 25 stage (Thisse *et al.*, 2004)

Zebra fish calsyntenin-1 has been identified and reported to NCBI database (clone number: BC052116). The expression profile has been investigated with i*n situ* hybridization (Figure 1). To look into the detailed expression pattern of calsyntenin-1 in zebra fish visual system, an *in situ* probe was designed according to the published cDNA sequence. Using cDNA obtained from brain tissue of zebra fish larvae, the PCR was perfermed for probe vector cloning. Instead of expected 660bp fragment, a 2089bp one was obtained (Figure 2). The fragment was cloned into vector for sequencing. The sequence was searched in NCBI database. It was discovered that the sequence belongs to an unidentified cDNA clone (BC127396), which represent a splicing variant of reported zebra fish calsyntenin-1. But whether the splicing variation is tissue specific or developmental stages specific is not clear. The studay of zebra fish calsynentnin-1 may help to understand its' highly conserved homologous in mammals.

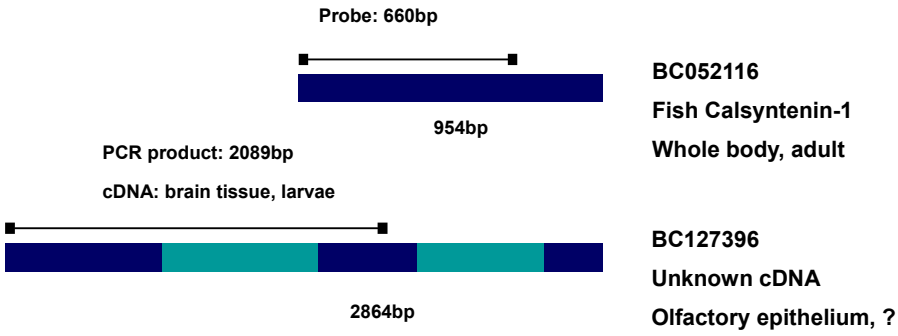

Figure 2: Identification of the splicing variant of zebra fish calsyntenin-1 in zebra fish larvae

Acknowledgments

I would like to acknowledge many people for supporting me during my Ph.D study. First and foremost, I would especially like to thank my advisor, Prof. Dr. Peter Streit, for his helpful guidance, support and encouragement. Further, I am very grateful for having an exceptional doctoral committee and wish to express thanks to my steering committee members: Prof. Dr. Peter Sonderegger, Prof. Dr. Beat Gähwiler and Prof. Dr. Urs Gerber for great assistance on my calsyntenin project and dissertation writing. Without their support, this dissertation would not have been possible.

I am grateful for the assistance and advices I received from Dr. Beat Kunz. I owe a special note of gratitude to colleagues working on calsyntenin project: Dr. Renato Frischknecht, Dr. Anetta Konecna, Alexander Ludwig, Martin Steuble, Sebastian Kirbach, Dr. Jessica Blume and Dr. José Mateos Melero. Thanks a lot for sharing materials and for inspiring discussion over the board topics which are very enlightening to me to improve my research.

I would like to thank the colleagues from Prof. Urs Gerber and Prof. Dr. Fritjof Helmchen's group for sharing ideas and knowledge during the regular department meeting and occasional department retreat. I extend many thanks to other colleagues: Lotty Rietschin for teaching me about organotypic culture techniques, Alexander Stephan for cooperation in primary neuronal culture preparation, Monica Dilkin for helping with animal experiments, and especially Beat Stierli for all the helps on many ordinary lab works during the past years. Many thanks go to Prof. Dr. Stephan Neuhauss for the support on zebrafish calsyntenin-1 experiment.

I can not express enough thanks to my "Chinese Supporting Network": Dr. Zhizhong Dong kindly shared his experiences on AAV production; Haiqing Hua and Ceng Zhang helped on accessing sequencing facilities and enzyme banks. I also benefit a lot from Dr. Chuan Cen's generosity for sparing precious antibodies to me. My sincere gratitude also goes to my "lunch partners" and good friends, Melody (Ying-yu) Huang, Natalie Wu and Wei Fan, for sharing delicious food and charting with our mother tongue Chinese over scientific and other interesting topics.

Finally, I would like to thank other Streits: Irina and Beatrice for their warmly hospitality to make me feel at home during my first days in Zurich. Many thanks go to my parents for their encouragement and enthusiasm. I am especially grateful to my husband Dr. Jingxuan Yang for his patience and consideration. His knowledge of molecular biology and computer science is extremely helpful to my doctoral work.